Advection of Passive Particles by Viscous Point Vortices

Gil Miguel Marques
Mestrado em Engenharia Matemática
Departamento de Matemática
2019

Orientador
Sílvio Marques de Almeida Gama, Professor Associado, FCUP

Coorientador
Maria João Pinto Sampaio Rodrigues, Professora Auxiliar, FCUP

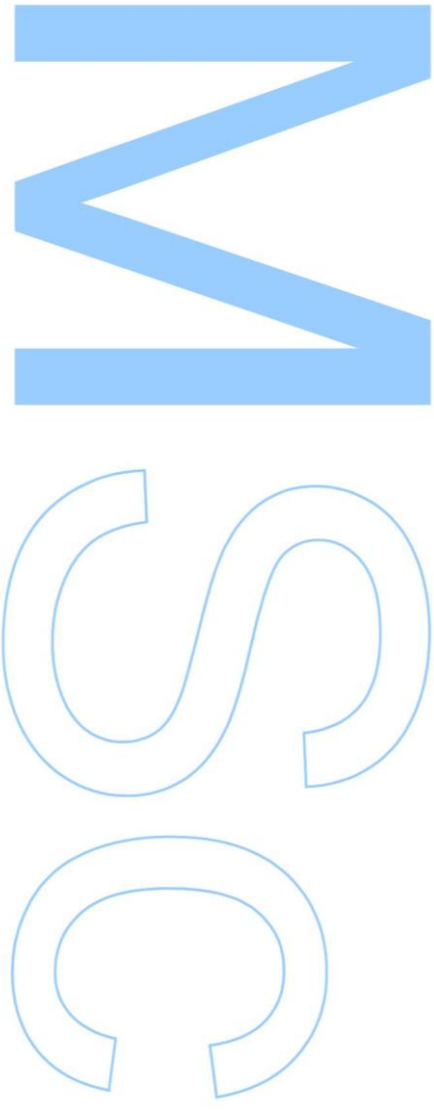

U.PORTO

FACULDADE DE CIÊNCIAS
UNIVERSIDADE DO PORTO

Todas as correções determinadas pelo júri, e só essas, foram efetuadas.

O Presidente do Júri,

Porto, _____/_____/_____

To my grandparents.

Acknowledgements

First and foremost, I would like to express my sincere gratitude to my supervisors Dr. Sílvio Gama and Dra. Maria João Rodrigues whose knowledge and support made my Master's Degree worth it so much more. Thank you also for believing and trusting in me even when I wouldn't trust myself.

I am grateful to all my other teachers for constantly filling my head with more knowledge, presenting me with new ways of thinking and giving me new tools to work with. A special word of thanks to professor João Gonçalves, who made me fall in love with mathematics on the 5^{th} grade and to Dra. Maria Helena Matos, who made me rediscover my love for mathematics early on my University life.

Thank you to my colleagues and friends from the Astronomy course, for being as welcoming and helpful as you were when I arrived in Oporto, 300 km away from my home and my friends. A special shout out to Joana Lima, Ana Afonso, Catarina Leite and João Maurício, for being my main support in those early years.

A special thank you to Raquel Albuquerque, for being my anchor in Oporto whenever I get into my darkest places. Thank you for always being there for me when I most need.

I must leave an enormous word of gratitude to music, for helping me and keeping me sane everyday. An extra shout out to all the friends and fellow travellers I made because of it, in particular to Ana Castro and Teresa Colaço. A special thank you to Björk Guðmundsdóttir for everything she has done for me.

To all my friends who have supported me throughout life and shaped me into a better person. Thank you to each and every one of you. You know who you are.

Last but not least, I am deeply grateful to my family: to my mom for all the support and sacrifices she made for me; to my grandparents, wherever you are, you are the reason for me to be the person I am, and you'll always be with me.

Abstract

The multitude of areas in which fluid dynamics is applicable justifies further investment in order to increase our knowledge on the behavior of fluids. In particular, fluid dynamics is of great importance in fields that concern the welfare of the whole human population, such as medicine or climate change.

As an alternative of the classical Navier-Stokes description, the behavior of fluids can be thought of as a consequence of the dynamics of structures such as vortices, which will generate the velocity field within the fluid.

The 2-dimensional approximation of a vortex is what we usually call a point vortex. The n-vortex problem in the plane is therefore the problem of finding the behavior of a system of n point vortices. This is no easy feat, as the problem is not integrable for $n \geq 4$ in the general case and therefore requires a numerical approach. This problem has been thoroughly studied in the inviscid case, but there is yet a lack of a consistent theory for viscous environments.

This dissertation focuses on the description of point vortices both in inviscid and viscous environments and tries to extend the idea of quantification of chaos in inviscid vortex systems of Babiano et al. [1] to viscous environments. In particular, we'll see that viscosity can disrupt stable dynamics and cause initially stable trajectories to go through chaotic behavior, before succumbing to viscosity completely. We also find that the logarithms of the duration of this chaotic behavior and the kinematic viscosity coefficient seem to be connected by a linear relationship.

Keywords

Fluid Dynamics, Navier-Stokes Equations, Incompressible Euler Equations, Hamiltonian Dynamics, Point Vortices, Viscous Point Vortices, Chaos, Lyapunov Exponents, Numerical Methods

Resumo

O grande número de área em que a dinâmica de fluídos é aplicável justifica um crescendo de investimento de modo a aumentar o nosso conhecimento acerca do comportamento de fluídos. Em particular, a dinâmica de fluídos é de extrema importância em áreas que afectam o bem-estar de toda a população, como a medicina ou as alterações climáticas.

Como alternativa à descrição clássica das equações de Navier-Stokes, o comportamento de fluídos pode ser pensado como consequência da dinâmica de estruturas como vórtices, que irão gerar um campo de velocidades no fluído.

A aproximação 2-dimensional de um vórtice é aquilo a que geralmente se demonima vórtice pontual. O problema dos n vórtices no plano é portanto o problema de encontrar o comportamento de um sistema de n vórtices pontuais. Isto não é fácil, pois o problema é, em geral, não integrável para $n \geq 4$ e requer, portanto, uma abordagem numérica. Este problema tem sido cuidadosamente no caso não viscoso, mas não existe ainda uma teoria consistente para ambientes viscosos.

Esta dissertação foca-se na descrição dos vórtices pontuais em ambientes viscosos e não-viscosos e tenta extender a ideia de quantificação do caos de sistemas de vórtices não viscosos de Babiano et al. [1] para ambientes viscosos. Em particular, ver-se-á que a viscosidade pode destruir dinâmicas estáveis e fazer com que trajectórias inicialmente estáveis passem a ter comportamento caótico antes de sucumbir completamente aos efeitos da viscosidade. Vê-se ainda que os logaritmos da duração deste comportamento caótico e o coeficiente de viscosidade cinemática parecem estar ligados através de uma relação linear.

Palavras chave

Dinâmica de Fluídos, Equações de Navier-Stokes, Equações de Euler Incompressíveis, Dinâmica Hamiltoniana, Vórtices Pontuais, Vórtices Pontuais Viscosos, Caos, Expoentes de Lyapunov, Métodos Numéricos

Contents

List of Figures

Chapter 1.

Introduction

Even though we might not notice or think about it on our daily lives, we are surrounded by flows everywhere: the flow of water all around the world in rivers and oceans; the flow of water or gas in the pipes and canals that make their way to our homes so that we can live comfortably as we are used to; or even the simple flow of air that enables us to breath and live.

Fluid dynamics is the field of physics dedicated to the description of flows, be them liquids or gases - usually referred to as fluids - and therefore is a vast field of research that addresses a countless number of phenomena, many of them crucial to human life.

The motion of fluids is critical to understanding phenomena as varied as the pumping of blood in our body, weather forecasting or even more exotic systems like the galaxy mergers. Fluid dynamics is there, at motion, at completely different scales. Other than its' wide range of applications, it should be noted that fluid dynamics is behind one of the most relevant problems of nowadays: climate change. It is impossible to deny that our climate has been changing drastically in last few decades and that its' affecting the living conditions of our planet, as well as the planet itself. As such, it is imperative that we do something to preserve our planet and the well-being of humanity itself.

In order to address this issue, it is mandatory to have a better understanding of the underlying mechanisms that affect Earth's climate. At the heart of that, we will always find fluid dynamics.

Fluid dynamics' most important equations are the Navier-Stokes equations, which have no general analytical solution and are usually very difficult equations to solve, even numerically. Therefore, further studies in this area should always be a key priority to improve our knowledge on various kind of phenomena

that may turn out crucial to our welfare.

The aim of this dissertation is to study the basic concepts of fluid dynamics and try to shed light on an alternative description of fluids which evades the direct resolution of the Navier-Stokes equations: the point vortices description. The idea is to describe fluids through a quantity that measures the local rotation of the flow (the vorticity) by modeling the objects that in fact generate that rotation. The n-vortex problem has been thoroughly studied throughout the years for inviscid environments, however, there is yet much to be done in this alternate description when we add viscosity into the equations. We follow the idea of Babiano et al. [1] on using Lyapunov exponents to quantify chaos on inviscid point vortex models and extend the study to a viscous environment.

Chapter 2 gives a short review on the basic concepts of fluid dynamics, its' vorticity formulation, Hamiltonian dynamics and the concepts of chaos and Lyapunov exponents. Chapter 3 deals with flows in the infinite plane and the dynamics of point vortices both in inviscid and viscous environments. These theoretical results will then be used to validate the code developed for the numerical integration of the equations, which is presented in Chapter 4. In Chapter 5 we tackle a non-integrable system in both inviscid and viscous environments, compare the results and draw some conclusions in Chapter 6.

Chapter 2.

Theoretical Basis

When studying fluids, as in every other science that deals with real phenomena, one needs to take hints from Nature itself to start developing models that help understanding the mechanisms that drive the observable consequences. One of the most important hints to construct a theory that is able to accurately describe the dynamics of fluid motion is that the individual behavior of molecules in fluids seems to be irrelevant in the overall behavior of the system they comprise.

2.1 THE NAVIER-STOKES EQUATION

The first natural hypothesis to make in order to develop a theory that can mathematically describe these systems is that the fluid forms a continuum, where a point represents a small volume of the real fluid. Such a point is called a fluid element (also sometimes denominated fluid parcel). Figure 2.1 shows a schematic representation of a fluid element.

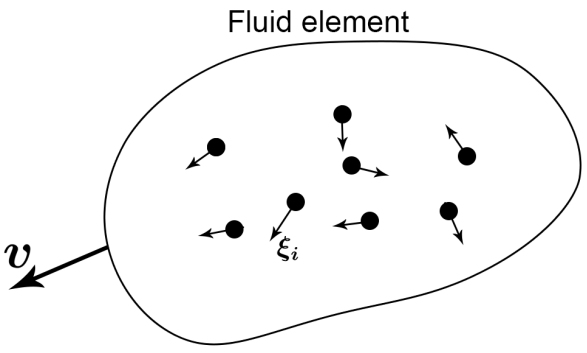

Figure 2.1: Schematic representation of a fluid element

Let the velocity $\boldsymbol{v}$ of a fluid element be defined by the velocities of the individual particles (noted $\boldsymbol{\xi_i},\ i = 1, 2, \dots$) that constitute that same fluid element at each time t as

$$\boldsymbol{v}\left(t, \boldsymbol{x}\left(t\right)\right) = \frac{1}{N\left(\boldsymbol{x}\left(t\right)\right)} \sum_{i=1}^{N(\boldsymbol{x}(t))} \boldsymbol{\xi_i}\left(\boldsymbol{x}\left(t\right)\right), \tag{2.1}$$

where $\boldsymbol{x}\left(t\right)$ denotes the position of the fluid element at time t and $N\left(\boldsymbol{x}\left(t\right)\right)$ is the number of particles inside the fluid element located at $\boldsymbol{x}\left(t\right)$. Using this description, one aims to describe the physical state of the fluid elements instead of individual molecules.

Consider a fluid element of volume V, with boundary ∂V. The mass of this fluid element will depend on the particles that constitute it at each time and, since the particles in it change in time, its' mass will also be time-varying. Assuming that the total mass of the system is conserved, the variation of mass inside a fluid element will be equal to the flux of mass that goes through its' boundary surface ∂V. Thus,

$$\frac{\partial m}{\partial t} = -\int_{\partial V} \rho \boldsymbol{v} \cdot \boldsymbol{n}\, dS, \tag{2.2}$$

where m is the mass, ρ is the density of the fluid element and $\boldsymbol{n}$ is the unit vector normal to the surface element dS. It is important to keep in mind that these quantities are time-dependent, but the explicit time dependence has been dropped in order to lighten notation. Since $m = \int_V \rho\, dV$ and using the divergence theorem, one can further write

$$\frac{\partial}{\partial t}\left(\int_V \rho\, dV\right) = -\int_{\partial V} \rho \boldsymbol{v} \cdot \boldsymbol{n}\, dS = -\int_V \nabla \cdot (\rho \boldsymbol{v})\ dV. \tag{2.3}$$

As ρ is a continuous and differentiable function, the integral and partial derivative can be interchanged, yielding

$$\int_V \left[\frac{\partial \rho}{\partial t} + \nabla \cdot (\rho \boldsymbol{v}) \right] dV = 0. \tag{2.4}$$

This must hold true for any volume V, therefore, in the limiting case where $V \to 0$ the integrand must be zero, which gives a continuity equation for the mass:

$$\frac{\partial \rho}{\partial t} + \nabla \cdot (\rho \boldsymbol{v}) = 0. \tag{2.5}$$

All fluids are compressible - their density changes due to variations in pressure and temperature - however, in a great number of situations, the changes in density are sufficiently negligible and can be ignored when modeling a flow in order to simplify the modeling of the system.

Definition 2.1.1 (Incompressible flow)**.** An incompressible flow is a flow in which each fluid element moving with the flow velocity does not expand nor compress.

From the definition of an incompressible flow, one has that the density of a fluid element moving with the flow velocity must remain constant in time: $\frac{d\rho}{dt} = 0$. For such a fluid element, making use of the continuity equation (2.5), it is possible to conclude easily that the divergence of the velocity field must be zero for any incompressible flow:

$$\frac{d\rho}{dt} = \frac{\partial \rho}{\partial t} + (\nabla \rho) \cdot \boldsymbol{v} = -\nabla \cdot (\rho \boldsymbol{v}) + (\nabla \rho) \cdot \boldsymbol{v} = -\rho \, (\nabla \cdot \boldsymbol{v}) = 0 \quad \Rightarrow \quad \nabla \cdot \boldsymbol{v} = 0. \tag{2.6}$$

Therefore, while there exist incompressible flows of compressible fluids, the reverse is not true: an incompressible fluid (characterized by having a constant density, i.e., $\frac{\partial \rho}{\partial t} = 0$) always undergoes an incompressible flow.

Consider once again the same fluid element with volume V. Since it is a part of some fluid, it should

be under the influence of both external volumetric and surface forces. Therefore, from Newton's Second Law of Motion, it is possible to write equations for each component of the total force as

$$\underbrace{\int_V F_i \, dV}_{\text{Total Volumetric Force}} + \underbrace{\int_{\partial V} T_i \, dS}_{\text{Total Superfical Force}} = \int_V \rho \, a_i \, dV, \tag{2.7}$$

where F_i represents the i^{th} component of the total volumetric force, T_i is the i^{th} component of the exerted tension and a_i is the i^{th} component of the acceleration. The exerted tensions T_i can be expressed, using the Einstein notation[1], as

$$T_i \left(\boldsymbol{x}_0, \boldsymbol{n} \right) = \tau_{ij} \left(\boldsymbol{x}_0 \right) n_j, \tag{2.8}$$

where τ is the tension tensor and τ_{ij} is the j^{th} component of the tension over the direction $\boldsymbol{e}_i$.

Using once again the divergence theorem, equation (2.7) can be re-written as

$$\begin{aligned} &\int_V F_i \, dV + \int_{\partial V} T_i \, dS = \int_V \rho \, a_i \, dV \Leftrightarrow \\ \Leftrightarrow &\int_V F_i \, dV + \int_{\partial V} \tau_{ij} n_j \, dS = \int_V \rho \, a_i \, dV \Leftrightarrow \\ \Leftrightarrow &\int_V \left[F_i + \partial_j \tau_{ij} \right] \, dV = \int_V \rho \, a_i \, dV \Leftrightarrow \\ \Leftrightarrow &\int_V \left[F_i + \tau_{ij,j} \right] \, dV = \int_V \rho \, a_i \, dV, \end{aligned} \tag{2.9}$$

where $\partial_i = \frac{\partial}{\partial x_i}$ and $\tau_{ij,j} = \partial_j \tau_{ij}$ for a more compact notation.

This last identity must hold true for any volume V, so, making $V \to 0$ results in $F_i + \tau_{ij,j} = \rho \, a_i$. If the fluid is at rest or if it is a perfect fluid[2] in movement, the exerted tension always has direction perpendicular to the fluid element, i.e., the tensions are purely normal; therefore one has $\tau_{ij} = -p\delta_{ij} \Rightarrow \tau_{ij,j} = -\partial_i p$, resulting in the vector equation

[1] Repeated indices in a single term imply summation over all possible values of that index

[2] A perfect fluid is one that can be completely characterized by density and pressure

$$-\nabla p + \boldsymbol{F} = \rho\, \boldsymbol{a}. \tag{2.10}$$

The set of equations

$$\begin{cases} -\nabla p + \boldsymbol{F} = \rho \dfrac{d\boldsymbol{v}}{dt} \\ \nabla \cdot \boldsymbol{v} = 0 \end{cases} \tag{2.11}$$

is usually known as the Euler Equations and is written in a Lagrangian coordinate system, where one must follow the movement of each particle in the fluid. This is not acceptable as there exists an enormous amount of particles in a fluid and it is impossible to follow each and every one of them. One work-around to this problem is to use an Eulerian coordinate system, describing the velocity of a particle at a certain position and at a certain time, regardless of which specific particle it actually is. As such, the Euler velocity can be defined as:

Definition 2.1.2 (Euler Velocity)**.** The Euler velocity, $\boldsymbol{u}(t, \boldsymbol{x})$, is the the velocity of any particle in the fluid that is located at position $\boldsymbol{x}$ at time t.

The Euler velocity can be related to the individual particle velocity $\boldsymbol{v}$ because $\boldsymbol{v}(t) = \boldsymbol{u}(t, \boldsymbol{x}(t))$ and $\boldsymbol{v}(t + \Delta t) = \boldsymbol{u}(t + \Delta t, \boldsymbol{x}(t + \Delta t)) = \boldsymbol{u}(t + \Delta t, \boldsymbol{x}(t) + \Delta \boldsymbol{x})$. As such,

$$\begin{aligned} \frac{d\boldsymbol{v}}{dt}(t) &= \lim_{\Delta t \to 0} \frac{\boldsymbol{v}(t + \Delta t) - \boldsymbol{v}(t)}{\Delta t} \\ &= \lim_{\Delta t \to 0} \frac{\boldsymbol{u}(t + \Delta t, \boldsymbol{x}(t) + \Delta \boldsymbol{x}) - \boldsymbol{u}(t, \boldsymbol{x}(t))}{\Delta t} \\ &= \lim_{\Delta t \to 0} \frac{\boldsymbol{u}(t + \Delta t, \boldsymbol{x}(t) + \Delta \boldsymbol{x}) - \boldsymbol{u}(t + \Delta t, \boldsymbol{x}(t))}{\Delta t} + \frac{\boldsymbol{u}(t + \Delta t, \boldsymbol{x}(t)) - \boldsymbol{u}(t, \boldsymbol{x}(t))}{\Delta t} \\ &= \underbrace{\lim_{\Delta t \to 0} \frac{\boldsymbol{u}(t + \Delta t, \boldsymbol{x}(t) + \Delta \boldsymbol{x}) - \boldsymbol{u}(t + \Delta t, \boldsymbol{x}(t))}{\Delta t}}_{\boldsymbol{L}} + \frac{\partial \boldsymbol{u}}{\partial t}(t, \boldsymbol{x}). \end{aligned} \tag{2.12}$$

And the i^{th} component of $\boldsymbol{L}$ can be expressed as

$$\begin{aligned} L_i &= \lim_{\Delta t \to 0} \frac{u_i\left(t+\Delta t, \boldsymbol{x}\right) + \left(\nabla u_i\left(t+\Delta t, \boldsymbol{x}\right)\right) \cdot \Delta \boldsymbol{x} + \mathcal{O}\left(\|\Delta \boldsymbol{x}\|^2\right) - u_i\left(t+\Delta t, \boldsymbol{x}\right)}{\Delta t} \\ &= \lim_{\Delta t \to 0} \frac{\left(\nabla u_i\left(t+\Delta t, \boldsymbol{x}\right)\right) \cdot \Delta \boldsymbol{x} + \mathcal{O}\left(\|\Delta \boldsymbol{x}\|^2\right)}{\Delta t} \\ &= \lim_{\Delta t \to 0} \nabla u_i\left(t+\Delta t, \boldsymbol{x}\right) \cdot \frac{\Delta \boldsymbol{x}}{\Delta t} + \frac{\mathcal{O}\left(\|\Delta \boldsymbol{x}\|^2\right)}{\Delta t} \\ &= \nabla u_i\left(t, \boldsymbol{x}\right) \cdot \boldsymbol{u}\left(t, \boldsymbol{x}\right) = \boldsymbol{u}\left(t, \boldsymbol{x}\right) \cdot \nabla u_i\left(t, \boldsymbol{x}\right). \end{aligned} \tag{2.13}$$

Therefore, $\boldsymbol{L} = \left(\boldsymbol{u} \cdot \nabla\right) \boldsymbol{u}$ and the Lagrangian and Eulerian velocities are related through

$$\frac{d\boldsymbol{v}}{dt} = \left(\frac{\partial}{\partial t} + \boldsymbol{u} \cdot \nabla\right) \boldsymbol{u}, \tag{2.14}$$

and thus, the Eulerian description of the fluid is given by the set of equations

$$\begin{cases} -\nabla p + \boldsymbol{F} = \rho \left[\dfrac{\partial \boldsymbol{u}}{\partial t} + \left(\boldsymbol{u} \cdot \nabla\right) \boldsymbol{u}\right] \\ \nabla \cdot \boldsymbol{u} = 0 \end{cases}. \tag{2.15}$$

If, however, the fluid is not at rest or if it moving but is not a perfect fluid, this description is not ideal, as it doesn't contemplate the existence of viscous forces. For the study of viscous fluids in movement, Taylor formulated 3 hypothesis:

1. The fluid is homogeneous and isotropic;
2. The tensor τ_{ij} depends on the deformation tensor $\tau_{ij} = \tau_{ij}\left(D_{kl}\right)$, where $D_{kl} = \frac{1}{2}\left(\frac{\partial v_k}{\partial x_l} + \frac{\partial v_l}{\partial x_k}\right)$;
3. When $\|\boldsymbol{v}\| \to 0, \quad \tau_{ij} \to -p\delta_{ij}$.

Expanding $\tau_{ij}\left(D_{kl}\right)$ in its' Taylor series gives

$$\begin{aligned}\tau_{ij} &= -p\delta_{ij} + \frac{\partial \tau_{ij}}{\partial D_{kl}} D_{kl} + \dots \\ &= -p\delta_{ij} + C_{ijkl} D_{kl} + \dots\end{aligned} \tag{2.16}$$

The most general expression for a fourth order tensor in an homogeneous and isotropic medium is given by [2] as being

$$C_{ijkl} = \lambda \delta_{ij}\delta_{kl} + \mu \left(\delta_{ik}\delta_{jl} + \delta_{il}\delta_{jk}\right), \tag{2.17}$$

where λ, $\mu \in \mathbb{R}$. To compute τ_{ij} notice first that

$$\begin{aligned}C_{ijkl} D_{kl} &= \left[\lambda \delta_{ij}\delta_{kl} + \mu \left(\delta_{ik}\delta_{jl} + \delta_{il}\delta_{jk}\right)\right] D_{kl} \\ &= \lambda \delta_{ij} D_{kk} + \mu \delta_{ik}\delta_{jl} D_{kl} + \mu \delta_{il}\delta_{jk} D_{kl} \\ &= \lambda \delta_{ij} D_{kk} + \mu D_{ij} + \mu D_{ji},\end{aligned} \tag{2.18}$$

$$D_{kk} = \frac{1}{2}\left(\frac{\partial v_k}{\partial x_k} + \frac{\partial v_k}{\partial x_k}\right) = \frac{\partial v_k}{\partial x_k} = v_{k,k} = \nabla \cdot \boldsymbol{v}. \tag{2.19}$$

Thus, since D_{ij} is symmetric, $C_{ijkl} D_{kl} = \lambda \delta_{ij} \nabla \cdot \boldsymbol{v} + 2\mu D_{ij}$ and since $\nabla \cdot \boldsymbol{v} = 0$ in an incompressible flow, the tension tensor can be expressed as $\tau_{ij} = -p\delta_{ij} + 2\mu D_{ij} + \dots$. Truncating this series at the first order term and calculating its' gradient in respect to j yields

$$\begin{aligned}\tau_{ij,j} &= -\partial_j p\delta_{ij} + 2\mu\partial D_{ij,j} \\ &= -\partial_j p\delta_{ij} + \mu\,[\,\underbrace{v_{i,jj}}_{(\nabla^2\boldsymbol{v})_i} + \underbrace{v_{j,ij}}_{[\nabla(\nabla\cdot\boldsymbol{v})]_i}\,] \\ &= -\partial_j p\delta_{ij} + \mu\, v_{i,jj}.\end{aligned} \tag{2.20}$$

Therefore, for a viscous and incompressible flow, one has

$$\begin{aligned}\tau_{ij,j} &= -\partial_i p + \mu\, v_{i,jj} \\ &= -\partial_i p + \mu\nabla^2 v_i,\end{aligned} \tag{2.21}$$

which, from Newton's Second Law of Motion, gives the equation of motion

$$\rho\frac{d\boldsymbol{v}}{dt} = -\nabla p + \mu\nabla^2\boldsymbol{v} + \boldsymbol{F}. \tag{2.22}$$

And in Eulerian coordinates, for an incompressible flow, this results in the well known Navier-Stokes equations:

$$\begin{cases}\dfrac{\partial\boldsymbol{u}}{\partial t} + (\boldsymbol{u}\cdot\nabla)\,\boldsymbol{u} = -\dfrac{1}{\rho}\nabla p + \nu\nabla^2\boldsymbol{u} + \dfrac{1}{\rho}\boldsymbol{F} \\ \nabla\cdot\boldsymbol{u} = 0\end{cases}, \tag{2.23}$$

where ν is the kinematic viscosity coefficient, which we'll refer to simply as viscosity hereafter (higher values of ν correspond to more viscous environments).

In 3 dimensions, any sufficiently smooth vector field that decays to zero rapidly enough at infinity can be decomposed in a solenoidal (divergence-free) and an irrotational (curl-free) component. This decomposition is due to Helmholtz [3] - and thereby usually called Helmholz decomposition. A proof of the theorem that gives this decomposition and an attempt of collecting the most common techniques for its' computation can be found in [4].

From this decomposition, if the conditions of Helmholtz's Theorem are met, the solution $\boldsymbol{u}$ to the

Navier-Stokes equations can then be written as

$$\boldsymbol{u} = \underbrace{\nabla \times \boldsymbol{\psi}}_{\text{divergence-less component}} + \underbrace{\nabla \varphi}_{\text{curl-less component}}, \tag{2.24}$$

where $\boldsymbol{\psi}$ is a solenoidal vector field and φ is a scalar field usually called the velocity potential. By calculating the divergence and curl of $\boldsymbol{u}$ it is possible to find differential equations for these two fields:

$$\nabla \cdot \boldsymbol{u} = \underbrace{\nabla \cdot (\nabla \times \boldsymbol{\psi})}_{0} + \nabla \cdot (\nabla \varphi) = 0 \quad \Leftrightarrow \quad \nabla^2 \varphi = 0, \tag{2.25}$$

$$\nabla \times \boldsymbol{u} = \nabla \times (\nabla \times \boldsymbol{\psi}) + \underbrace{\nabla \times (\nabla \varphi)}_{0} = \nabla \left(\underbrace{\nabla \cdot \boldsymbol{\psi}}_{0} \right) - \nabla^2 \boldsymbol{\psi} \quad \Leftrightarrow \quad \nabla^2 \boldsymbol{\psi} = -\nabla \times \boldsymbol{u}. \tag{2.26}$$

Notice that this decomposition isn't guaranteed to be unique. When dealing with incompressible flows in an unbound domain, if the velocity field $\boldsymbol{u}$ decays quickly to 0 at infinity, it is possible to prove that there exists a solenoidal vector field ψ such that the velocity field can be obtained directly from its' curl and therefore the curl-less component of this decomposition will be zero. Throughout the remainder of this work, the velocity field will be assumed to satisfy these conditions.

2.2 THE VORTICITY EQUATION

Many observed phenomena in Nature are easier to model or better explained in terms of the local rotation of the flow instead of the usual velocity field characterization. An alternate description of flows can therefore be derived for a quantity measuring this local rotation:

Definition 2.2.1. The vorticity of a flow is $\boldsymbol{\omega} \stackrel{\text{def}}{=} \nabla \times \boldsymbol{u}$ and quantifies the local rotation of the flow.

Some useful identities can be obtained by taking the divergence and curl of $\boldsymbol{\omega}$:

$$\begin{cases} \nabla \cdot \boldsymbol{\omega} = \nabla \cdot (\nabla \times \boldsymbol{u}) = 0 \\ \nabla \times \boldsymbol{\omega} = \nabla \times (\nabla \times \boldsymbol{u}) = \nabla \underbrace{(\nabla \cdot \boldsymbol{u})}_{0} - \nabla^2 \boldsymbol{u} = -\nabla^2 \boldsymbol{u} \end{cases}. \tag{2.27}$$

The first identity arises from the fact that the curl of any vector field is divergence-less and shows that the components of the vorticity are related in the same way as the components of the velocity of an incompressible flow; the second identity shows that each component of the velocity satisfies a Poisson equation.

Before deriving the equation that rules the time evolution of vorticity, it is worthy to mention another important quantity in fluid dynamics that is closely related to vorticity: the circulation.

Definition 2.2.2. The circulation of the fluid around a simple closed curve C is $\Gamma \stackrel{\text{def}}{=} \oint_C \boldsymbol{u} \cdot d\boldsymbol{s}$

By Stoke's Theorem, circulation can be directly related to vorticity:

$$\Gamma = \oint_C \boldsymbol{u} \cdot d\boldsymbol{s} = \int_S \boldsymbol{\omega} \cdot \boldsymbol{n} dS, \tag{2.28}$$

where S is the surface enclosed by the curve C. The equality between the two integrals in (2.28) gives rise to an alternative interpretation of the circulation as the flux of vorticity through the surface S. There is also an important result related to circulation, which is due to Lord Kelvin:

Theorem 2.2.1 (Kelvin's Circulation Theorem)**.** *In an ideal, incompressible fluid, if all forces acting on it are conservative, the circulation Γ around any closed material curve that is moving with the fluid is constant, i.e., $\frac{d\Gamma}{dt} = 0$.*

Proof. From the definition of the circulation and a curve moving with the fluid, one has

$$\frac{d\Gamma}{dt} = \frac{d}{dt}\left(\oint_C \boldsymbol{u} \cdot d\boldsymbol{s}\right) = \oint_C \frac{d\boldsymbol{u}}{dt} \cdot d\boldsymbol{s} + \oint_C \boldsymbol{u} \cdot d\boldsymbol{u}. \tag{2.29}$$

So, using the Navier-Stokes equation (2.23) for an inviscid[3] flow ($\nu = 0$) yields

$$\begin{aligned}\frac{d\Gamma}{dt} &= \oint_C \left(-\frac{1}{\rho}\nabla p + \frac{1}{\rho}\boldsymbol{F}\right)\cdot d\boldsymbol{s} + \oint_C \boldsymbol{u}\cdot d\boldsymbol{u} = \frac{1}{\rho}\oint_C (-\nabla p + \boldsymbol{F})\cdot d\boldsymbol{s} + \oint_C \boldsymbol{u}\cdot d\boldsymbol{u} \\ &= \frac{1}{\rho}\int_S (-\nabla\times\nabla p + \nabla\times\boldsymbol{F})\cdot\boldsymbol{n}\, dS + \frac{1}{2}\oint_C \nabla\left(|\boldsymbol{u}|^2\right)\cdot d\boldsymbol{s} \\ &= 0,\end{aligned} \tag{2.30}$$

because every term is zero: the gradient of any scalar function is always curl-less, the forces $\boldsymbol{F}$ are conservative (i.e., they can be written as a gradient of a scalar function) and the second integral is the integral of an exact differential over a closed loop.

■

As one may suppose, circulation is not conserved for flows of viscous fluids. In the viscous case, the extra term $-\nu\nabla^2\boldsymbol{u}$ in the Navier-Stokes equations originates a change in circulation over time:

$$\frac{d\Gamma}{dt} = \oint_C \left(-\nu\nabla^2\boldsymbol{u}\right)\cdot d\boldsymbol{s} = -\nu\oint_C \left(\nabla^2\boldsymbol{u}\right)\cdot d\boldsymbol{s} = -\nu\oint_C (\nabla\times\boldsymbol{\omega})\cdot d\boldsymbol{s}. \tag{2.31}$$

In order to get the vorticity description of a flow, one needs to re-write the Navier-Stokes equations in terms of the vorticity. This is readily done by taking the curl of the Navier-Stokes equations:

$$\begin{aligned} & \nabla\times\left(\frac{\partial\boldsymbol{u}}{\partial t} + (\boldsymbol{u}\cdot\nabla)\,\boldsymbol{u}\right) = \nabla\times\left(-\frac{1}{\rho}\nabla p + \nu\nabla^2\boldsymbol{u} + \frac{1}{\rho}\boldsymbol{F}\right) \Leftrightarrow \\ \Leftrightarrow\quad & \frac{\partial}{\partial t}(\nabla\times\boldsymbol{u}) + \nabla\times(\boldsymbol{u}\cdot\nabla)\,\boldsymbol{u} = -\frac{1}{\rho}\nabla\times\nabla p + \nu\nabla\times\nabla^2\boldsymbol{u} + \frac{1}{\rho}\nabla\times\boldsymbol{F} \Leftrightarrow \\ \Leftrightarrow\quad & \frac{\partial\boldsymbol{\omega}}{\partial t} + (\boldsymbol{u}\cdot\nabla)\,\boldsymbol{\omega} - (\boldsymbol{\omega}\cdot\nabla)\,\boldsymbol{u} = \nu\nabla^2\boldsymbol{\omega} + \frac{1}{\rho}\nabla\times\boldsymbol{F} \Leftrightarrow \\ \Leftrightarrow\quad & \frac{\partial\boldsymbol{\omega}}{\partial t} + (\boldsymbol{u}\cdot\nabla)\,\boldsymbol{\omega} = (\boldsymbol{\omega}\cdot\nabla)\,\boldsymbol{u} + \nu\nabla^2\boldsymbol{\omega} + \frac{1}{\rho}\nabla\times\boldsymbol{F}. \end{aligned} \tag{2.32}$$

[3] Viscous forces are not conservative in nature, so this result is not valid for viscous flows.

It should also be noted that it is in fact the vorticity that appears in the right-hand side of equation (2.26), so the solenoidal vector field $\boldsymbol{\psi}$ is directly related to the vorticity: $\nabla^2\boldsymbol{\psi} = -\boldsymbol{\omega}$. This gives a Poisson equation for each component of $\boldsymbol{\psi}$ that can be solved through the usual techniques; its' solution can be written formally in terms of the Green's Function for the Laplacian as

$$\boldsymbol{\psi}(\boldsymbol{r}) = \int G(\boldsymbol{r} - \boldsymbol{r_0})\,\boldsymbol{\omega}(\boldsymbol{r_0})\,d\boldsymbol{r_0}. \tag{2.33}$$

The Green's function $G(\boldsymbol{r})$ will depend on the geometry of the space we are solving the equation in. For the unbound spaces $\mathbb{R}^2$ and $\mathbb{R}^3$ one has:

$$G(\boldsymbol{r}) = \begin{cases} -\dfrac{1}{2\pi}\log\|\boldsymbol{r}\|, & \text{in } \mathbb{R}^2 \\ \dfrac{1}{4\pi\|\boldsymbol{r}\|}, & \text{in } \mathbb{R}^3 \end{cases}. \tag{2.34}$$

Hence, for an incompressible flow, the velocity field at each time can be computed easily provided one knows the vorticity field:

$$\boldsymbol{u}(\boldsymbol{r}) = \nabla \times \boldsymbol{\psi}(\boldsymbol{r}) = \nabla \times \int G(\boldsymbol{r} - \boldsymbol{r_0})\,\boldsymbol{\omega}(\boldsymbol{r_0})\,d\boldsymbol{r_0} = \int \nabla G(\boldsymbol{r} - \boldsymbol{r_0}) \times \boldsymbol{\omega}(\boldsymbol{r_0})\,d\boldsymbol{r_0}. \tag{2.35}$$

An alternative way to express the velocity field in matricial form is

$$\boldsymbol{u}(\boldsymbol{r}) = \int \boldsymbol{K}(\boldsymbol{r} - \boldsymbol{r_0})\,\boldsymbol{\omega}(\boldsymbol{r_0})\,d\boldsymbol{r_0}, \tag{2.36}$$

where $K(\boldsymbol{r})$ is the Biot-Savart Kernel, defined as usual:

$$\boldsymbol{K}(\boldsymbol{r}) = \begin{cases} \dfrac{1}{2\pi\|\boldsymbol{r}\|^2}(-y, x), & \text{in } \mathbb{R}^2 \\ \dfrac{1}{4\pi\|\boldsymbol{r}\|^3}\begin{pmatrix} 0 & z & -y \\ -z & 0 & x \\ y & -x & 0 \end{pmatrix}, & \text{in } \mathbb{R}^3 \end{cases}. \tag{2.37}$$

2.3 POINT VORTICES

Consider some vorticity field in a 3-dimensional fluid. Any curve that is everywhere tangent to the local vorticity vectors named vortex line. Furthermore, the vortex lines passing through any closed curve in the fluid form a tubular surface that is called a vortex tube. Vortex tubes can therefore be defined by the equation $\boldsymbol{\omega} \cdot \boldsymbol{n} = 0$. The strength of a vortex tube is defined as the circulation of any closed loop on the vortex tube that circles it only once; thus, the strength of a vortex tube is the same along the whole tube and from Kelvin's Circulation Theorem, it is possible to conclude that for an inviscid, ideal and incompressible fluid, vortex tubes' strength does not change in time. Hence, these tubes must be closed, extend into infinity or terminate at solid boundaries or fluid-fluid interfaces. In the viscous case, however, viscosity creates changes in the strength of a vortex tube over time and therefore it may change its' geometric configuration. If a vortex tube is surrounded by irrotational fluid, it is usually called a vortex filament.

A vortex filament in the 3-dimensional space, by definition, usually has a small cross section in comparison to it's curvature. Making a cut in a plane that is locally orthogonal to the vortex filament, will result in a 2-dimensional vorticity distribution that is highly concentrated in the vicinity of the centerline of the filament. For such an object, if the centerline of the filament is localized at a point $\boldsymbol{r_0}$ in the plane, one can usually assume that the vorticity field has radial symmetry and is of the form

$$\omega(\boldsymbol{r}) = \frac{\Gamma}{2\pi}\phi_\epsilon(\boldsymbol{r} - \boldsymbol{r_0}), \tag{2.38}$$

where $\phi_\epsilon(\boldsymbol{r}) = \phi(\boldsymbol{r}/\epsilon)/\epsilon$ and ϕ is a suitable radially symmetric function such that its' integral over all space equals 1.

The limiting case $\epsilon \to 0$ is what it is usually called a point vortex, where the vorticity is completely concentrated in one point in space. Mathematically this corresponds to choosing $\phi_\epsilon = \delta(\boldsymbol{r})$, the usual Dirac-delta function.

Hence, it should be useful to investigate the the simplified 2-dimensional problem to try and understand the dynamics of the vortex filaments and the velocity fields produced by them. The vorticity equation (2.32) simplifies to a scalar equation because $\boldsymbol{\omega} = \omega\, \boldsymbol{e_3}$ and the $(\boldsymbol{\omega} \cdot \nabla)\, \boldsymbol{u}$ term vanishes. In a system where no external forces are applied the 2D vorticity equation becomes

$$\frac{\partial \omega}{\partial t} + (\boldsymbol{u} \cdot \nabla)\, \omega = \nu \nabla^2 \omega. \tag{2.39}$$

So, while in the inviscid case, vorticity is conserved throughout the trajectory of a fluid element $\left(\frac{d\omega}{dt} = 0\right)$, it is dissipated in the viscous case due to the viscosity term in the equation.

The Poisson equation (2.26) will also simplify to a scalar equation as the first and second components of $\boldsymbol{\psi}$ will always be zero. The function $\psi = \boldsymbol{\psi} \cdot \boldsymbol{e_3}$ in the 2-dimensional case is usually called the stream function of the flow and can be used to compute the velocity field easily because of its' direct relation with velocity:

$$\boldsymbol{u} = \left(\frac{\partial \psi}{\partial y}, -\frac{\partial \psi}{\partial x}\right). \tag{2.40}$$

Therefore, since the equation of a particle moving in the fluid is given by $\dot{\boldsymbol{r}} = (\dot{x}, \dot{y}) = \boldsymbol{u}$, it is possible to see that this is an Hamiltonian system, as this is the form of Hamilton's equations:

$$\begin{cases} \dot{x} = \dfrac{\partial H}{\partial y} \\ \dot{y} = -\dfrac{\partial H}{\partial x} \end{cases}. \tag{2.41}$$

So, the stream function here plays the role of the Hamiltonian H in Hamiltonian dynamics, while the coordinates x, y play the role of the canonically conjugate variables in this formalism.

Remark: In fluid dynamics it's usual to express the equations in terms of the Reynolds Number, Re. The Reynolds Number gives the ratio of inertial forces to viscous forces within a fluid and is defined as $Re = \frac{uL}{\nu}$, where u and L are characteristic velocities and linear dimension of the problem in hand. It is usual to take both of these to be 1, yielding $Re = \frac{1}{\nu}$ and allowing the equations of fluid dynamics to be written in dimensionless form.

2.4 HAMILTONIAN DYNAMICS

This section gives a summary of some important results of Hamiltonian Dynamics that will be useful in the subsequent analysis of the problems in hand. For an extensive discussion of Lagrangian and Hamiltonian Dynamics one can find the works of Goldstein [5] or (for a more advanced and deeper presentation) Arnold [6] very useful.

The Hamiltonian Dynamics approach is a reformulation of classical mechanics, making use of a different and more powerful - yet more abstract - mathematical formalism. The predictions of classical physical systems remain the same in this context, yet it opened way to later developing theories such as Quantum Physics, which can not be described by a classical approach.

The original formulation of Hamiltonian Dynamics rests in two fundamental principles:

- One should try to express the state of a physical system with the minimum number of variables possible;
- A physical system always tries to minimize its' action at each instant.

The action of a system is a functional of a function usually called the Lagrangian: a function that

contains the information about the dynamics of the physical system. This function is usually given in terms of some generalized coordinates $\boldsymbol{q} \in \mathbb{R}^n$ and their time derivatives; the usual notation for a Lagrangian is $L(\boldsymbol{q}, \dot{\boldsymbol{q}}, t)$. Therefore, the action S between two time instants t_1 and t_2 is

$$S[\boldsymbol{q}] \stackrel{\text{def}}{=} \int_{t_1}^{t_2} L(\boldsymbol{q}, \dot{\boldsymbol{q}}, t)\, dt. \tag{2.42}$$

The second fundamental principal of Hamiltonian Dynamics, usually called Hamilton's Principle can therefore be expressed as

$$\frac{\delta S}{\delta q_k(t)} = 0, \quad k = 1, \ldots, n. \tag{2.43}$$

The Lagrangian can take many forms, depending of the system which one is trying to model; it is, however, possible to give general expressions of the Lagrangian for a vast kind of systems that share a set of properties. For example, for a non-relativistic system of particles, the Lagrangian can be simply written as the difference between the kinetic and potential energy (T and V, respectively) of the system: $L = T - V$.

From Hamilton's Principle it is possible to deduce a set of equations of motion for the system, called the Euler-Lagrange equations:

$$\frac{d}{dt}\left(\frac{\partial L}{\partial \dot{q}_k}\right) - \frac{\partial L}{\partial q_k} = 0, \quad k = 1, \ldots, n. \tag{2.44}$$

The core function of Hamiltonian dynamics is, in fact, the Hamiltonian, which is defined as the Legendre transform of the Lagrangian. Using the generalized momenta $p_k = \frac{\partial L}{\partial \dot{q}_k}$, one can write

$$H\left(\boldsymbol{q},\boldsymbol{p},t\right)=\sum_{k=1}^{n}p_k\dot{q_k}-L\left(\boldsymbol{q},\dot{\boldsymbol{q}},t\right). \tag{2.45}$$

Like the Lagrangian, the Hamiltonian can have different forms depending on the physical system under study; for a non-relativistic system of particles for which the Lagrangian does not explicitly depend on time, however, the Hamiltonian takes again a simple form, as the sum of kinetic and potential energies: $H=T+V$.

To get Hamilton's equations one must first write the total differential of the Lagrangian and do some manipulations:

$$\begin{aligned}
& dL=\sum_{k=1}^{n}\left(\frac{\partial L}{\partial q_k}dq_k+\frac{\partial L}{\partial \dot{q_k}}d\dot{q_k}\right)+\frac{\partial L}{\partial t}dt && \Leftrightarrow \\
\Leftrightarrow\quad & dL=\sum_{k=1}^{n}\left(\frac{\partial L}{\partial q_k}dq_k+p_k d\dot{q_k}\right)+\frac{\partial L}{\partial t}dt && \Leftrightarrow \\
\Leftrightarrow\quad & dL=\sum_{k=1}^{n}\left(\frac{\partial L}{\partial q_k}dq_k+d\left(p_k\dot{q_k}\right)-\dot{q_k}dp_k\right)+\frac{\partial L}{\partial t}dt && \Leftrightarrow \\
\Leftrightarrow\quad & \underbrace{d\left(\sum_{k=1}^{n}p_k\dot{q_k}-L\right)}_{dH}=\sum_{k=1}^{n}\left(-\frac{\partial L}{\partial q_k}dq_k+\dot{q_k}dp_k\right)-\frac{\partial L}{\partial t}dt.
\end{aligned} \tag{2.46}$$

Comparing the coefficients from the total differential of the Hamiltonian

$$dH=\sum_{k=1}^{n}\left(\frac{\partial H}{\partial q_k}dq_k+\frac{\partial H}{\partial p_k}dp_k\right)+\frac{\partial H}{\partial t}dt, \tag{2.47}$$

and using the Euler-Lagrange equations (2.44), one arrives at the canonical form of Hamilton's equations:

$$\dot{q_k}=\frac{\partial H}{\partial p_k},\qquad \dot{p_k}=-\frac{\partial H}{\partial q_k}. \tag{2.48}$$

Noether's Theorem is a key result in Hamiltonian Dynamics that can help to classify and solve the equations of Hamiltonian systems. This theorem states that to every continuous symmetry in a system, there corresponds a conserved quantity of the system. Noether's Theorem is usually given in the Lagrangian formulation and can be formulated mathematically as follows

Theorem 2.4.1 (Noether's Theorem)**.** *Given the infinitesimal transformations (*$|\epsilon| << 1$*)*

$$\begin{aligned} t \to t' &= t + \epsilon X\left(q\left(t\right), t\right), \\ q_k \to q'_k &= q_k + \epsilon \psi_k\left(q\left(t\right), t\right), \quad k = 1, \ldots, n \end{aligned} \tag{2.49}$$

where X *and* ψ *are some functions of* q *and* t*, if the action remains invariant, then the quantity*

$$Q = \sum_{k=1}^{n} \frac{\partial L}{\partial \dot{q}_k}\left(\dot{q}_k X - \psi\right) - XL \tag{2.50}$$

is conserved throughout the dynamics of the system.

Proof. Suppose the system undergoes some infinitesimal transformations like the ones defined in the statement of the theorem. From them, one has

$$\begin{aligned} \frac{dt'}{dt} &= 1 + \epsilon \dot{X} \\ \frac{dq'_k\left(t\right)}{dt'} = \frac{dq_k}{dt}\frac{dt}{dt'} &= \frac{\dot{q}_k + \epsilon \dot{\psi}_k}{1 + \epsilon \dot{X}} = \left(\dot{q}_k + \epsilon \dot{\psi}_k\right)\left(1 - \epsilon \dot{X} + \mathcal{O}\left(\epsilon^2\right)\right) \\ &= \dot{q}_k + \epsilon \underbrace{\left(\dot{\psi}_k - \dot{q}_k \dot{X}\right)}_{\xi_k} + \mathcal{O}\left(\epsilon^2\right). \end{aligned} \tag{2.51}$$

By keeping only the terms which are of first order in ϵ, one can write the change in the action due to these infinitesimal transformation as

$$\begin{aligned}
\delta S &= \int_{t_1'}^{t_2'} L\left(\boldsymbol{q}+\epsilon\boldsymbol{\psi}, \dot{\boldsymbol{q}}+\epsilon\boldsymbol{\xi}, t+\epsilon X\right)(1+\epsilon X)\, dt - \int_{t_1}^{t_2} L\left(\boldsymbol{q}, \dot{\boldsymbol{q}}, t\right) dt \\
&= \int_{t_1}^{t_2} \left[L\left(\boldsymbol{q}+\epsilon\boldsymbol{\psi}, \dot{\boldsymbol{q}}+\epsilon\boldsymbol{\xi}, t+\epsilon X\right) - L\left(\boldsymbol{q}, \dot{\boldsymbol{q}}, t\right)\right] dt + \epsilon \int_{t_1}^{t_2} \dot{X} L\left(\boldsymbol{q}+\epsilon\boldsymbol{\psi}, \dot{\boldsymbol{q}}+\epsilon\boldsymbol{\xi}, t+\epsilon X\right) dt \\
&= \int_{t_1}^{t_2} \left[\frac{L\left(\boldsymbol{q}', \dot{\boldsymbol{q}}', t'\right) - L\left(\boldsymbol{q}', \dot{\boldsymbol{q}}', t\right)}{\epsilon X}\epsilon X + \sum_{k=1}^{n} \frac{L\left(q_k', \dot{q}_k', t\right) - L\left(q_k', \dot{q}_k, t\right)}{\epsilon \xi_k}\epsilon\xi_k \right. \\
&\quad \left. + \sum_{k=1}^{n} \frac{L\left(q_k', \dot{q}_k, t\right) - L\left(q_k, \dot{q}_k, t\right)}{\epsilon \psi_k}\epsilon\psi_k + \epsilon \dot{X} L\left(\boldsymbol{q}', \dot{\boldsymbol{q}}', t'\right)\right] dt \\
&= 0.
\end{aligned} \tag{2.52}$$

So, when $\epsilon \to 0$, since this should hold true for any times t_1 and t_2,

$$\begin{aligned}
& X\frac{\partial L}{\partial t} + \sum_{k=1}^{n} \frac{\partial L}{\partial \dot{q}_k}\left(\dot{\psi}_k - \dot{q}_k \dot{X}\right) + \sum_{k=1}^{n} \frac{\partial L}{\partial q_k}\psi_k + \dot{X} L = 0 \quad \Leftrightarrow \\
\Leftrightarrow \quad & \dot{X}\left(L - \sum_{k=1}^{n} \dot{q}_k \frac{\partial L}{\partial \dot{q}_k}\right) + X\frac{\partial L}{\partial t} + \sum_{k=1}^{n}\left[\psi_k \frac{\partial L}{\partial q_k} + \dot{\psi}_k \frac{\partial L}{\partial \dot{q}_k}\right] = 0 \quad \Leftrightarrow \\
\Leftrightarrow \quad & \dot{X}\left(L - \sum_{k=1}^{n} \dot{q}_k \frac{\partial L}{\partial \dot{q}_k}\right) + X\frac{\partial L}{\partial t} + \sum_{k=1}^{n}\left[\psi_k \frac{d}{dt}\left(\frac{\partial L}{\partial \dot{q}_k}\right) + \dot{\psi}_k \frac{\partial L}{\partial \dot{q}_k}\right] = 0 \quad \Leftrightarrow \\
\Leftrightarrow \quad & \dot{X}\left(L - \sum_{k=1}^{n} \dot{q}_k \frac{\partial L}{\partial \dot{q}_k}\right) + X\frac{d}{dt}\left[L - \sum_{k=1}^{n} \dot{q}_k \frac{\partial L}{\partial \dot{q}_k}\right] + \sum_{k=1}^{n}\left[\psi_k \frac{d}{dt}\left(\frac{\partial L}{\partial \dot{q}_k}\right) + \dot{\psi}_k \frac{\partial L}{\partial \dot{q}_k}\right] = 0 \quad \Leftrightarrow \\
\Leftrightarrow \quad & \frac{d}{dt}\left[X\left(L - \sum_{k=1}^{n} \dot{q}_k \frac{\partial L}{\partial \dot{q}_k}\right) - \sum_{k=1}^{n} \psi_k \frac{\partial L}{\partial \dot{q}_k}\right] = 0 \\
\Leftrightarrow \quad & \frac{d}{dt}\left[\sum_{k=1}^{n} \frac{\partial L}{\partial \dot{q}_k}\left(\dot{q}_k X - \psi\right) - XL\right] = 0
\end{aligned} \tag{2.53}$$

and therefore $Q = \sum_{k=1}^{n} \frac{\partial L}{\partial \dot{q}_k}\left(\dot{q}_k X - \psi\right) - XL$ is an invariant of the system.

■

More general and complex formulations of Noether's Theorem exist; one of them makes use of a quantity that is fundamental in Hamiltonian Dynamics: the Poisson Bracket. This quantity can also be a useful tool to identify conserved quantities of Hamiltonian Systems, even without making explicit use of Noether's Theorem.

Definition 2.4.1 (Canonical Poisson Bracket)**.** Consider two functions of class C^1: $f\left(\boldsymbol{q}, \boldsymbol{p}, t\right)$ and

$g(\boldsymbol{q}, \boldsymbol{p}, t)$, defined on the $2n$ phase space. Their Canonical Poisson Bracket is defined as

$$\{f, g\} \stackrel{\text{def}}{=} \sum_{k=1}^{n} \left(\frac{\partial f}{\partial q_k} \frac{\partial g}{\partial p_k} - \frac{\partial f}{\partial p_k} \frac{\partial g}{\partial q_k} \right). \tag{2.54}$$

The Poisson Bracket has some useful properties which have straightforward proofs (it suffices to use the definition and properties of the derivatives):

1. $\{f, g\} = -\{g, f\}$
2. $\{f + g, h\} = \{f, h\} + \{g, h\}$
3. $\{f, \{g, h\}\} + \{g, \{h, f\}\} + \{h, \{f, g\}\} = 0$ (Jacobi's identity)
4. $\{fg, h\} = f\{g, h\} + g\{f, h\}$ (Leibniz identity)

Remark: The first three identities define a Lie algebra.

Definition 2.4.2. Two functions are said to be in involution with one another (or to Poisson commute) if the Poisson bracket between them is zero.

If one takes the full time derivative of a C^1 function $f(\boldsymbol{q}, \boldsymbol{p}, t)$, one gets

$$\begin{aligned} \frac{df}{dt} &= \sum_{k=1}^{n} \left(\frac{\partial f}{\partial q_k} \frac{\partial q_k}{\partial t} + \frac{\partial f}{\partial p_k} \frac{\partial p_k}{\partial t} \right) + \frac{\partial f}{\partial t} = \\ &= \sum_{k=1}^{n} \left(\frac{\partial f}{\partial q_k} \frac{\partial H}{\partial p_k} - \frac{\partial f}{\partial p_k} \frac{\partial H}{\partial q_k} \right) + \frac{\partial f}{\partial t} = \\ &= \{f, H\} + \frac{\partial f}{\partial t} \end{aligned} \tag{2.55}$$

and therefore, for a system characterized by the Hamiltonian H, f is a conserved quantity if it is time-independent and is in involution with the Hamiltonian. Furthermore, if one knows two conserved quantities in some Hamiltonian system, it is possible to generate further conserved quantities by the following result:

Theorem 2.4.2. *Given two C^1 functions f and g that are conserved quantities in an Hamiltonian system, $\{f, g\}$ is also a conserved quantity.*

Proof. From Jacobi's identity, $\left\{ f, \underbrace{\{g, H\}}_{0} \right\} + \left\{ g, \underbrace{\{H, f\}}_{0} \right\} + \{H, \{f, g\}\} = 0 \Rightarrow \{H, \{f, g\}\} = 0.$

■

Remark: The above theorem does not guarantee that the conserved quantity $\{f, g\}$ is a new one.

The Hamiltonian statement of Noether's Theorem makes use of the Poisson Bracket formalism, which seems natural, as the Poisson Bracket is closely connect to conserved quantities. However, in order to derive Noether's Theorem in the Hamiltonian formalism, one needs an extra definition:

Definition 2.4.3. A canonical transformation of coordinates and momenta is a transformation that preserves the form of Hamilton's equations.

Equivalently, one can say that a transformation from $(\boldsymbol{q}, \boldsymbol{p})$ to $(\boldsymbol{Q}, \boldsymbol{P})$ is canonical if their Poisson Brackets are preserved. Infinitesimal canonical transformations can be expressed in terms of a generating function on the phase space. The details of these infinitesimal transformations and their generating functions are out of the scope of this work; however, it should be useful to have in mind that these generating functions are what actually links symmetries and conserved quantities in Hamiltonian systems:

Theorem 2.4.3 (Alternate form of Noether's Theorem)**.** *Q is a conserved quantity of a system described by the Hamiltonan H if and only if Q generates some continuous symmetry of the Hamiltonan.*

Proof (sketch). The change in some observable g due to the symmetry generated by Q can be written as $\delta g = \{g, Q\}$. Since the Hamiltonan is invariant under a symmetry, it holds that $\delta H = \{H, Q\} = 0$. As the Poisson bracket is anti-symmetric, one must have $0 = \{Q, H\} = \dot{Q}$, therefore Q is a conserved quantity of the system.

■

For a deeper analysis on the concepts of canonical transformations and their connection to Poisson brackets and conserved quantities, refer to the already mentioned works of Goldstein [5] and Arnold [6]. Furthermore, Struckmeier's work [7] generalizes Noether's Theorem in the framework of Hamiltonian point dynamics by putting the time and space variables on equal footing and extending the usual set of canonical transformations to include transformations that also map time and energy.

2.5 CHAOS AND LYAPUNOV EXPONENTS

A chaotic system is essentially characterized by its' non predictability, meaning that it is impossible to know its' time evolution for some generic initial condition. Lyapunov exponents are quantities that can help to quantify chaos. They measure the rates of divergence or convergence of nearby trajectories in phase space: a negative Lyapunov exponent means that trajectories approach one another, while a positive one indicates the divergence of the nearby orbits and therefore chaotic behavior (a zero Lyapunov exponent means that the nearby trajectories maintain their distance).

If one considers a ball of points in the n-dimensional phase space - corresponding to nearby configurations of the system - and let it evolve through the system's dynamical equations, after some time that ball of points will either maintain its' form, shrink and (eventually) collapse to a single point or become distorted in some direction(s) becoming somewhat ellipsoidal. In fact, the Lyapunov exponents measure the expansions and contractions of this ball of points in phase space, and therefore there are n Lyapunov exponents in a system with a n-dimensional phase space.

Consider a system ruled by some equation $\dot{\boldsymbol{x}} = f(\boldsymbol{x})$, where x_k, $k = 1, \ldots, n$ are the state-space variables and a trajectory $\boldsymbol{x}(t)$ of this system. Furthermore, consider a second trajectory, $\tilde{\boldsymbol{x}}(t)$, close to the latter, such that $\boldsymbol{\delta} = \tilde{\boldsymbol{x}} - \boldsymbol{x}$ at some point in time, with $|\boldsymbol{\delta}| << 1$. The dynamics of the separation $\boldsymbol{\delta}$ should then follow

$$\begin{aligned} \dot{\boldsymbol{\delta}} &= f(\tilde{\boldsymbol{x}}) - f(\boldsymbol{x}) \\ &= f(\boldsymbol{x}) + Df(\boldsymbol{x})\,\boldsymbol{\delta} - f(\boldsymbol{x}) + \mathcal{O}\left(|\boldsymbol{\delta}|^2\right) \\ &= Df(\boldsymbol{x})\,\boldsymbol{\delta} + \mathcal{O}\left(|\boldsymbol{\delta}|^2\right). \end{aligned} \tag{2.56}$$

Letting $\boldsymbol{\delta} \to \mathbf{0}$ and denoting $J_f(\boldsymbol{x}) = Df(\boldsymbol{x})\,\boldsymbol{\delta}$ for the Jacobian matrix, one finds the dynamical equation for the separation $\boldsymbol{\delta}$:

$$\dot{\boldsymbol{\delta}} = J_f(\boldsymbol{x})\,\boldsymbol{\delta}. \tag{2.57}$$

Thus, integrating this equation throughout the trajectory $\boldsymbol{x}(t)$ yields the time evolution of the separation vector,

$$\boldsymbol{\delta}(t) = M(t)\,\boldsymbol{\delta}(0), \tag{2.58}$$

for some matrix $M(t)$. It is also possible to get the dynamical equation that describes the time evolution of M by differentiating (2.58) and using (2.57):

$$\dot{M} = J_f(\boldsymbol{x})\,M. \tag{2.59}$$

Computing M requires, therefore, the joint integration of $\dot{\boldsymbol{x}} = f(\boldsymbol{x})$ and $\dot{M} = J_f(\boldsymbol{x})\,M$, which is usually a difficult analytical task.

Now, consider a small ball of points in state-space such that $|\boldsymbol{\delta}(0)|^2 = \delta_0^2 \in \mathbb{R}^+$ around the initial point $\boldsymbol{x}(0)$ of some trajectory $\boldsymbol{x}(t)$. After some time t, each of the initial separations on the small ball will have evolved into $\boldsymbol{\delta}(t) = M(t)\,\boldsymbol{\delta}(0)$. If M is invertible, from the identity $\boldsymbol{\delta}^T(0)\,\boldsymbol{\delta}(0) = \delta_0^2$, one can write

$$\begin{aligned} &\boldsymbol{\delta}^T(t)\,M^{-T}(t)\,M^{-1}(t)\,\boldsymbol{\delta}(t) = \delta_0^2 \quad \Leftrightarrow \\ \Leftrightarrow \quad &\boldsymbol{\delta}^T(t)\,G(t)\boldsymbol{\delta}(t) = 1, \end{aligned} \tag{2.60}$$

where $G(t) = \delta_0^{-2} M^{-T}(t)\,M^{-1}(t)$ is a positive definite matrix. This equation defines the surface of an

ellipsoid with principal axes given by the eigenvectors of G, each of them with semi-axis length $g_k^{-1/2}$, where g_k is the eigenvalue associated to the k^{th} eigenvector of G. One can consider the singular value decomposition of M to gain more insight on how its' eigenvalues are connected with the eigenvalues of G. Let $M = USV^T$, where U and V are orthogonal matrices ($UU^T = VV^T = id$) and S is a diagonal matrix with elements s_k, $k = 1, \ldots, n$ on the diagonal. One can easily compute that $M^T M = VS^2V^T$ and $MM^T = US^2U^T$. Therefore $M^T M$ and MM^T have the same set of eigenvalues which are the squares of the entries of the diagonal of S. Furthermore, one can write

$$G = \delta_0^{-2} M^{-T} M^{-1} = \delta_0^{-2} \left(MM^T\right)^{-1} = \delta_0^{-2} \left(US^2U^T\right)^{-1} = \delta_0^{-2} \left(US^{-2}U^T\right). \tag{2.61}$$

So, the spectrum of G is $\left\{\delta_0^{-2} s_k^{-2},\, k = 1, \ldots, n\right\}$ and one can conclude that M transforms the ball of points of radius δ_0 into an ellipsoid with semi-axis of lengths $g_k^{-1/2} = \delta_0 s_k$, $k = 1, \ldots, n$.

From the eigenvalues of $M^T M$ one can define mathematically the Lyapunov exponents:

Definition 2.5.1 (Lyapunov Exponents)**.** Given a system ruled by an equation $\dot{\boldsymbol{x}} = f(\boldsymbol{x})$, a trajectory $\boldsymbol{x}(t)$ and a matrix M as defined above such that the spectrum of $M^T M$ is $\{s_k^2,\, k = 1, \ldots, n\}$, the Lyapunov exponents of $\boldsymbol{x}(t)$ are the quantities

$$\lambda_k = \lim_{t \to \infty} \frac{1}{t} \log |s_k|. \tag{2.62}$$

Remark: Lyapunov exponents are usually ordered from the largest to the smallest: $\lambda_1 \geq \lambda_2 \geq \cdots \geq \lambda_n$.

In order to connect the definition of the Lyapunov exponents to their physical meaning, consider the quantity $\frac{1}{t} \log \frac{|\boldsymbol{\delta}(t)|}{|\boldsymbol{\delta}(0)|}$:

$$\frac{1}{t} \log \frac{|\boldsymbol{\delta}(t)|}{|\boldsymbol{\delta}(0)|} = \frac{1}{t} \log \frac{\left(\boldsymbol{\delta}^T(t)\, \boldsymbol{\delta}(t)\right)^{1/2}}{\delta_0} = \frac{1}{2t} \log \frac{\boldsymbol{\delta}_0^T M^T M \boldsymbol{\delta}_0}{\delta_0^2}, \tag{2.63}$$

since $M^T M$ and MM^T have the same eigenvalues, one can conclude that the eigenvalues of $M^T M$ are

$\left\{g_k^{-1}\delta_0^{-2},\, k=1,\ldots,n\right\}$ from the fact that $G^{-1}=\delta_0^2 MM^T$. Therefore, for a separation vector $\boldsymbol{\delta}_0$ in the direction of the k^{th} eigenvector of M^TM, one has

$$\frac{1}{t}\log\frac{|\boldsymbol{\delta}\,(t)\,|}{|\boldsymbol{\delta}\,(0)\,|}=\frac{1}{2t}\log\frac{\boldsymbol{\delta}_0^T g_k^{-1}\delta_0^{-2}\boldsymbol{\delta}_0}{\delta_0^2}=\frac{1}{2t}\log s_k^2=\frac{1}{t}\log|s_k|. \tag{2.64}$$

Taking the limit $t\to\infty$, one retrieves the definition of the k^{th} Lyapunov exponent. So, Lyapunov exponents should be related to the time evolution of the separations between close trajectories. The largest Lyapunov exponent, λ_1, is the easiest to interpret: one has that for an initial separation $\boldsymbol{\delta}_0$ in the direction of largest growth, $\lambda_1=\lim_{t\to\infty}\frac{1}{t}\log\frac{|\boldsymbol{\delta}(t)|}{|\boldsymbol{\delta}(0)|}$. This is equivalent to assuming that nearby trajectories diverge (or converge) at an exponential rate $|\boldsymbol{\delta}\,(t)\,|\sim|\boldsymbol{\delta}\,(0)\,|e^{\lambda_1 t}$. Similarly, if one takes three nearby trajectories and applies the same thought, one can see that the sum $\lambda_1+\lambda_2$ is the exponential growth rate of small areas between the three trajectories. So, for k nearby trajectories, the sum $\lambda_1+\cdots+\lambda_k$ gives the exponential growth rate of the k-volume between the k trajectories.

The complexity of computing Lyapunov exponents analytically grows with the complexity of the dynamical equations of the system, as the equations for M can get be highly complex and, usually, impossible to solve analytically. In fact, even the numeric computation of Lyapunov exponent is no easy task, as the matrices M can become highly ill-conditioned in the case that the ball of points in phase space is transformed into highly elongated ellipsoids.

There are various methods that can be used to calculate these Lyapunov exponents, such as Benettin's [8, 9], Wolf's [10], Rosenstein's [11] or Kantz's [12]. Each of them has some advantages or disadgvantages over the others. Awrejcewicz's [13] paper has a nice description and comparison between these methods and some others.

Usually, only the largest Lyapunov exponent is studied, because it is the one that gives the information about the largest expansion direction - yielding the most insight into the system's behavior - and it is the easiest one to calculate numerically. This work will focus only on the largest Lyapunov exponent λ_1, which can be calculated through the simple algorithm developed by Benettin et al. [8, 9]. One first considers two nearby trajectories starting at $\boldsymbol{x}\,(0)$ and $\boldsymbol{x}\,(0)+\boldsymbol{\delta_0}$ separated by a distance $|\boldsymbol{\delta_0}|=\delta_0<<1$. These two trajectories are integrated for some time T, after which one evaluates the separation $|\boldsymbol{\delta}\,(T)\,|=\delta\,(T)$.

At this point, one renormalizes the separation vector to its' original length δ_0 and repeats the process. After doing so N times, this will result in a set of separation vectors $\{\boldsymbol{\delta}(kT),\, k = 1, \ldots, N\}$ that will, for a sufficient total integration time, point in the direction of largest growth and therefore give information about λ_1. The numerical estimator of λ_1 is then

$$\lambda_1 \approx \frac{1}{NT} \sum_{k=1}^{N} \log \frac{|\boldsymbol{\delta}(kT)|}{\delta_0}. \tag{2.65}$$

There are, however, two major problems with this method: first, what should be a good value for the initial separation δ_0? Second, what should be a good value for the normalization time T? The initial separation should be small enough so that the approximation of exponential divergence/convergence of the trajectories holds valid, but it can't be too small or numerical errors may arise in the computations. The normalization time T should also not be too big as to not get out of the exponential regime, but should also not be too small, or the separation of the two trajectories will not be noticeable. Unfortunately, there appears that no simple answer exists for these questions, as every system is different and behaves in distinct ways. Therefore, for each problem, one should always try to first run some simpler tests for different pairs of values of δ_0 and T in order to try to guarantee the validity of most complex studies.

Chapter 3.

Vortices in 2D Flows

3.1 INVISCID POINT VORTICES

Consider a 2-dimensional inviscid flow extending to infinity, inhabited by some number of point vortices. What are the dynamics of this system? Answering this question corresponds, mathematically, to solving the vorticity equation in the unbound plane for some initial condition describing the desired point vortices.

In the unbound plane, if the system is composed by only one point vortex located in $\boldsymbol{r_0}$, the stream function at point $\boldsymbol{r}$ can be written as

$$\psi(\boldsymbol{r}) = -\frac{\Gamma}{2\pi}\log\|\boldsymbol{r} - \boldsymbol{r_0}\|. \tag{3.1}$$

Since the relation between velocity and vorticity is linear, the velocity field created by n point vortices can be written as the linear superposition of the velocity field created by each point vortex. In fact if each vortex has a circulation of Γ_α and is located in the position $\boldsymbol{r_\alpha}$, it can be shown that the Hamiltonian of the system can be written as

$$H = -\frac{1}{4\pi}\sum_{\alpha\neq\beta}\Gamma_\alpha\Gamma_\beta \log\|\boldsymbol{r}_\alpha - \boldsymbol{r}_\beta\|. \tag{3.2}$$

Therefore, using Hamilton's equations, the movement equations for the point vortices can be written as

$$\begin{cases} \Gamma_\alpha \dot{x_\alpha} = \dfrac{\partial H}{\partial y_\alpha} = -\dfrac{\Gamma_\alpha}{2\pi}\displaystyle\sum_{\beta\neq\alpha}\Gamma_\beta\frac{y_\alpha - y_\beta}{r_{\alpha\beta}^2} \\ \Gamma_\alpha \dot{y_\alpha} = -\dfrac{\partial H}{\partial x_\alpha} = \dfrac{\Gamma_\alpha}{2\pi}\displaystyle\sum_{\beta\neq\alpha}\Gamma_\beta\frac{x_\alpha - x_\beta}{r_{\alpha\beta}^2} \end{cases}, \tag{3.3}$$

where $r_{\alpha\beta}^2 = (x_\alpha - x_\beta)^2 + (y_\alpha - y_\beta)^2$. These equations can be re-written in Hamilton's canonical form (2.48) by taking, for instance, the choice of $q_\alpha = x_\alpha$ and $p_\alpha = \Gamma_\alpha y_\alpha$ for the generalized position and momentum. There are other choices that can be made for these generalized coordinates; the results that arise from the analysis, however, are independent of this choice as they follow from the intrinsic behavior of the system.

Thus, it is easy to see that, for this model, one can choose a phase space that only differs from the physical configuration space by a rescaling of the y-axis. This is a feature that has profound consequences in the statistical physics and chaotic advection of the system, as noted by Aref [14].

By using complex variables $z_\alpha(t) = x_\alpha(t) + iy_\alpha(t)$ it is possible to express the movement equations (3.3) in a more compact form (which will be useful in some future analysis):

$$\dot{z}_\alpha^* = \frac{1}{2\pi i}\sum_{\beta\neq\alpha}^{n}\frac{\Gamma_\beta}{z_\alpha - z_\beta}. \tag{3.4}$$

3.1.1 Conserved Quantities and Symmetries

One of the main interests of the Hamiltonian description of the problem in hand is that the Poisson bracket defined in (2.4.1) provides an easy way to check for invariants of the system. Other than the Hamiltonian, which is invariant by definition, the n-vortex system also has the following conserved quantities:

1. $Q = \sum_{\alpha=1}^{n} \Gamma_\alpha x_\alpha$;
2. $P = \sum_{\alpha=1}^{n} \Gamma_\alpha y_\alpha$;
3. $I = \sum_{\alpha=1}^{n} \Gamma_\alpha |z_\alpha|^2$;
4. $I_0 = \frac{1}{2i} \sum_{\alpha=1}^{n} \Gamma_\alpha \left(z_\alpha^* \dot{z}_\alpha - z_\alpha \dot{z}_\alpha^*\right) = \frac{1}{2\pi} \sum_{\alpha=1}^{n} \sum_{\beta<\alpha} \Gamma_\alpha \Gamma_\beta$

$Q + iP$ is called the linear impulse and, when divided by the total circulation $\Gamma = \sum_{\alpha=1}^{n} \Gamma_\alpha$, gives the vorticity center of the system; I is called the angular impulse.

The time invariance of the first three quantities can be easily checked through their Poisson bracket with the Hamiltonan, as none of them has an explicit dependence on time:

$$\begin{aligned} \{Q, H\} &= \sum_{\alpha=1}^{n} \Gamma_\alpha \{x_\alpha, H\} = \sum_{\alpha=1}^{n} \Gamma_\alpha \{q_\alpha, H\} = \sum_{\alpha=1}^{n} \Gamma_\alpha \dot{q}_\alpha = \sum_{\alpha=1}^{n} \Gamma_\alpha \dot{x}_\alpha \\ &= -\frac{1}{2\pi} \sum_{\alpha=1}^{n} \sum_{\beta \neq \alpha} \underbrace{\Gamma_\alpha \Gamma_\beta \frac{y_\alpha - y_\beta}{r_{\alpha\beta}^2}}_{\xi_{\alpha\beta}} = 0, \end{aligned} \tag{3.5}$$

because $\xi_{\alpha\beta} = -\xi_{\beta\alpha}$ and thus every term of the sum cancels with its' symmetric. The conservation of P follows in a analogous fashion:

$$\begin{aligned} \{P, H\} &= \sum_{\alpha=1}^{n} \{\Gamma_\alpha y_\alpha, H\} = \sum_{\alpha=1}^{n} \{p_\alpha, H\} = \sum_{\alpha=1}^{n} \dot{q}_\alpha = \sum_{\alpha=1}^{n} \Gamma_\alpha \dot{y}_\alpha \\ &= \frac{1}{2\pi} \sum_{\alpha=1}^{n} \sum_{\beta \neq \alpha} \underbrace{\Gamma_\alpha \Gamma_\beta \frac{x_\alpha - x_\beta}{r_{\alpha\beta}^2}}_{\eta_{\alpha\beta}} = 0, \end{aligned} \tag{3.6}$$

again, because $\eta_{\alpha\beta} = -\eta_{\beta\alpha}$.

The angular impulse I also stays constant in time:

$$\begin{aligned}
\{I,H\} &= \sum_{\alpha=1}^{n}\left\{\Gamma_\alpha\left(x_\alpha^2+y_\alpha^2\right),H\right\} = \sum_{\alpha=1}^{n}\Gamma_\alpha\left[\left\{x_\alpha^2,H\right\}+\left\{y_\alpha^2,H\right\}\right] = \\
&= 2\sum_{\alpha=1}^{n}\Gamma_\alpha\left[x_\alpha\left\{x_\alpha,H\right\}+y_\alpha\left\{y_\alpha,H\right\}\right] = 2\sum_{\alpha=1}^{n}\Gamma_\alpha\left[x_\alpha\dot{x}_\alpha+y_\alpha\dot{y}_\alpha\right] = \\
&= \frac{1}{\pi}\sum_{\alpha=1}^{n}\sum_{\beta\neq\alpha}\frac{\Gamma_\alpha\Gamma_\beta}{r_{\alpha\beta}^2}\left[x_\alpha\left(y_\beta-y_\alpha\right)+y_\alpha\left(x_\alpha-x_\beta\right)\right] = \frac{1}{\pi}\sum_{\alpha=1}^{n}\sum_{\beta\neq\alpha}\underbrace{\frac{\Gamma_\alpha\Gamma_\beta}{r_{\alpha\beta}^2}\left[x_\alpha y_\beta-y_\alpha x_\beta\right]}_{\kappa_{\alpha\beta}} = 0,
\end{aligned} \tag{3.7}$$

once more, because $\kappa_{\alpha\beta} = -\kappa_{\beta\alpha}$ and every term in the sum cancels with a symmetric one.

I_0 is obviously a conserved quantity as it is the sum of constant quantities. One just needs to prove that the definition of I_0 is equal to the sum $\frac{1}{2\pi}\sum_{\alpha=1}^{n}\sum_{\beta<\alpha}\Gamma_\alpha\Gamma_\beta$:

$$\begin{aligned}
I_0 &= \frac{1}{2i}\sum_{\alpha=1}^{n}\Gamma_\alpha\left(z_\alpha^*\dot{z}_\alpha-z_\alpha\dot{z}_\alpha^*\right) = \frac{1}{2i}\sum_{\alpha=1}^{n}\sum_{\beta\neq\alpha}\left[-\frac{\Gamma_\alpha\Gamma_\beta}{2\pi i}\frac{z_\alpha^*}{z_\alpha^*-z_\beta^*}-\frac{\Gamma_\alpha\Gamma_\beta}{2\pi i}\frac{z_\alpha}{z_\alpha-z_\beta}\right] = \\
&= \frac{1}{4\pi}\sum_{\alpha=1}^{n}\sum_{\beta\neq\alpha}\Gamma_\alpha\Gamma_\beta\left(\frac{z_\alpha}{z_\alpha-z_\beta}+\frac{z_\alpha^*}{z_\alpha^*-z_\beta^*}\right) = \frac{1}{2\pi}\sum_{\alpha=1}^{n}\sum_{\beta\neq\alpha}\Gamma_\alpha\Gamma_\beta Re\left(\frac{z_\alpha}{z_\alpha-z_\beta}\right) = \\
&= \frac{1}{2\pi}\sum_{\alpha=1}^{n}\sum_{\beta\neq\alpha}\frac{\Gamma_\alpha\Gamma_\beta}{|z_\alpha-z_\beta|^2}\left[|z_\alpha|^2-Re\left(z_\alpha z_\beta^*\right)\right] = \\
&= \frac{1}{2\pi}\sum_{\alpha=1}^{n}\sum_{\beta\neq\alpha}\frac{\Gamma_\alpha\Gamma_\beta}{|z_\alpha-z_\beta|^2}\left(x_\alpha^2+y_\alpha^2-x_\alpha x_\beta-y_\alpha y_\beta\right) \\
&= \frac{1}{2\pi}\sum_{\alpha=1}^{n}\sum_{\beta<\alpha}\frac{\Gamma_\alpha\Gamma_\beta}{|z_\alpha-z_\beta|^2}\underbrace{\left(x_\alpha^2+y_\alpha^2-2x_\alpha x_\beta-2y_\alpha y_\beta+x_\beta^2+y_\beta^2\right)}_{|z_\alpha-z_\beta|^2} = \frac{1}{2\pi}\sum_{\alpha=1}^{n}\sum_{\beta<\alpha}\Gamma_\alpha\Gamma_\beta.
\end{aligned} \tag{3.8}$$

Though Noether's Theorem it is possible to associate each of these conserved quantities to a symmetry of the system. The conservation of the Hamiltonian is connected to a time translation symmetry, the conservation of the linear impulse gives a space translation symmetries, while rotational symmetry is linked to the conservation of angular impulse. Finally, the conservation of I_0 is related to scale transformation symmetry. Chapman's paper [15] gives a detailed description of these conserved quantities and symmetries.

Discrete symmetries do not generate conserved quantities, but nevertheless they can be useful to have in mind when studying or solving a complex problem. In particular, the n-vortex system has some discrete symmetries:

1. $t \to -t, \quad \Gamma_\alpha \to -\Gamma_\alpha$;

2. $z \to -z$;

3. $\Gamma_\alpha \to -\Gamma_\alpha, \quad z \to z^*$;

4. Cyclic permutations of indices.

3.1.2 Integrability of the System

A common strategy to address the question of integrability of some system of differential equations is to look for first integrals of the system, or, equivalently, quantities that are conserved, mutually involutive and functionally independent. For the n-vortex system this is also a valid method. One can find easily a couple of useful Poisson bracket identities by just using their properties and the fundamental brackets $\{x_\alpha, x_\beta\} = 0 = \{y_\alpha, y_\beta\}$ and $\{x_\alpha, y_\beta\} = -\{y_\beta, x_\alpha\} = \Gamma_\beta^{-1}\delta_{\alpha\beta}$:

1. $\{Q, P\} = \sum_{\alpha=1}^{n}\sum_{\beta=1}^{n}\Gamma_\alpha\Gamma_\beta\{x_\alpha, y_\beta\} = \sum_{\alpha=1}^{n}\sum_{\beta=1}^{n}\Gamma_\alpha\delta_{\alpha\beta} = \sum_{\alpha=1}^{n}\Gamma_\alpha = \Gamma$

2. $\{Q, I\} = \sum_{\alpha=1}^{n}\sum_{\beta=1}^{n}\Gamma_\alpha\Gamma_\beta\left\{x_\alpha, x_\beta^2 + y_\beta^2\right\} = 2\sum_{\alpha=1}^{n}\sum_{\beta=1}^{n}\Gamma_\alpha\Gamma_\beta\left[x_\beta\{x_\alpha, x_\beta\} + y_\beta\{x_\alpha, y_\beta\}\right] =$
$= 2\sum_{\alpha=1}^{n}\sum_{\beta=1}^{n}\Gamma_\alpha y_\beta\delta_{\alpha\beta} = 2\sum_{\alpha=1}^{n}\Gamma_\alpha y_\alpha = 2P$

3. $\{P, I\} = \sum_{\alpha=1}^{n}\sum_{\beta=1}^{n}\Gamma_\alpha\Gamma_\beta\left\{y_\alpha, x_\beta^2 + y_\beta^2\right\} = 2\sum_{\alpha=1}^{n}\sum_{\beta=1}^{n}\Gamma_\alpha\Gamma_\beta\left[x_\beta\{y_\alpha, x_\beta\} + y_\beta\{y_\alpha, y_\beta\}\right] =$
$= -2\sum_{\alpha=1}^{n}\sum_{\beta=1}^{n}\Gamma_\beta x_\beta\delta_{\alpha\beta} = -2\sum_{\beta=1}^{n}\Gamma_\beta x_\beta = -2Q$

4. $\{P^2 + Q^2, H\} = 2P\{P, H\} + 2Q\{Q, H\} = 0$

5. $\{P^2 + Q^2, I\} = 2P\{P, I\} + 2Q\{Q, I\} = 2P(-2Q) + 2Q(2P) = 0$

In an Hamiltonian system with n degrees of freedom (equivalently, a phase space of dimension $2n$), if there are k conserved quantities that are in involution with one another and are functionally independent, one can reduce the phase space dimension by $2k$.

Definition 3.1.1 (Integrability)**.** If there are n conserved quantities that are in involution with one another and are functionally independent in the n-vortex system, the system is said to be integrable.

Theorem 3.1.1. *For $n \leq 3$, the n-vortex problem is integrable for any $\Gamma_\alpha\,(\alpha = 1, \ldots, n)$. If $\Gamma = 0$, the 4-vortex system is also integrable.*

Proof. For $n = 1$ and $n = 2$, the system is trivially integrable (the integration for $n = 2$ will be explicitly made in section 3.1.3). For $n = 3$, the quantities H, $P^2 + Q^2$ and I are functionally independent and are in involution with one another for all combinations of circulations of the 3 vortices [16, 17, 18], hence the system is integrable. If $\Gamma = 0$, the quantities H, P, Q and I are mutually involutive since it is possible to change the origin of the system of coordinates to a point such that $P = 0 = Q$. This change of coordinates does not affect the Poisson brackets since it only adds constant values to P and Q, thus, the problem for $n = 4$ is integrable if $\Gamma = 0$.

■

Remark: In fact, the non-integrability for $n = 4$ in the case $\Gamma \neq 0$ has been proven by various authors such as Ziglin [19], Koiller & Carvalho [20, 21] or Castilla et al. [22].

In order to study the solutions of the n-vortex system in the integrable cases, one can take any of the descriptions formulated to tackle the problem. Let's use the complex description to do so:

$$\dot{z}_k^* = \frac{1}{2\pi i} \sum_{j \neq k}^{n} \frac{\Gamma_j}{z_k - z_j}. \tag{3.9}$$

For a system comprised of only one point vortex, the integration of (3.9) is trivial, and the point vortex will remain in its' initial position at all times, since it doesn't feel its' own vorticity field (and therefore the velocity field created by it) and there are no other sources of vorticity in the system.

3.1.3 Dynamics of 2 Point Vortices

For a system formed by two point vortices of circulations Γ_1 and Γ_2, we have the following system of differential equations

$$\begin{cases} \dot{z}_1^* = \dfrac{1}{2\pi i}\dfrac{\Gamma_2}{z_1 - z_2} \\ \dot{z}_2^* = \dfrac{1}{2\pi i}\dfrac{\Gamma_1}{z_2 - z_1} \end{cases} . \tag{3.10}$$

One can first notice that the distance between the two vortices, $D = \sqrt{(z_1 - z_2)(z_1 - z_2)^*}$, is a conserved quantity:

$$\begin{aligned} \left\{D^2, H\right\} &= (z_1 - z_2)\left\{(z_1 - z_2)^*, H\right\} + \left\{z_1 - z_2, H\right\}(z_1 - z_2)^* \\ &= (z_1 - z_2)(\dot{z}_1 - \dot{z}_2)^* + (\dot{z}_1 - \dot{z}_2)(z_1 - z_2)^* \\ &= \frac{1}{2\pi i}\left[(z_1 - z_2)\left(\frac{\Gamma_2}{z_1 - z_2} + \frac{\Gamma_1}{z_2 - z_1}\right) - \left(\frac{\Gamma_2}{(z_1 - z_2)^*} + \frac{\Gamma_1}{(z_2 - z_1)^*}\right)(z_1 - z_2)^*\right] \\ &= \frac{1}{2\pi i}\left[(\Gamma_2 - \Gamma_1) - (\Gamma_2 - \Gamma_1)\right] \\ &= 0. \end{aligned} \tag{3.11}$$

Therefore the system (3.10) can be re-written as

$$\begin{cases} \dot{z}_1 = \dfrac{i\Gamma_2}{2\pi D^2}(z_1 - z_2) \\ \dot{z}_2 = \dfrac{i\Gamma_1}{2\pi D^2}(z_2 - z_1) \end{cases} . \tag{3.12}$$

As such, it's easy to see that $\Gamma_1\dot{z}_1 + \Gamma_2\dot{z}_2 = 0$, and the linear impulse is conserved, as expected. Thus, $\{\Gamma_1 z_1 + \Gamma_2 z_2, H\} = 0$. To solve the system (3.12) we introduce a simple change of variables $z_+ = z_1 + z_2,\ z_- = z_1 - z_2$ and we get

$$\begin{cases} \dot{z}_+ = \dfrac{i}{2\pi D^2}(\Gamma_2 - \Gamma_1)\, z_- \\ \dot{z}_- = \dfrac{i}{2\pi D^2}(\Gamma_1 + \Gamma_2)\, z_- \end{cases} . \tag{3.13}$$

We need to distinguish between two cases here: $\Gamma_1 + \Gamma_2 = 0$ and $\Gamma_1 + \Gamma_2 \neq 0$.

a) $\boldsymbol{\Gamma_1 + \Gamma_2 = 0}$

The integration is trivial and yields

$$\begin{cases} z_+ = \dfrac{i}{2\pi D^2}\left(\Gamma_2 - \Gamma_1\right) At + B, \\ z_- = A \end{cases}, \tag{3.14}$$

where $A, B \in \mathbb{C}$ can be easily determined provided one knows the initial positions of the point vortices: $A = z_1(0) - z_2(0)$, $B = z_1(0) + z_2(0)$. Therefore, the positions of the point vortices at all times are given by

$$\begin{cases} z_1(t) = z_1(0) + \dfrac{i\Gamma_1}{2\pi D}\left[z_2(0) - z_1(0)\right] t \\ z_2(t) = z_2(0) - \dfrac{i\Gamma_2}{2\pi D}\left[z_2(0) - z_1(0)\right] t \end{cases}, \tag{3.15}$$

and they move in straight lines, parallel to one another and with constant velocity $\Gamma_1 / (2\pi D^2)$.

b) $\boldsymbol{\Gamma_1 + \Gamma_2 \neq 0}$:

While not as straightforward as in the previous case, the integration is also simple and it gives

$$\begin{cases} z_+ = \dfrac{\Gamma_2 - \Gamma_1}{\Gamma_1 + \Gamma_2} A \exp(i\theta t) + B, \\ z_- = A \exp(i\theta t) \end{cases}, \tag{3.16}$$

where $\theta = (\Gamma_1 + \Gamma_2) / (2\pi D^2)$ and $A, B \in \mathbb{C}$ can be easily determined provided we know the initial positions of the point vortices as

$$\begin{cases} A = z_1(0) - z_2(0) \\ B = 2\dfrac{\Gamma_1 z_1(0) + \Gamma_2 z_2(0)}{\Gamma_1 + \Gamma_2} \end{cases}. \tag{3.17}$$

Therefore, after a little bit of algebra, one arrives at expressions for the point vortices' position at all times:

$$\begin{cases} z_1(t) = \dfrac{1}{\Gamma_1+\Gamma_2}\left[\Gamma_1 z_1(0) + \Gamma_2 z_2(0) + \Gamma_2\left[z_1(0) - z_2(0)\right]e^{i\theta t}\right] \\ z_2(t) = \dfrac{1}{\Gamma_1+\Gamma_2}\left[\Gamma_1 z_1(0) + \Gamma_2 z_2(0) - \Gamma_1\left[z_1(0) - z_2(0)\right]e^{i\theta t}\right] \end{cases}, \tag{3.18}$$

and the vortices rotate around a common point - the center of vorticity of the system - at a velocity that is in inverse proportion to their separation distance.

3.1.4 Dynamics of 3 Point Vortices

For a system comprised of 3 or more vortices, integration is not as trivial even if one knows all the conserved quantities of the system. In fact, if the system is integrable, odds are that carrying out the explicit integration will require knowledge of transformation and reduction theory (the works of Lichtenberg and Lieberman [23] or Goldstein [5] cover the basics, for example), which enables one to find a special set of coordinates, called the action-angle coordinates, $(\boldsymbol{I}, \boldsymbol{\theta})$, defined in subregions of the phase space and an Hamiltonian, $\tilde{H}(\boldsymbol{I})$, independent of the $\boldsymbol{\theta}$ variables such that the equations of motion simplify to

$$\begin{cases} \dot{I}_k = -\dfrac{\partial \tilde{H}}{\partial \theta_k} = 0 \\ \dot{\theta}_k = \dfrac{\partial \tilde{H}}{\partial I_k} = \omega_k(\boldsymbol{I}) \end{cases}, \quad k = 1, \ldots, n. \tag{3.19}$$

So, the first n equations give us the n conserved quantities of the system, while the remaining n are the angles - $\theta_k \in [0, 2\pi]$ - that increase as some linear combination of the invariants I_k.

For analysis of systems with $n \geq 3$, it is usually useful to rewrite the equations for the n-vortex system for the distance between pairs of vortices, usually called the intervortex separations. Let $\ell_{\alpha\beta} = |z_\alpha - z_\beta|$. There are two invariant quantities that can be written directly from the intervortex separations and, therefore, are independent of the specific coordinates of each vortex. One is the Hamiltonian,

$$H = -\frac{1}{4\pi} \sum_{\alpha \neq \beta} \Gamma_\alpha \Gamma_\beta \log\left(\ell_{\alpha\beta}\right), \tag{3.20}$$

and the other is a combination of the integrals P, Q and I defined in Section 3.1.1:

$$\begin{aligned} M &= \frac{1}{2} \sum_{\alpha=1}^{n} \sum_{\beta \neq \alpha} \Gamma_\alpha \Gamma_\beta \ell_{\alpha\beta} = \Gamma \sum_{\alpha=1}^{n} \Gamma_\alpha \left(x_\alpha^2 + y_\alpha^2\right) - \left(\sum_{\alpha=1}^{n} \Gamma_\alpha x_\alpha\right)^2 - \left(\sum_{\alpha=1}^{n} \Gamma_\alpha y_\alpha\right)^2 \\ &= \Gamma I - \left(Q^2 + P^2\right) \end{aligned} \tag{3.21}$$

Even without the advanced techniques of transformation and reduction theory, it is still possible to characterize the equilibria and collapse states of the 3 vortices problem.

Definition 3.1.2 (Vortex Configuration)**.** The geometrical object formed by the set of vortices in a system at any given time is called a vortex configuration. If this geometrical object does not rotate or suffers translations in time, one says that it is a fixed equilibrium of the system. Otherwise, one calls it a relative equilibrium.

Remark: It is straightforward to notice that for $n = 2$, there are no fixed equilibria, whichever may be the initial conditions or the circulations of the vortices. All solutions of the 2-vortices system are, therefore, relative equilibria.

Due to the discreet symmetries of the n-vortex described in section 3.1.1, one can reduce the 3-vortex problem to the case where $\Gamma_1 \geq \Gamma_2 \geq 0$ and $\Gamma_3 \in \mathbb{R}$, as all the other cases can be obtained from these symmetries. From here on, the analysis will be performed in a system assuming these vortex circulations. In order to simplify notation, for a system of 3 vortices, one can write $s_1 = \ell_{23}$, $s_2 = \ell_{31}$ and $s_3 = \ell_{12}$. With this, the Hamiltonian and the M integral have pretty straightforward expressions:

$$H = -\frac{1}{4\pi} \left[\Gamma_2\Gamma_3 \log\left(s_1^2\right) + \Gamma_1\Gamma_3 \log\left(s_2^2\right) + \Gamma_1\Gamma_2 \log\left(s_3^2\right)\right], \tag{3.22}$$

$$M = \Gamma_2\Gamma_3 s_1^2 + \Gamma_1\Gamma_3 s_2^2 + \Gamma_1\Gamma_2 s_3^2. \tag{3.23}$$

Notice that it is possible to easily compute the fundamental Poisson brackets between pairs of the squares of these new variables, such as s_1^2 and s_2^2:

$$\begin{aligned}
\left\{s_1^2, s_2^2\right\} &= \left\{(x_2-x_3)^2 + (y_2-y_3)^2, (x_3-x_1)^2 + (y_3-y_1)^2\right\} = \\
&= 4\left[(x_2-x_3)(y_3-y_1)\left\{x_2-x_3, y_3-y_1\right\} + (y_2-y_3)(x_3-x_1)\left\{y_2-y_3, x_3-x_1\right\}\right] = \\
&= 4\left[-(x_2-x_3)(y_3-y_1)\Gamma_3^{-1} + (y_2-y_3)(x_3-x_1)\Gamma_3^{-1}\right] = \\
&= -\frac{8}{\Gamma_3}\frac{x_1y_2 + x_2y_3 + x_3y_1 - x_1y_3 - x_3y_2 - x_2y_1}{2} \\
&= -\frac{8}{\Gamma_3}\Delta,
\end{aligned} \tag{3.24}$$

where Δ is the area of the triangle defined by the positions of the vortices z_1, z_2 and z_3, affected by the sign of the permutation of the indices, i.e., it is positive if the triangle has vertices 123 counterclockwise and negative if the vertices appear clockwise. The other two fundamental Poisson brackets can be obtain analogously:

$$\left\{s_1^2, s_2^2\right\} = -\frac{8}{\Gamma_3}\Delta, \quad \left\{s_2^2, s_3^2\right\} = -\frac{8}{\Gamma_1}\Delta, \quad \left\{s_3^2, s_1^2\right\} = -\frac{8}{\Gamma_2}\Delta. \tag{3.25}$$

With these brackets, it becomes straightforward to derive the differential equations for the squares of the intervortex separations, since these quantities do not explicitly depend on time:

$$\begin{aligned}\frac{d\left(s_1^2\right)}{dt} = \left\{s_1^2, H\right\} &= -\frac{1}{4\pi}\left[\Gamma_2\Gamma_3\left\{s_1^2, \log\left(s_1^2\right)\right\} + \Gamma_1\Gamma_3\left\{s_1^2, \log\left(s_2^2\right)\right\} + \Gamma_1\Gamma_2\left\{s_1^2, \log\left(s_3^2\right)\right\}\right] \\ &= -\frac{1}{4\pi}\left[\frac{\Gamma_2\Gamma_3}{s_1^2}\left\{s_1^2, s_1^2\right\} + \frac{\Gamma_1\Gamma_3}{s_2^2}\left\{s_1^2, s_2^2\right\} + \frac{\Gamma_1\Gamma_2}{s_3^2}\left\{s_1^2, s_3^2\right\}\right] \\ &= \frac{2}{\pi}\Gamma_1\Delta\left(\frac{1}{s_2^2} - \frac{1}{s_3^2}\right).\end{aligned} \tag{3.26}$$

The remaining two equations can be found through similar computations, forming together the system of ordinary differential equations

$$\begin{cases}\dfrac{d\left(s_1^2\right)}{dt} = \dfrac{2}{\pi}\Gamma_1\Delta\left(\dfrac{1}{s_2^2} - \dfrac{1}{s_3^2}\right) \\ \dfrac{d\left(s_2^2\right)}{dt} = \dfrac{2}{\pi}\Gamma_2\Delta\left(\dfrac{1}{s_3^2} - \dfrac{1}{s_1^2}\right) \\ \dfrac{d\left(s_3^2\right)}{dt} = \dfrac{2}{\pi}\Gamma_3\Delta\left(\dfrac{1}{s_1^2} - \dfrac{1}{s_2^2}\right)\end{cases}. \tag{3.27}$$

Remark: The area of the triangle formed by the positions of the 3 vortices, $|\Delta|$, can also be expressed in a more desirable way when working with equations (3.27) by Heron's formula $|\Delta| = \sqrt{p\left(p-s_1\right)\left(p-s_2\right)\left(p-s_3\right)}$, where $p = 0.5\left(s_1+s_2+s_3\right)$ is the semi-perimeter of the triangle. This equation and (3.27) form therefore a closed system provided that the 3 vortices don't go through collinear states, where Δ changes sign. To analyze what happens when the three vortices go through a collinear state, one requires a dynamical equation for Δ.

Theorem 3.1.2 (Fixed equilibria of the 3 vortex system)**.** *The necessary and sufficient conditions for a fixed equilibria configuration of 3 vortices in the plane are*

(i) The vortices must be collinear and their positions be such that $\Gamma_3\left(z_2 - z_1\right) = \Gamma_2\left(z_1 - z_3\right)$

(ii) $\sum_{\alpha\neq\beta}\Gamma_\alpha\Gamma_\beta = 0$

Proof. From the dynamical equations

$$\dot{z}_\alpha^* = \frac{1}{2\pi i}\sum_{\beta\neq\alpha}\frac{\Gamma_\beta}{z_\alpha - z_\beta}, \tag{3.28}$$

the necessary condition for a fixed equilibrium is $\dot{z}_\alpha^* = 0$, so, for $\alpha = 1$ one gets

$$\frac{\Gamma_2}{z_1 - z_2} + \frac{\Gamma_3}{z_1 - z_3} = 0, \tag{3.29}$$

which is equivalent to $\Gamma_3 (z_2 - z_1) = \Gamma_2 (z_1 - z_3)$. This also shows that the vectors in the complex plane that connect z_2 to z_1 and z_3 to z_1 must be scalar multiples of one another and therefore the three vortices must present a collinear configuration.

From the dynamical equations for the 3 vortices, the conditions $\dot{z}_\alpha^* = 0,\ \alpha \in \{1, 2, 3\}$ give rise to

$$\begin{cases} \dfrac{\Gamma_2}{z_1 - z_2} + \dfrac{\Gamma_3}{z_1 - z_3} = 0 \\ \dfrac{\Gamma_3}{z_2 - z_3} + \dfrac{\Gamma_1}{z_2 - z_1} = 0 \\ \dfrac{\Gamma_1}{z_3 - z_1} + \dfrac{\Gamma_2}{z_3 - z_2} = 0 \end{cases}. \tag{3.30}$$

Multiplying each of these three equations by $\Gamma_1 z_1$, $\Gamma_2 z_2$ and $\Gamma_3 z_3$ respectively and summing them gives

$$\begin{aligned} &\frac{\Gamma_2\Gamma_1 z_1}{z_1 - z_2} + \frac{\Gamma_3\Gamma_1 z_1}{z_1 - z_3} + \frac{\Gamma_3\Gamma_3 z_2}{z_2 - z_3} + \frac{\Gamma_1\Gamma_2 z_2}{z_2 - z_1} + \frac{\Gamma_1\Gamma_3 z_3}{z_3 - z_1} + \frac{\Gamma_2\Gamma_3 z_3}{z_3 - z_2} = 0 \Leftrightarrow \\ \Leftrightarrow\ &\frac{\Gamma_1\Gamma 1 (z_1 - z_2)}{z_1 - z_2} + \frac{\Gamma_2\Gamma 3 (z_2 - z_3)}{z_2 - z_3} + \frac{\Gamma_3\Gamma_1 (z_1 - z_3)}{z_1 - z_3} = 0 \Leftrightarrow \\ \Leftrightarrow\ &\Gamma_1\Gamma_2 + \Gamma_2\Gamma_3 + \Gamma_3\Gamma_1 = 0. \end{aligned} \tag{3.31}$$

To prove the sufficiency of these conditions, one starts with $\sum_{\alpha\neq\beta} \Gamma_\alpha\Gamma_\beta = 0$. It is possible to write expressions for Γ_2 and Γ_3 in terms of the other two circulations:

$$\Gamma_2 = -\frac{\Gamma_1\Gamma_3}{\Gamma_1 + \Gamma_3}, \quad \Gamma_3 = -\frac{\Gamma_1\Gamma_2}{\Gamma_1 + \Gamma_2}. \tag{3.32}$$

With these two identities and the condition $\Gamma_3 (z_2 - z_1) = \Gamma_2 (z_1 - z_3)$ it is possible to use derive

similar expressions for each pair of Γ_α's, yielding

$$\begin{cases} \Gamma_3 (z_2 - z_1) = \Gamma_2 (z_1 - z_3) \\ \Gamma_1 (z_3 - z_2) = \Gamma_2 (z_1 - z_3) \\ \Gamma_3 (z_2 - z_1) = \Gamma_1 (z_3 - z_2) \end{cases}. \tag{3.33}$$

And using these three identities in the dynamical equations, it is straightforward to see that $\dot{z}^*_\alpha = 0$ for $\alpha \in \{1, 2, 3\}$.

■

Theorem 3.1.3 (Relative equilibria of the 3 vortex system)**.** *The only relative equilibria configurations for a system of 3 vortices in the plane are collinear configurations and equilateral triangles. Furthermore,*

(i) all equilateral triangles with side s constitute relative equilibria rotating rigidly around their center of vorticity with frequency $\frac{\Gamma}{2\pi s^2}$. In the limiting case where $\Gamma = 0$, the center of vorticity is located at infinity and all vortices travel in parallel to one another with velocity $\sqrt{\frac{\Gamma_1^2+\Gamma_2^2+\Gamma_3^2}{8\pi^2 s^2}}$.

(ii) Collinear states can form relative equilibria if and only if

$\frac{s_3^2-s_2^2}{s_1^2}(\Gamma_2+\Gamma_3) + \frac{s_1^2-s_3^2}{s_2^2}(\Gamma_3+\Gamma_1) + \frac{s_2^2-s_1^2}{s_3^2}(\Gamma_1+\Gamma_2) = 0.$

Proof. For the system to be in relative equilibrium, the time derivatives of s_1, s_2 and s_3 must go to zero at all times. As it can be seen from the equations (3.27), this only happens when either $\Delta = 0$, which corresponds to a collinear configuration, or when $s_1 = s_2 = s_3$, which corresponds to an equilateral triangle configuration.

Now, let the system be in a equilateral triangle configuration of side s and $\Gamma = \sum_{\alpha=1}^3 \Gamma_\alpha \neq 0$. The center of vorticity of the system is defined as

$$z_{cv} = \frac{\sum_{\alpha=1}^3 \Gamma_\alpha z_\alpha}{\Gamma}. \tag{3.34}$$

Therefore one can write the equations of motion for the three vortices as

$$\begin{aligned}\dot{z}_\alpha &= -\frac{1}{2\pi i}\sum_{\beta\neq\alpha}\frac{\Gamma_\beta}{(z_\alpha - z_\beta)^*} = -\frac{1}{2\pi i}\sum_{\beta\neq\alpha}\frac{\Gamma_\beta\,(z_\alpha - z_\beta)}{(z_\alpha - z_\beta)^*\,(z_\alpha - z_\beta)} = \\ &= -\frac{1}{2\pi i s^2}\sum_{\beta\neq\alpha}\left[\Gamma_\beta\,(z_\alpha - z_\beta)\right] = -\frac{1}{2\pi i s^2}\sum_{\beta\neq\alpha}\left[\Gamma_\beta z_\alpha - \Gamma_\beta z_\beta + \Gamma_\alpha z_\alpha - \Gamma_\alpha z_\alpha\right] \\ &= -\frac{1}{2\pi i s^2}\left[\sum_{\beta=1}^{3}\Gamma_\beta z_\alpha - \sum_{\beta=1}^{3}\Gamma_\beta z_\beta\right] = \frac{i\Gamma}{2\pi s^2}\left[z_\alpha - z_{cv}\right].\end{aligned} \tag{3.35}$$

Since z_{cv} is defined only by conserved quantities of the equations of motion, it is a fixed point in space ($\dot{z}_{cv} = 0$), these equations can be easily integrated:

$$z_\alpha - z_{cv} = K_\alpha e^{i\frac{\Gamma}{2\pi s^2}t}, \quad K_\alpha \in \mathbb{C}, \tag{3.36}$$

where $K_\alpha = z_\alpha\,(t=0) - z_{cv}$ for each vortex. Thus, each of the vortices rotates around the center of vorticity with an angular frequency of $\frac{\Gamma}{2\pi s^2}$.

Now, if $\Gamma = 0$, equations (3.35) become

$$\dot{z}_\alpha = \frac{1}{2\pi i s^2}\sum_{\beta=1}^{3}\Gamma_\beta z_\beta, \quad \forall\alpha \in \{1,2,3\}, \tag{3.37}$$

so each of the three vortices moves with the same velocity; the three of them move like a rigid body with velocity such that

$$|\dot{z}_\alpha|^2 = \frac{1}{4\pi^2 s^4}|\Gamma_1 z_1 + \Gamma_2 z_2 + \Gamma_3 z_3| = \frac{1}{4\pi^2 s^4}|Q + iP| = \frac{Q^2 + P^2}{4\pi^2 s^4}. \tag{3.38}$$

From the definition of the M invariant (3.21), it is possible to see that, for a system under these

conditions, $Q^2+P^2=-\left(\Gamma_1\Gamma_2+\Gamma_2\Gamma_3+\Gamma_3\Gamma_1\right)s^2$ and from $\Gamma=0$ it is easy to conclude that $Q^2+P^2=\frac{1}{2}\left(\Gamma_1^2+\Gamma_2^2+\Gamma_3^2\right)s^2$. Therefore, the three vortices travel in parallel, as a rigid body, with linear velocity $\sqrt{\frac{\Gamma_1^2+\Gamma_2^2+\Gamma_3^2}{8\pi^2 s^2}}$.

To prove the second point of the theorem it is necessary to first derive an equation for the dynamics of Δ. Using the fundamental brackets $\{x_\alpha,x_\beta\}=0=\{y_\alpha,y_\beta\}$, $\{x_\alpha,y_\beta\}=-\{y_\beta,x_\alpha\}=\Gamma_\beta^{-1}\delta_{\alpha\beta}$ and the fact that $2\Delta=x_1y_2+x_2y_3+x_3y_1-x_1y_3-x_3y_2-x_2y_1$, it is possible to calculate the following Poisson brackets:

$$\begin{cases}\left\{s_1^2,2\Delta\right\}=\left(\dfrac{1}{\Gamma_2}-\dfrac{1}{\Gamma_3}\right)s_1^2+\left(\dfrac{1}{\Gamma_2}+\dfrac{1}{\Gamma_3}\right)\left(s_2^2-s_3^2\right)\\ \left\{s_2^2,2\Delta\right\}=\left(\dfrac{1}{\Gamma_3}-\dfrac{1}{\Gamma_1}\right)s_2^2+\left(\dfrac{1}{\Gamma_3}+\dfrac{1}{\Gamma_1}\right)\left(s_3^2-s_1^2\right)\\ \left\{s_3^2,2\Delta\right\}=\left(\dfrac{1}{\Gamma_1}-\dfrac{1}{\Gamma_2}\right)s_3^2+\left(\dfrac{1}{\Gamma_1}+\dfrac{1}{\Gamma_2}\right)\left(s_1^2-s_2^2\right)\end{cases}. \tag{3.39}$$

With these it becomes easy to deduce a dynamical equation for Δ,

$$\begin{aligned}\frac{d\Delta}{dt}=\{\Delta,H\}&=-\frac{1}{4\pi}\left[\frac{\Gamma_2\Gamma_3}{s_1^2}\left\{\Delta,s_1^2\right\}+\frac{\Gamma_3\Gamma_1}{s_2^2}\left\{\Delta,s_2^2\right\}+\frac{\Gamma_1\Gamma_2}{s_3^2}\left\{\Delta,s_3^2\right\}\right]\\&=-\frac{1}{8\pi}\left[\frac{s_3^2-s_2^2}{s_1^2}\left(\Gamma_2+\Gamma_3\right)+\frac{s_1^2-s_3^2}{s_2^2}\left(\Gamma_3+\Gamma_1\right)+\frac{s_2^2-s_1^2}{s_3^2}\left(\Gamma_1+\Gamma_2\right)\right],\end{aligned} \tag{3.40}$$

which should vanish for any collinear configuration in relative equilibrium.

■

The stability of these equilibria is a much more sensitive subject, and depends mostly on the values of the circulations of the vortices. Aref [17] developed an extensive study of the stability of all the possible equilibria of the 3-vortex problem.

There is yet another interesting solution for the 3 vortices system that one can analyze with the formalism here used: the self-similar collapse of the vortices. First, however, one needs to mathematically define the concept of self-similar motion:

Definition 3.1.3 (Self-similar motion)**.** A system of vortices is said to evolve self-similarly if $z_\alpha(t)=\lambda_\alpha f(t)$ for all $\alpha=1,\ldots,n$, where $\lambda\in\mathbb{C}$ are complex-valued scale factors and $f(t)$ is a complex-valued

function of time.

The self-similar collapse of 3 vortices is easily analyzed in terms of the intervortical distances s_1^2, s_2^2 and s_3^2. If the collapse is self-similar, the ratios between the sides of the triangle formed by the positions of the vortices must remain constant. Therefore, one can define the constant ratios

$$\lambda_1 = \frac{s_3^2}{s_2^2}, \qquad \lambda_2 = \frac{s_1^2}{s_2^2}. \tag{3.41}$$

The Hamiltonian (3.22) for the system can be re-written as

$$\tilde{H} = \exp\left(-\frac{4\pi H}{\Gamma_1\Gamma_2\Gamma_3}\right) = \left(s_1^2\right)^{1/\Gamma_1}\left(s_2^2\right)^{1/\Gamma_2}\left(s_3^2\right)^{1/\Gamma_3} = \lambda_1^{1/\Gamma_3}\lambda_2^{1/\Gamma_1}\left(s_2^2\right)^{\frac{1}{\Gamma_1}+\frac{1}{\Gamma_2}+\frac{1}{\Gamma_3}}, \tag{3.42}$$

and since $\dot{H} = 0 \Rightarrow \dot{\tilde{H}} = 0$, one has that

$$\dot{\tilde{H}} = 0 \Leftrightarrow \lambda_1^{1/\Gamma_3}\lambda_2^{1/\Gamma_1}\left(s_2^2\right)^{\frac{1}{\Gamma_1}+\frac{1}{\Gamma_2}+\frac{1}{\Gamma_3}-1}\left(\frac{1}{\Gamma_1}+\frac{1}{\Gamma_2}+\frac{1}{\Gamma_3}\right)\frac{d\left(s_2^2\right)}{dt} = 0. \tag{3.43}$$

Therefore, for the Hamiltonian to be conserved, one must have $\frac{1}{\Gamma_1}+\frac{1}{\Gamma_2}+\frac{1}{\Gamma_3} = 0$, since all the other multiplicative terms of the equation must be non-zero for some time in the evolution of the system.

The other invariant of the system, M (3.23), yields, for a self-similar motion of the system,

$$M = \Gamma_2\Gamma_3 s_1^2 + \Gamma_1\Gamma_3 s_2^2 + \Gamma_1\Gamma_2 s_3^2 = \left(\Gamma_2\Gamma_3\lambda_2 + \Gamma_1\Gamma_3 + \Gamma_1\Gamma_2\lambda_1\right)s_2^2. \tag{3.44}$$

Since in the moment of collapse one has $s_2^2 = 0$, M must be zero at that time, and thus M must be zero during the whole time evolution of the system.

Using the ratios (3.41), the dynamical equations for the intervortical distances can be re-written as

$$\begin{cases} \dfrac{d\left(s_2^2\right)}{dt} = \dfrac{2}{\pi}\Gamma_1\Delta\left(\dfrac{\lambda_1-1}{\lambda_1\lambda_2}\right)\dfrac{1}{s_2^2} \\ \dfrac{d\left(s_2^2\right)}{dt} = \dfrac{2}{\pi}\Gamma_2\Delta\left(\dfrac{\lambda_2-\lambda_1}{\lambda_1\lambda_2}\right)\dfrac{1}{s_2^2} \\ \dfrac{d\left(s_2^2\right)}{dt} = \dfrac{2}{\pi}\Gamma_3\Delta\left(\dfrac{1-\lambda_2}{\lambda_1\lambda_2}\right)\dfrac{1}{s_2^2} \end{cases}, \tag{3.45}$$

which give the following relations

$$\Gamma_1\left(\lambda_1-1\right) = \Gamma_2\left(\lambda_2-\lambda_1\right) = \Gamma_3\left(1-\lambda_2\right). \tag{3.46}$$

Writing $\Delta = sgn\left(\Delta\right)|\Delta|$ and making use of one of Henon's formulas for the area of the triangle,

$$\begin{aligned} 4|\Delta| &= \sqrt{4\left(s_1^2s_2^2+s_1^2s_3^2+s_2^2s_3^3\right)-\left(s_1^2+s_2^+s_3^2\right)^2} = \\ &= \sqrt{4\left(\lambda_2+\lambda_1\lambda_2+\lambda_1\right)s_2^4-\left(\lambda_1+1+\lambda_2\right)^2s_2^4} \\ &= s_2^2\sqrt{2\left(\lambda_1+\lambda_2\right)-\left(\lambda_1-\lambda_2\right)^2-1} = \gamma s_2^2, \end{aligned} \tag{3.47}$$

if one defines $\Lambda = \frac{\Gamma_2}{2\pi}\left(\frac{\lambda_1-\lambda_2}{\lambda_1\lambda_2}\right)\gamma$, the dynamical equation for s_2^2 can be written as

$$\frac{d\left(s_2^2\right)}{dt} = -sgn\left(\Delta\right)\Lambda. \tag{3.48}$$

This equation has the simple solution

$$s_2(t) = \sqrt{-sgn(\Delta)\Lambda t + s_2^2(0)}. \tag{3.49}$$

So, if $sgn(\Delta)\Lambda > 0$, the self-similar collapse should happen at time $t^* = s_2^2(0)/\Lambda$; if $sgn(\Delta)\Lambda < 0$, then the configuration expands indefinitely.

Theorem 3.1.4 (Self-similar collapse of the 3 vortices system)**.** *The self-similar collapse of the 3 vortices system happens if and only if*

(i) $\frac{1}{\Gamma_1} + \frac{1}{\Gamma_2} + \frac{1}{\Gamma_3} = 0$;

(ii) $M = 0$;

(iii) *the initial vortex configuration is not an equilibrium;*

(iv) $sgn(\Delta)\Lambda > 0$

Proof. The necessity of these conditions has been shown beforehand, while analyzing what happens in a situation where the three vortices collide self-similarly. One now needs to show that these conditions are also sufficient to guarantee the collapse. In fact, (i) and (ii) are just the conditions for self-similar motion, while (iii) guarantees that the intervortical distances change in time.

Using the triangle inequalities and trilinear coordinates

$$b_\alpha = \frac{s_\alpha}{\Gamma_\alpha}, \quad \alpha = 1, 2, 3, \tag{3.50}$$

it is possible to show that regions in the (b_1, b_2, b_3) space corresponding to physical acceptable solutions are bounded by conic sections satisfying

$$(\Gamma_1 b_1)^2 + (\Gamma_2 b_2)^2 + (\Gamma_3 b_3)^2 \leq 2(\Gamma_1\Gamma_2 b_1 b_2 + \Gamma_2\Gamma_3 b_2 b_3 + \Gamma_3\Gamma_1 b_3 b_1). \tag{3.51}$$

From (i), one finds that $\Gamma_3 < 0$. Furthermore, (ii) gives the identity $b_1 + b_2 + b_3 = 0$ and therefore the phase trajectories can be analyzed in the (b_1, b_2) plane, with $b_3 = -(b_1 + b_2)$. Using this in (3.51) yields a standard equation for a degenerate conic section defining a wedge-shaped region.

In fact, from the Hamiltonian, it is possible to write a function

$$\tilde{f}(b_1, b_2) = b_1^{1/\Gamma_1} b_2^{1/\Gamma_2} (b_1 + b_2)^{1/\Gamma_3} = b_1^{1/\Gamma_1} b_2^{1/\Gamma_2} (b_1 + b_2)^{-1/\Gamma_1 - 1/\Gamma_2}, \tag{3.52}$$

such that each level curve of $\tilde{f}$ is a phase trajectory of the vortex system. One can notice that any line of positive slope in the (b_1, b_2) that goes through the origin is a phase curve of $\tilde{f}$. Thus, all level curves of $\tilde{f}$ satisfy $b_2 = \lambda b_1$ for some $\lambda > 0$, corresponding to a level $1/\theta$ such that $\theta = (1 + \lambda)^{1/\Gamma_1} (1 + \lambda^{-1})^{1/\Gamma_2}$.

The minimum value of θ is obtained for $\lambda = \frac{\Gamma_1}{\Gamma_2}$ and each point on this trajectory actually corresponds to a triangular configuration that is rotating rigidly. The lines that form the boundary of the wedge-like region of physical acceptable solutions are also formed by equilibrium points of the system, each of them relating to some collinear configuration of vortices that is rotating rigidly.

All of these are, as seen before, relative equilibria of the system and therefore the initial configuration will not lie on any of these lines if the system collapses. Therefore, the collapsing states should lie in the remaining phase trajectories. Since $b_2 = \lambda b_1$ and $b_3 = -(1 + \lambda) b_1$, s_2 and s_3 must be proportional to s_1 and the right-hand sides of equations (3.27) are all constant. If $sgn(\Delta)\Lambda > 0$, the collapse occurs as it was shown beforehand.

■

3.2 VISCOUS VORTICES

While the inviscid case has been thoroughly studied throughout the years, the study of point vortices in a viscous environment still has a long way to go. By considering fluids with non-zero viscosity the complexity of the problem grows, nevertheless, one expects the results to come much closer to what we find in Nature, as most fluids exhibit viscous properties.

3.2.1 Lamb-Oseen Vortex

In a viscous environment, the dynamics are described by the Navier-Stokes equation, which was deduced in Section 2.1. By formulating the problem through the vorticity description in the unbound 2-dimensional plane, for a single point vortex of circulation Γ located at z_0 one arrives at

$$\begin{cases} \dfrac{\partial \omega}{\partial t} + (\boldsymbol{u} \cdot \nabla)\,\omega = \nu \nabla^2 \omega \\ \omega\,(z, t=0) = \Gamma \delta\,(z - z_0) \end{cases}. \tag{3.53}$$

Solving this problems corresponds to finding the vorticity field caused by the point vortex described above. The exact solution is well-known and usually called the Lamb-Oseen vortex:

$$\omega\,(z,t) = \frac{\Gamma}{4\pi\nu t} \exp\left(-\frac{|z - z_0|^2}{4\nu t}\right), \tag{3.54}$$

which generates a velocity field

$$\dot{z}^*\,(z,t) = \frac{\Gamma}{2\pi i}\frac{1}{z}\left[1 - \exp\left(-\frac{|z - z_0|^2}{4\nu t}\right)\right]. \tag{3.55}$$

As these vorticity and velocity profiles make clear, the time evolution of the Lamb-Oseen vortex is such that the vorticity is diffused radially outward with a Gaussian profile. This vorticity diffusion can also be quantified by the radius of the vortex core $r = \sqrt{4\nu t}$. Even though the Lamb-Oseen vortex is an exact and simple solution of the vorticity equation, explicit analytical solutions for a general initial condition are still not available.

One important result on the Lamb-Oseen vortex is that it is an asymptotically stable attracting solution of the vorticity equation for any integrable initial vorticity configuration, as was proven by Gallay & Wayne [24]. The superposition of n point vortices - $\omega\,(z, t=0) = \sum_{\alpha=1}^{n} \Gamma_\alpha \delta\,(z - z_\alpha)$ - is one such configuration.

3.2.2 Multi-Gaussian Model

This idea gave rise to the multi-Gaussian model of point vortices, that assumes that the vorticity field is a superposition of Lamb-Oseen vortices at all times: each of the initial point vortices spread axisymmetrically as if it they were isolated, modeling the diffusive term in the vorticity equation ($\nu\nabla^2\omega$); the center position of each vortex, however, is affected by all the other vortices and moves according to the velocity field created by them, as it is expected due to the convective term $(\boldsymbol{u}\cdot\nabla)\,\omega$.

Gallay showed, in a more recent work [25], that under certain conditions, the solution of the Navier-Stokes equation in the inviscid limit $\nu \to 0$ for δ-Dirac initial conditions converges to a superposition of Lamb-Oseen vortices. This provides yet another reason for the viability of the multi-Gaussian model in the description of fluids.

Thus, for the study of viscous point vortices, we will use the multi-Gaussian model. The vorticity field for a system of n vortices located at z_α, $\alpha = 1, 2, \ldots, n$ is therefore

$$\omega\left(z,t\right) = \frac{1}{4\pi\nu t}\sum_{\alpha=1}^{n}\Gamma_\alpha \exp\left(-\frac{|z-z_\alpha|^2}{4\nu t}\right), \tag{3.56}$$

and gives rise to a velocity field

$$\dot{z}^*\left(z,t\right) = \frac{1}{2\pi i}\sum_{\alpha=1}^{n}\frac{\Gamma_\alpha}{z-z_\alpha}\left[1-\exp\left(-\frac{|z-z_\alpha|^2}{4\nu t}\right)\right]. \tag{3.57}$$

Hence, the equations of motion for the vortex α are

$$\dot{z}^*_\alpha = \frac{1}{2\pi i}\sum_{\beta\neq\alpha}^{n}\frac{\Gamma_\beta}{z_\alpha-z_\beta}\left[1-\exp\left(-\frac{|z_\alpha-z_\beta|^2}{4\nu t}\right)\right]. \tag{3.58}$$

One can also write a kind of generalized Hamiltonian, a function G such that Hamilton's equations hold. Such function should coincide with the classical Hamiltonian (3.2) in the limit $\nu \to 0$. Suppose G is of the form

$$G = \frac{1}{2\pi} \sum_{\alpha=1}^{n} \sum_{\beta>\alpha} \Gamma_\alpha \Gamma_\beta F(\chi, t), \tag{3.59}$$

where $\chi(z_\alpha, z_\beta) = \sqrt{(x_\alpha - x_\beta)^2 + (y_\alpha - y_\beta)^2}$.

Therefore G shall satisfy

$$\Gamma_\alpha \dot{z}_\alpha^* = \Gamma_\alpha \dot{x}_\alpha - i\Gamma_\alpha \dot{y}_\alpha = \frac{\partial G}{\partial y_\alpha} + i\frac{\partial G}{\partial x_\alpha} = 2i\frac{\partial G}{\partial z_\alpha}. \tag{3.60}$$

On the other hand, differentiating (3.59),

$$\begin{aligned}
\frac{\partial G}{\partial z_\gamma} &= -\frac{1}{2\pi} \sum_{\alpha=1}^{n} \sum_{\beta>\alpha} \Gamma_\alpha \Gamma_\beta \frac{\partial F}{\partial \chi} \frac{\partial \chi}{\partial z_\alpha} \frac{\partial z_\alpha}{\partial z_\gamma} \\
&= -\frac{1}{2\pi} \sum_{\alpha=1}^{n} \sum_{\beta>\alpha} \Gamma_\alpha \Gamma_\beta \frac{\partial F}{\partial \chi} \frac{\partial \chi}{\partial z_\alpha} \delta_{\alpha\gamma} \\
&= -\frac{1}{2\pi} \sum_{\alpha=1}^{n} \sum_{\beta>\alpha} \Gamma_\alpha \Gamma_\beta \frac{\partial F}{\partial \chi} \left[(\frac{1}{2\chi} \left(z_\alpha^* - z_\beta^* \right) \right] \delta_{\alpha\gamma} \\
&= -\frac{1}{4\pi} \sum_{\beta\neq\gamma} \frac{\Gamma_\gamma \Gamma_\beta}{\chi} \left(z_\gamma^* - z_\beta^* \right) \frac{\partial F}{\partial \chi}.
\end{aligned} \tag{3.61}$$

Finally, by comparing this expression with $\frac{\partial G}{\partial z_\alpha} = \frac{\Gamma_\alpha z_\alpha^*}{2i}$ and using the equations of motion (3.58), it is possible to see that F must satisfy the differential equation

$$\frac{\partial F}{\partial \chi} = \frac{1}{\chi} \left[1 - \exp\left(-\frac{\chi^2}{4\nu t} \right) \right], \tag{3.62}$$

and in the limit $\nu \to 0$, one can retrieve the classical Hamiltonian for a system of inviscid vortices. Solving this equation for F and plugging it in on G, one obtains the analytical expression for the generalized Hamiltonian, which will be a measure of the energy of the system:

$$G = \frac{1}{2\pi} \sum_{\alpha=1}^{n} \sum_{\beta>\alpha} \Gamma_\alpha \Gamma_\beta \left[\log\left(\ell_{\alpha\beta}\right) - \int_0^{\ell_{\alpha\beta}} \frac{1}{s} \exp\left(-\frac{s^2}{4\nu t}\right) ds \right], \tag{3.63}$$

which will now vary in time, and therefore is not conserved due to the viscous dissipation of energy:

$$\frac{dG}{dt} = \frac{\partial G}{\partial t} = -\frac{1}{2\pi} \sum_{\alpha=1}^{n} \sum_{\beta>\alpha} \Gamma_\alpha \Gamma_\beta \int_0^{\ell_{\alpha\beta}} \frac{1}{s} \exp\left(-\frac{s^2}{4\nu t}\right) ds. \tag{3.64}$$

3.2.3 Conserved Quantities

The viscous n-vortex at hand problem cannot be analyzed via classical Hamiltonian methods: since viscosity dissipates energy, it isn't possible to write a classical Hamiltonian for the system. However, some of the conservation laws analyzed in the inviscid environment (in Section 3.1.1) still hold for viscous flows. In particular, the linear impulse, $Q + iP$, and angular impulse, I, are conserved:

$$\begin{aligned} \frac{d}{dt}\left(Q + iP\right) = \frac{d}{dt}\left(\sum_{\alpha=1}^{n} \Gamma_\alpha z_\alpha\right) = \sum_{\alpha=1}^{n} \Gamma_\alpha \dot{z}_\alpha = \\ = \frac{1}{2\pi i} \sum_{\alpha=1}^{n} \sum_{\beta\neq\alpha} \frac{\Gamma_\alpha \Gamma_\beta}{z_\alpha^* - z_\beta^*} \left[1 - \exp\left(-\frac{|z_\alpha - z_\beta|^2}{4\nu t}\right)\right] = 0, \end{aligned} \tag{3.65}$$

since $\left(z_\alpha^* - z_\beta^*\right)^{-1} = -\left(z_\beta^* - z_\alpha^*\right)^{-1}$ and therefore each term of the sum will cancel with its' symmetric.

$$\begin{aligned}
\frac{dI}{dt} &= \frac{d}{dt}\left(\sum_{\alpha=1}^{n}\Gamma_\alpha|z_\alpha|^2\right) = \frac{d}{dt}\left(\sum_{\alpha=1}^{n}\Gamma_\alpha z_\alpha z_\alpha^*\right) = \sum_{\alpha=1}^{n}\Gamma_\alpha\left(\dot{z}_\alpha z_\alpha^* + z_\alpha\dot{z}_\alpha^*\right) = \\
&= \frac{1}{2\pi i}\sum_{\alpha=1}^{n}\sum_{\beta\neq\alpha}\Gamma_\alpha\Gamma_\beta\left[-\frac{z_\alpha^*}{z_\alpha^*-z_\beta^*}+\frac{z_\alpha}{z_\alpha-z_\beta}\right]\left[1-\exp\left(-\frac{|z_\alpha-z_\beta|^2}{4\nu t}\right)\right] = \\
&= \frac{1}{\pi}\sum_{\alpha=1}^{n}\sum_{\beta\neq\alpha}\Gamma_\alpha\Gamma_\beta Im\left(\frac{z_\alpha}{z_\alpha-z_\beta}\right)\left[1-\exp\left(-\frac{|z_\alpha-z_\beta|^2}{4\nu t}\right)\right] = \\
&= \frac{1}{\pi}\sum_{\alpha=1}^{n}\sum_{\beta\neq\alpha}\frac{\Gamma_\alpha\Gamma_\beta}{|z_\alpha-z_\beta|^2}Im\left(z_\alpha\left(z_\alpha^*-z_\beta^*\right)\right)\left[1-\exp\left(-\frac{|z_\alpha-z_\beta|^2}{4\nu t}\right)\right] = \\
&= -\frac{1}{\pi}\sum_{\alpha=1}^{n}\sum_{\beta\neq\alpha}\frac{\Gamma_\alpha\Gamma_\beta}{|z_\alpha-z_\beta|^2}Im\left(z_\alpha z_\beta^*\right)\left[1-\exp\left(-\frac{|z_\alpha-z_\beta|^2}{4\nu t}\right)\right] = \\
&= 0,
\end{aligned} \tag{3.66}$$

since $Im\left(z_\alpha z_\beta^*\right) = -Im\left(z_\beta z_\alpha^*\right)$ and thus each term of the sum will cancel with its' symmetric.

Remark: The quantity M defined in (3.21) is also conserved since it is a combination of the conserved quantities Q, P and I.

3.2.4 Dynamics of 2 Vortices

Consider now a system comprised of two Lamb-Oseen vortices evolving according to (3.58). First, one can notice that the distance $D = |z_1 - z_2|$ between the two vortices remains constant, as in the inviscid case. To condensate the discussion hereafter, define $h\left(z_1, z_2, t\right) = 1 - \exp\left(-\frac{|z_1-z_2|^2}{4\nu t}\right)$.

$$\begin{aligned}
\frac{d\left(D^2\right)}{dt} &= \frac{d}{dt}\left[\left(z_1-z_2\right)\left(z_1-z_2\right)^*\right] = \left(\dot{z}_1-\dot{z}_2\right)\left(z_1-z_2\right)^* + \left(z_1-z_2\right)\left(\dot{z}_1-\dot{z}_2\right)^* \\
&= \frac{h\left(z_1,z_2,t\right)}{2\pi i}\left[-\left(\frac{\Gamma_2}{\left(z_1-z_2\right)^*}+\frac{\Gamma_1}{\left(z_2-z_1\right)^*}\right)\left(z_1-z_2\right)^* + \left(z_1-z_2\right)\left(\frac{\Gamma_2}{z_1-z_2}+\frac{\Gamma_1}{z_2-z_1}\right)\right] \\
&= \frac{h\left(z_1,z_2,t\right)}{2\pi i}\left[-\left(\Gamma_2-\Gamma_1\right)+\left(\Gamma_2-\Gamma_1\right)\right] \\
&= 0.
\end{aligned} \tag{3.67}$$

So, in fact, since D^2 is constant, h depends only on time and the initial positions of the vortices. For some set of initial positions $z_1\left(0\right), z_2\left(0\right)$, one can therefore write $h\left(t\right) = h\left(z_1, z_2, t\right)$.

Using these facts, specifying the motion equations for the two vortices yields

$$\begin{cases} \dot{z}_1 = \dfrac{i\Gamma_2}{2\pi D^2}\left(z_1 - z_2\right) h\left(t\right) \\ \dot{z}_2 = \dfrac{i\Gamma_1}{2\pi D^2}\left(z_2 - z_1\right) h\left(t\right) \end{cases}. \tag{3.68}$$

From the conservation of the linear impulse one has $\Gamma_1 \dot{z}_1 + \Gamma_2 \dot{z}_2 = 0$ and therefore

$$\Gamma_1 z_1\left(t\right) + \Gamma_2 z_2\left(t\right) = \Gamma_1 z_1\left(0\right) + \Gamma_2 z_2\left(0\right), \quad \forall t \in \mathbb{R} \tag{3.69}$$

As in the inviscid case, one defines new variables $z_+ = z_1 + z_2,\ z_- = z_1 - z_2$. The differential equations for z_+ and z_- are

$$\begin{cases} \dot{z}_+ = \dfrac{i\left(\Gamma_2 - \Gamma_1\right)}{2\pi D^2} h\left(t\right) z_- \\ \dot{z}_- = \dfrac{i\left(\Gamma_1 + \Gamma_2\right)}{2\pi D^2} h\left(t\right) z_- \end{cases}. \tag{3.70}$$

Once again, there are two possible cases depending on the values of Γ_1 and Γ_2.

a) $\boldsymbol{\Gamma_1 + \Gamma_2 = 0}$

The integration on the variables z_+ and z_- is easy, yielding

$$\begin{cases} z_+ = z_1\left(0\right) + z_2\left(0\right) + \dfrac{i\left(\Gamma_2 - \Gamma_1\right)}{2\pi D^2}\left[z_1\left(0\right) - z_2\left(0\right)\right] \displaystyle\int h\left(t\right) dt, \\ z_- = z_1\left(0\right) - z_2\left(0\right) \end{cases}, \tag{3.71}$$

where $\int h\left(t\right) dt = t - \int \exp\left(-\frac{D^2}{4\nu t}\right) dt$. This integral cannot be expressed in terms of analytical functions, however it can be related to the well-known Exponential integral function. The positions of the vortices at all times are given by

$$\begin{cases} z_1(t) = z_1(0) + \dfrac{i\Gamma_1}{2\pi D^2}\left[z_2(0) - z_1(0)\right]\left[t - \displaystyle\int \exp\left(-\frac{D^2}{4\nu t}\right) dt\right] \\ z_2(t) = z_2(0) - \dfrac{i\Gamma_2}{2\pi D^2}\left[z_2(0) - z_1(0)\right]\left[t - \displaystyle\int \exp\left(-\frac{D^2}{4\nu t}\right) dt\right] \end{cases}, \tag{3.72}$$

and as in the inviscid case, the vortices travel in straight lines, parallel to one another; however their velocity is not constant and decreases with time because $\frac{dh}{dt} = -\frac{D^2}{4\nu t^2}\exp\left(-\frac{D^2}{4\nu t}\right)$.

b) $\boldsymbol{\Gamma_1 + \Gamma_2 \neq 0}$

Although the solution is a little bit more complicated than in the previous case, one can also find the solution in terms of the integral $\int h(t)\, dt$. Integrating for z_- yields

$$z_- = \left[z_1(0) - z_2(0)\right] \exp\left(\frac{i\left(\Gamma_1 + \Gamma_2\right)}{2\pi D^2} \int h(t)\, dt\right). \tag{3.73}$$

Writing $\theta = \left(\Gamma_1 + \Gamma_2\right) / \left(2\pi D^2\right)$ and using the conservation of linear impulse, it is possible to write explicit expressions for the positions of both vortices:

$$\begin{cases} z_1(t) = \dfrac{1}{\Gamma_1 + \Gamma_2}\left[\Gamma_1 z_1(0) + \Gamma_2 z_2(0) + \Gamma_2\left[z_1(0) - z_2(0)\right] e^{i\theta t} e^{-i\theta \int \exp\left(-\frac{D^2}{4\nu t}\right) dt}\right] \\ z_2(t) = \dfrac{1}{\Gamma_1 + \Gamma_2}\left[\Gamma_1 z_1(0) + \Gamma_2 z_2(0) - \Gamma_1\left[z_1(0) - z_2(0)\right] e^{i\theta t} e^{-i\theta \int \exp\left(-\frac{D^2}{4\nu t}\right) dt}\right] \end{cases}. \tag{3.74}$$

Once again, the vortices rotate around the center of vorticity of the system, but this time with a velocity that decreases with time.

3.2.5 Dynamics of 3 Vortices

The dynamics of a system of three vortices in a viscous environment is a much more difficult problem to analyze than the inviscid case. Thus, the aim of this section is just to provide some intuition on how the dynamics are distinct from those in an environment with no viscosity at all.

As in the inviscid case, one can write the equations of motion for each individual vortex from (3.58) or

write the differential equations for the intervortex separations. Once again, to condensate the discussion, one can write $s_1^2 = |z_2 - z_3|^2$, $s_2^2 = |z_1 - z_3|^2$, $s_3^2 = |z_1 - z_2|^2$ and $h\left(s_\alpha^2, t\right) = 1 - \exp\left(-\frac{s_\alpha^2}{4\nu t}\right)$, $\alpha \in \{1, 2, 3\}$. This yields, after extensive calculations, the following system of differential equations:

$$\begin{cases} \dfrac{d\left(s_1^2\right)}{dt} = \dfrac{2\Gamma_1}{\pi}\Delta\left[\dfrac{1}{s_2^2}h\left(s_3^2, t\right) - \dfrac{1}{s_3^2}h\left(s_2^2, t\right)\right] \\ \dfrac{d\left(s_2^2\right)}{dt} = \dfrac{2\Gamma_2}{\pi}\Delta\left[\dfrac{1}{s_3^2}h\left(s_1^2, t\right) - \dfrac{1}{s_1^2}h\left(s_3^2, t\right)\right] \\ \dfrac{d\left(s_3^2\right)}{dt} = \dfrac{2\Gamma_3}{\pi}\Delta\left[\dfrac{1}{s_1^2}h\left(s_2^2, t\right) - \dfrac{1}{s_2^2}h\left(s_1^2, t\right)\right] \end{cases}, \tag{3.75}$$

where Δ is, once again, the area of the triangle defined by the positions of the three vortices, affected by the sign of the permutation of the indices.

In the inviscid case, the only fixed equilibrium configurations were collinear states. On an viscous environment, one can see, from the same arguments, that if fixed equilibria exist, they must also correspond to collinear configurations of the vortices. It suffices to analyze the equation for one of the vortices, for example, for $\alpha = 1$, the equation of motion reads

$$\dot{z}_1^* = \frac{1}{2\pi i}\left[\frac{\Gamma_2}{z_1 - z_2}h\left(s_3^2, t\right) + \frac{\Gamma_3}{z_1 - z_3}h\left(s_2^2, t\right)\right], \tag{3.76}$$

and therefore, since for any fixed equilibrium one has to have $\dot{z}_\alpha = 0$ for all α and all times, the following expression must hold true for all times:

$$\begin{aligned} &\frac{\Gamma_2}{z_1 - z_2}h\left(s_3^2, t\right) + \frac{\Gamma_3}{z_1 - z_3}h\left(s_2^2, t\right) = 0 \Leftrightarrow \\ \Leftrightarrow \quad &\Gamma_2\left(z_1 - z_3\right)h\left(s_3^2, t\right) + \Gamma_3\left(z_1 - z_2\right)h\left(s_2^2, t\right) = 0. \end{aligned} \tag{3.77}$$

Excluding the unphysical case of infinite viscosity (which would obviously correspond to a fixed equilibrium for any vortex configuration, as the vorticity would be 0 everywhere), this expression implies that for

a fixed equilibrium, $z_1 - z_2$ and $z_1 - z_3$ must be scalar multiples of one another at all times, and therefore the vortices have to be in a collinear configuration at all times.

While in an inviscid environment there are some collinear configurations which correspond to fixed equilibria, the same does not hold true in the viscous case. In fact, these configurations constitute unstable equilibria of the inviscid problem and the presence of viscosity triggers the instability of the system and the vortices start rotating unsteadily. This was shown in the recent work of Jing et al. [26], where they give the full details of the problem.

Relative equilibria are, however, permitted in viscous environments. If one allows the vortex configuration to rotate or suffer translations in time, while maintaining its' geometrical shape, the only constraints are that the intervortex separations remain constant for all times. From this condition, the equations (3.75) give two possibilities for characterizing relative equilibria: either $\Delta = 0$ or the three expressions between square brackets should go to zero at all times.

The first case, $\Delta = 0$, corresponds to collinear configurations. For these configurations, one can only have a relative equilibrium configuration if the three vortices remain collinear at all times. To analyze that, one needs first to find an equation for the dynamics of Δ and check if it is possible to have $\dot{\Delta} = 0$ for all times for collinear configurations.

The second case, gives the conditions

$$\begin{cases} \frac{1}{s_2^2} h\left(s_3^2, t\right) - \frac{1}{s_3^2} h\left(s_2^2, t\right) = 0 \\ \frac{1}{s_3^2} h\left(s_1^2, t\right) - \frac{1}{s_1^2} h\left(s_3^2, t\right) = 0 \\ \frac{1}{s_1^2} h\left(s_2^2, t\right) - \frac{1}{s_2^2} h\left(s_1^2, t\right) = 0 \end{cases}, \tag{3.78}$$

which should be verified for all t. In particular, these should hold at $t = 0$, there h goes to 1 whichever may the s_α be. Therefore, if non-collinear relative equilibria exist, they must be equilateral triangles such that $s_1^2 = s_2^2 = s_3^2 = s^2$ and one can write $h(s_\alpha^2, t) = h\,(t) = 1 - \exp\left(-\frac{s^2}{4\nu t}\right)$.

The analysis is similar to the inviscid case once again:

$$\begin{aligned}\dot{z}_\alpha &= -\frac{1}{2\pi i}\sum_{\beta\neq\alpha}\frac{\Gamma_\beta}{(z_\alpha - z_\beta)^*}h(t) = -\frac{1}{2\pi i}\sum_{\beta\neq\alpha}\frac{\Gamma_\beta (z_\alpha - z_\beta)}{(z_\alpha - z_\beta)^* (z_\alpha - z_\beta)}h(t) = \\ &= -\frac{1}{2\pi i s^2}\sum_{\beta\neq\alpha}\left[\Gamma_\beta (z_\alpha - z_\beta)\right]h(t) = -\frac{1}{2\pi i s^2}\sum_{\beta\neq\alpha}\left[\Gamma_\beta z_\alpha - \Gamma_\beta z_\beta + \Gamma_\alpha z_\alpha - \Gamma_\alpha z_\alpha\right]h(t) \\ &= -\frac{1}{2\pi i s^2}\left[\sum_{\beta=1}^{3}\Gamma_\beta z_\alpha - \sum_{\beta=1}^{3}\Gamma_\beta z_\beta\right]h(t).\end{aligned} \tag{3.79}$$

So, if $\Gamma = \sum_{\beta=1}^{3}\Gamma_\beta = 0$, one gets $\dot{z}_\alpha = -\frac{ih(t)}{2\pi s^2}\sum_{\beta=1}^{3}\Gamma_\beta z_\beta$, so the three vortices suffer a translation in time with the same velocity:

$$|\dot{z}_\alpha|^2 = \frac{h^2(t)}{4\pi^2 s^4}|\Gamma_1 z_1 + \Gamma_2 z_2 + \Gamma_3 z_3| = \frac{h^2(t)}{4\pi^2 s^4}|Q + iP| = \frac{Q^2 + P^2}{4\pi^2 s^4}h^2(t). \tag{3.80}$$

As in the inviscid case, $Q^2 + P^2 = \frac{1}{2}\left(\Gamma_1^2 + \Gamma_2^2 + \Gamma_3^2\right)s^2$ and therefore, the three vortices travel in parallel, as a rigid body, with a linear velocity that decreases in time $|\dot{z}_\alpha| = \sqrt{\frac{\Gamma_1^2+\Gamma_2^2+\Gamma_3^2}{8\pi^2 s^2}}\left[1 - \exp\left(-\frac{s^2}{4\nu t}\right)\right]$.

If $\Gamma \neq 0$, one can define the center of vorticity of the system as before and get

$$\dot{z}_\alpha = -\frac{i\Gamma h(t)}{2\pi s^2}\sum_{\beta=1}^{3}\Gamma_\beta z_\beta\left[z_\alpha - z_{cv}\right]. \tag{3.81}$$

Once again, these equations can be easily integrated to yield

$$z_\alpha - z_{cv} = K_\alpha e^{i\frac{\Gamma}{2\pi s^2}\int\left[1-\exp\left(-\frac{s^2}{4\nu t}\right)\right]dt}, \quad K_\alpha \in \mathbb{C}, \tag{3.82}$$

where $K_\alpha = z_\alpha(t=0) - z_{cv}$ for each vortex. Therefore, each of the vortices rotates around the center of vorticity with an angular frequency of $\frac{\Gamma}{2\pi s^2}\left[1 - \exp\left(-\frac{s^2}{4\nu t}\right)\right]$, stopping completely at infinity.

These dynamics of the system are all self-similar, since the trajectory of each vortex evolves according to the same function. However, one can wonder if there are other self-similar motions of the 3-vortices systems, such as a the self-similar collapse, analogous to the inviscid case.

Suppose that the vortices have a self-similar motion and write $z_\alpha(t) = \lambda_\alpha g(t)$, $\alpha \in \{1,2,3\}$ for

some function $g(t)$ such that $g(0) = 1$. Therefore, λ_α are simply the initial positions of the vortices and differentiating with respect to time $\dot{z}_\alpha(t) = \lambda_\alpha \dot{g}(t)$ yields

$$\begin{aligned} & \lambda_\alpha \dot{g}(t) = -\frac{1}{2\pi i} \sum_{\beta \neq \alpha} \frac{\Gamma_\beta}{z_\alpha^* - z_\beta^*} \left[1 - \exp\left(-\frac{|z_\alpha - z_\beta|^2}{4\nu t}\right)\right] \Leftrightarrow \\ \Leftrightarrow \quad & \dot{g}(t)\, g^*(t) = -\frac{1}{2\pi i} \sum_{\beta \neq \alpha} \frac{\Gamma_\beta}{\lambda_\alpha \left(\lambda_\alpha^* - \lambda_\beta^*\right)} \left[1 - \exp\left(-\frac{|\lambda_\alpha - \lambda_\beta|^2 |g(t)|^2}{4\nu t}\right)\right]. \end{aligned} \tag{3.83}$$

This expression should hold true for all t. Also, since the left side is independent of α, the right side should also be independent of α. One can write down this expression for any pair of α's and, for example, equating this for $\alpha = 1, 2$ one arrives at the identity

$$\begin{aligned} & \frac{\Gamma_2}{\lambda_1 (\lambda_1^* - \lambda_2^*)} \left[1 - \exp\left(-\frac{|\lambda_1 - \lambda_2|^2 |g(t)|^2}{4\nu t}\right)\right] + \\ & \qquad \frac{\Gamma_3}{\lambda_1 (\lambda_1^* - \lambda_3^*)} \left[1 - \exp\left(-\frac{|\lambda_1 - \lambda_3|^2 |g(t)|^2}{4\nu t}\right)\right] = \\ = & \frac{\Gamma_1}{\lambda_2 (\lambda_2^* - \lambda_1^*)} \left[1 - \exp\left(-\frac{|\lambda_2 - \lambda_1|^2 |g(t)|^2}{4\nu t}\right)\right] + \\ & \qquad \frac{\Gamma_3}{\lambda_2 (\lambda_2^* - \lambda_3^*)} \left[1 - \exp\left(-\frac{|\lambda_2 - \lambda_3|^2 |g(t)|^2}{4\nu t}\right)\right], \end{aligned} \tag{3.84}$$

which should hold for all t. Since the exponential functions form an orthonormal basis, this can only happen if $|\lambda_1 - \lambda_2|^2 = |\lambda_1 - \lambda_3|^2 = |\lambda_2 - \lambda_3|^2$ and therefore the initial configuration has to be an equilateral triangle.

From the expression of the invariant M (3.23) for a system of 3 vortices, one can also write

$$\begin{aligned} & M = \Gamma_1 \Gamma_2 |z_1 - z_2|^2 + \Gamma_2 \Gamma_3 |z_2 - z_3|^2 + \Gamma_3 \Gamma_1 |z_3 - z_1|^2 \Leftrightarrow \\ \Leftrightarrow \quad & M = \left(\Gamma_1 \Gamma_2 |\lambda_1 - \lambda_2|^2 + \Gamma_2 \Gamma_3 |\lambda_2 - \lambda_3|^2 + \Gamma_3 \Gamma_1 |\lambda_3 - \lambda_1|^2\right) |g(t)|^2 \Leftrightarrow \\ \Leftrightarrow \quad & \frac{M}{\Gamma_1 \Gamma_2 \Gamma_3} = \left(\Gamma_3^{-1} |\lambda_1 - \lambda_2|^2 + \Gamma_1^{-1} |\lambda_2 - \lambda_3|^2 + \Gamma_2^{-1} |\lambda_3 - \lambda_1|^2\right) |g(t)|^2. \end{aligned} \tag{3.85}$$

Since $\frac{M}{\Gamma_1\Gamma_2\Gamma_3}$ is constant for all t, the right side of the above equation must also be constant for all t. There are two possibilities for this to hold true: either $|g(t)|^2$ is constant, which corresponds to the rigid motions analyzed beforehand, or $\Gamma_3^{-1}|\lambda_1-\lambda_2|^2+\Gamma_1^{-1}|\lambda_2-\lambda_3|^2+\Gamma_2^{-1}|\lambda_3-\lambda_1|^2=0$. From the fact that self-similar motions must begin as equilateral triangles, one has that, in particular, $\Gamma_1^{-1}+\Gamma_2^{-1}+\Gamma_3^{-1}=0$. So, if there exist other types of self-similar motions other than the rigid motion, those must satisfy this condition while having a non-constant $|g(t)|^2$.

From the conservation of the linear impulse, one can also write:

$$\begin{aligned}\frac{d}{dt}(Q+iP) &= \Gamma_1\lambda_1\dot{g}(t)+\Gamma_2\lambda_2\dot{g}(t)+\Gamma_3\lambda_3\dot{g}(t)\\ &= (\Gamma_1\lambda_1+\Gamma_2\lambda_2+\Gamma_3\lambda_3)\,\dot{g}(t)=0,\end{aligned} \tag{3.86}$$

hence, $\Gamma_1\lambda_1+\Gamma_2\lambda_2+\Gamma_3\lambda_3=0$. Analogously, from the conservation of angular impulse, one has

$$\begin{aligned}\frac{dI}{dt} &= \Gamma_1|\lambda_1|^2\frac{d}{dt}\left(|g(t)|^2\right)+\Gamma_2|\lambda_2|^2\frac{d}{dt}\left(|g(t)|^2\right)+\Gamma_3|\lambda_3|^2\frac{d}{dt}\left(|g(t)|^2\right)\\ &= \left(\Gamma_1|\lambda_1|^2+\Gamma_2|\lambda_2|^2+\Gamma_3|\lambda_3|^2\right)\frac{d}{dt}\left(|g(t)|^2\right)=0,\end{aligned} \tag{3.87}$$

and therefore $\Gamma_1|\lambda_1|^2+\Gamma_2|\lambda_2|^2+\Gamma_3|\lambda_3|^2=0$ because we are looking for non rigid self-similar motions.

But these two last conditions only hold for $\Gamma_1=\Gamma_2=\Gamma_3=0$, which is not possible as this is the same as if there were no vortices in the system. Therefore there are no other self-similar motions for the three-vortices problem other than rigid motions with an equilateral triangular configuration.

This excludes, in particular, the self-similar collapse that was possible in inviscid environments. In fact, it is possible to show that one never has a finite-time collapse in this viscous model. For that one first defines inter-vortical vectors for each pair of vortices:

$$q_1=z_2-z_3,\quad q_2=z_3-z_1,\quad q_3=z_1-z_2 \tag{3.88}$$

And the differential equations for these quantities are

$$\begin{cases} \dot{q}_1^* = \dfrac{1}{2\pi i}\left[\dfrac{\Gamma_2+\Gamma_3}{q_1}\left(1-e^{-\frac{|q_1|^2}{4\nu t}}\right)-\dfrac{\Gamma_1}{q_2}\left(1-e^{-\frac{|q_2|}{4\nu t}}\right)-\dfrac{\Gamma_1}{q_3}\left(1-e^{-\frac{|q_3|}{4\nu t}}\right)\right] \\ \dot{q}_2^* = \dfrac{1}{2\pi i}\left[\dfrac{\Gamma_1+\Gamma_3}{q_2}\left(1-e^{-\frac{|q_2|^2}{4\nu t}}\right)-\dfrac{\Gamma_2}{q_3}\left(1-e^{-\frac{|q_3|}{4\nu t}}\right)-\dfrac{\Gamma_2}{q_1}\left(1-e^{-\frac{|q_1|}{4\nu t}}\right)\right] \\ \dot{q}_3^* = \dfrac{1}{2\pi i}\left[\dfrac{\Gamma_1+\Gamma_2}{q_3}\left(1-e^{-\frac{|q_3|^2}{4\nu t}}\right)-\dfrac{\Gamma_3}{q_1}\left(1-e^{-\frac{|q_1|}{4\nu t}}\right)-\dfrac{\Gamma_3}{q_2}\left(1-e^{-\frac{|q_2|}{4\nu t}}\right)\right] \end{cases}. \tag{3.89}$$

Suppose now that there is a total collapse of the vortices at time $t = t_c > 0$ at the origin. Then one can write $q_k = (t_c - t)^{\gamma_k}\,\xi_k(t)$ with $\gamma_k > 0$ and $\xi_k(t_c) \neq 0$ for $k \in \{1,2,3\}$. The functions ξ_k and the exponents γ_k may be different for each k. Let γ_1 be the minimum of the exponents. Near $t \approx t_c$, the exponential terms in equations (3.89) can be approximated by the first terms in their Taylor series. For example,

$$1-\exp\left(-\frac{|q_1|^2}{4\nu t}\right) \approx \frac{|q_1|^2}{4\nu t} \approx \frac{|t-t_c|^2|\xi_1(t)|^2}{4\nu t}. \tag{3.90}$$

Therefore, the dynamical equation for q_1 near $t \approx t_c$ becomes (asymptotically)

$$\begin{aligned} &\gamma_1 (t_c-t)^{\gamma_1-1}\,\xi_1^*(t) + (t_c-t)^{\gamma_1}\,\dot{\xi}_1^*(t) = \\ &\quad = \frac{1}{2\pi i}\left[\frac{(\Gamma_2+\Gamma_3)(t_c-t)^{\gamma_1}|\xi_1(t)|^2}{4\nu t\,\xi_1(t)} - \frac{\Gamma_1(t_c-t)^{\gamma_2}|\xi_2(t)|^2}{4\nu t\,\xi_2(t)} - \frac{\Gamma_1(t_c-t)^{\gamma_3}|\xi_3(t)|^2}{4\nu t\,\xi_3(t)}\right]. \end{aligned} \tag{3.91}$$

If one divides this equation by $(t_c - t)^{\gamma_1}$ and let $t \to t_c$, one gets the equation that describes asymptotically the dynamics near t_c:

$$\gamma_1 \xi_1^* + (t_c - t)\,\dot{\xi}_1^* = 0, \tag{3.92}$$

which has the solution $\xi_1(t) = A(t_c - t)^{\gamma_1}$, $A \in \mathbb{C}$. However, this contradicts the assumption that $\xi_1(t_c) \neq 0$ and therefore there is no total collapse of the three vortices system in a viscous environment in a finite time.

Chapter 4.

Numerical Method and Validation of the Code

4.1 THE RUNGE-KUTTA-FEHLBERG METHOD

As mentioned before, for $n \geq 4$, in general, the system

$$\dot{z}_\alpha^* = \frac{1}{2\pi i} \sum_{\beta \neq \alpha}^{n} \frac{\Gamma_\beta}{z_\alpha - z_\beta} \left[1 - \exp\left(-\frac{|z_\alpha - z_\beta|^2}{4\nu t} \right) \right] \tag{4.1}$$

is not integrable, even for $\nu = 0$. Therefore, in order to analyze the behaviour of these systems, one needs to resort to numerical methods, which will give an approximation of the solution of the problem. One such method is the Runge-Kutta-Fehlberg method, which is a combination of Runge-Kutta methods of orders 4 and 5.

The aim is to find an approximation of the solution of some (system of) differential equation(s) $y'(t) = f(t, y(t))$, where $y : [t_0, T] \to \mathbb{C}^n$ and $f : [t_0, T] \times \mathbb{C}^n \to \mathbb{C}^n$, given some initial condition $y(t_0) = y_0 \in \mathbb{C}^n$.

First, one needs to discretize the interval $[t_0, T]$ in $N+1$ points $t_0, t_1, \ldots, t_N = T$ such that $t_k = t_0 + kh$ with $h = \frac{T - t_o}{N}$. Then, if one knows the (approximate) solution $y_k \approx y(t_k)$, the objective is to find the approximate solution at $y_{k+1} \approx y(t_{k+1})$.

The Runge-Kutta-Fehlberg method constructs the approximation of the solution at time t_{k+1} as

$$y_{k+1} = y_k + \frac{16}{135}K_1(t_k, y_k) + \frac{6656}{12825}K_3(t_k, y_k) + \frac{28561}{56430}K_4(t_k, y_k) - \frac{9}{50}K_5(t_k, y_k) + \frac{2}{55}K_6(t_k, y_k), \quad (4.2)$$

where the functions K_α, $\alpha \in \{1, 2, 3, 4, 5, 6\}$ are the following:

$$\begin{aligned}
K_1(t, y) &= h\, f(t, y) \\
K_2(t, y) &= h\, f\left(t + \frac{1}{4}h, y + \frac{1}{4}K_1(t, y)\right) \\
K_3(t, y) &= h\, f\left(t + \frac{3}{8}h, y + \frac{3}{32}K_1(t, y) + \frac{9}{32}K_2(t, y)\right) \\
K_4(t, y) &= h\, f\left(t + \frac{12}{13}h, y + \frac{1932}{2197}K_1(t, y) - \frac{7200}{2197}K_2(t, y) + \frac{7296}{2197}K_3(t, y)\right) \\
K_5(t, y) &= h\, f\left(t + h, y + \frac{439}{216}K_1(t, y) - 8K_2(t, y) + \frac{3680}{513}K_3(t, y) - \frac{845}{4104}K_4(t, y)\right) \\
K_6(t, y) &= h\, f\left(t + \frac{1}{2}h, y - \frac{8}{27}K_1(t, y) + 2K_2(t, y) - \frac{3544}{2565}K_3(t, y) + \frac{1859}{4104}K_4(t, y) + \right. \\
&\qquad \left. - \frac{11}{40}K_5(t, y)\right).
\end{aligned} \quad (4.3)$$

For more details on the method and how it compares computationally to other Runge-Kutta methods, refer to the original paper of Fehlberg [27]. Using this integration method, it is possible to obtain approximate solutions for the n-vortex problem with relatively good accuracy.

Since the problem is complex and non-integrable for $n \geq 4$, it is important to first check if the developed code against the few cases for which the analytical solution is available and for those where one at least knows the behavior of the solutions. The code was developed in FORTRAN90 and can be found in Appendix A.

4.2 NUMERICAL CALCULATION OF THE LARGEST LYAPUNOV EXPONENT

The largest Lyapunov exponent was calculated through the algorithm developed by Bennetin et al. [8, 9] which was explained in Section 2.5. In fact, the algorithm calculates the estimator of λ_1 at the end of some integration period T, yielding a quantity $\lambda(t) = \frac{1}{t}\log\frac{|\boldsymbol{\delta}(t)|}{|\boldsymbol{\delta_0}|}$ which should approach λ_1 as $t \to \infty$. After validating the integration algorithm, we ran some other test runs to fine-tune the parameters of this algorithm and found consistent results for a period $T = 1$ and an initial perturbation of $|\boldsymbol{\delta_0}| = 10^{-5}$.

These values were used for all simulations hereafter, even though they are not guaranteed to be optimal.

4.3 INVISCID VORTICES

The simplest case that one can test is the system composed by two inviscid point vortices. The code should be able to simulate the well-known dynamics of this system both if the total circulation of the system is zero or not.

4.3.1 Case I: Two inviscid point vortices with non-zero total circulation

The simulation was made using two inviscid point vortices of circulations $\Gamma_1 = 2$ and $\Gamma_2 = -1$, initially placed at positions $z_1 = 2$ and $z_2 = -1 - i$ in the complex plane. The integration step was set at $h = 2 \times 10^{-3}$ and the integration ran up until $t = 10^6$. The quantities P, Q, I and H were indeed conserved during the whole run, as can be seen from the left panel of Figure 4.1. There are little oscillations in these four quantities, but the relative variations never exceed $\sim 10^{-11}$ and are therefore purely numerical artifacts. Comparing with the analytical solution for z_1 and z_2, one finds that the relative error never exceeds numbers of the order of $\sim 10^{-7}$, even for the largest integration times.

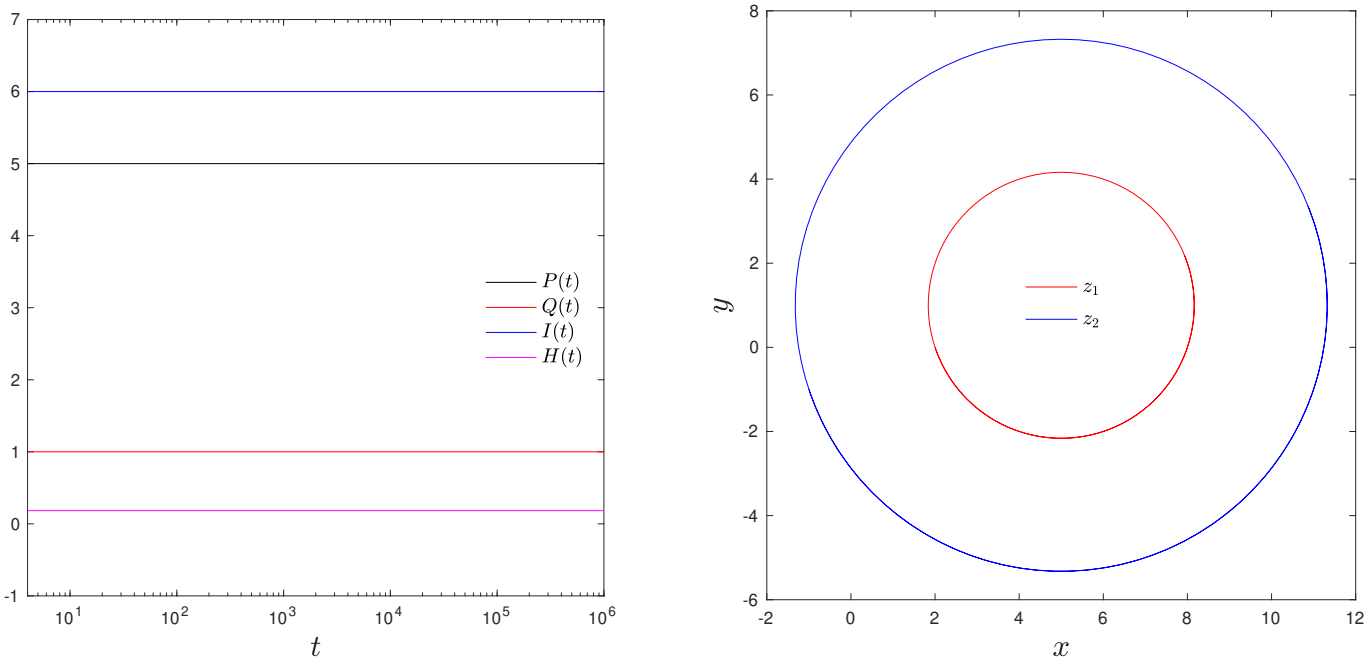

Figure 4.1: Numerical results for the simulation of the system of two inviscid point vortices of circulations $\Gamma_1 = 2$ and $\Gamma_2 = -1$, placed initially at $z_1 = 2$ and $z_2 = -1 - i$. The left panel shows the conserved quantities P, Q, I and H for the whole run of 10^6 units of time. The right panel shows the trajectories of the two vortices: two closed loops with the same center (the center of vorticity of the system).

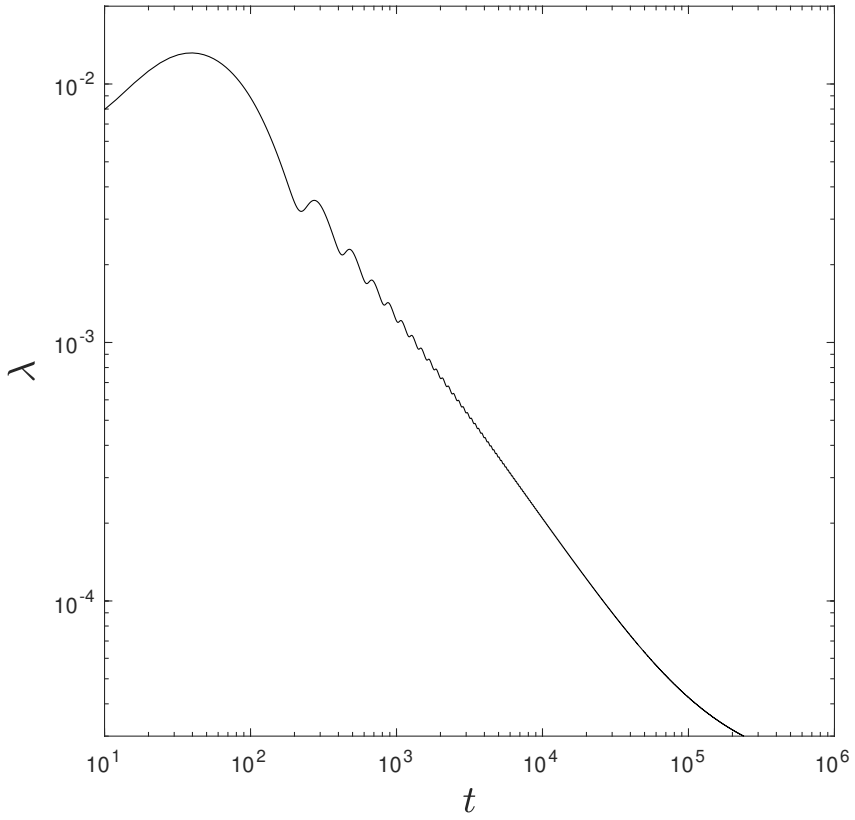

Figure 4.2: Numerical results for $\lambda(t) = \frac{1}{t}\log\frac{|\boldsymbol{\delta}(t)|}{|\boldsymbol{\delta_0}|}$ for the simulation of the system of two inviscid point vortices of circulations $\Gamma_1 = 2$ and $\Gamma_2 = -1$, placed initially at $z_1 = 2$ and $z_2 = -1 - i$. This suggests $\lambda_1 = 0$.

The right panel of Figure 4.1 shows the trajectories described by these point vortices: two closed loops with a common center. This is the expected behavior, as the two vortices should orbit their center of vorticity in a closed, simple trajectory.

As can be seen from the explicit solutions of this problem, presented in Section 3.1.3, any small perturbation $\boldsymbol{\delta_0}$ in the initial conditions will keep the perturbed trajectory close to the unperturbed one. As such, one expects to measure zero for the largest Lyapunov Exponent, λ_1. In Figure 4.2 one can see the behavior of the quantity $\lambda(t)$ for an initial perturbation of $|\boldsymbol{\delta_0}| = 10^{-5}$. As expected, the rapidly decreasing $\lambda(t)$ suggests that $\lambda_1 = 0$.

4.3.2 Case II: Two inviscid point vortices with zero total circulation

Similar results arise for the analysis of two vortices with circulations $\Gamma_1 = 1$ and $\Gamma_2 = -1$, initially placed at positions $z_1 = 2$ and $z_2 = -1 - i$ in the complex plane: the four invariant quantities remain constant in the whole run (of 10^6 units of time, with integration step set at $h = 2 \times 10^{-3}$) as can be seen in the left panel of Figure 4.3, presenting only small oscillations that never exceed $\sim 10^{-8}$ which are the

usual numerical artifacts. Comparing with the analytical solution for z_1 and z_2, ir is possible to observe that the relative error never exceeds $\sim 10^{-8}$ even for the largest integration times.

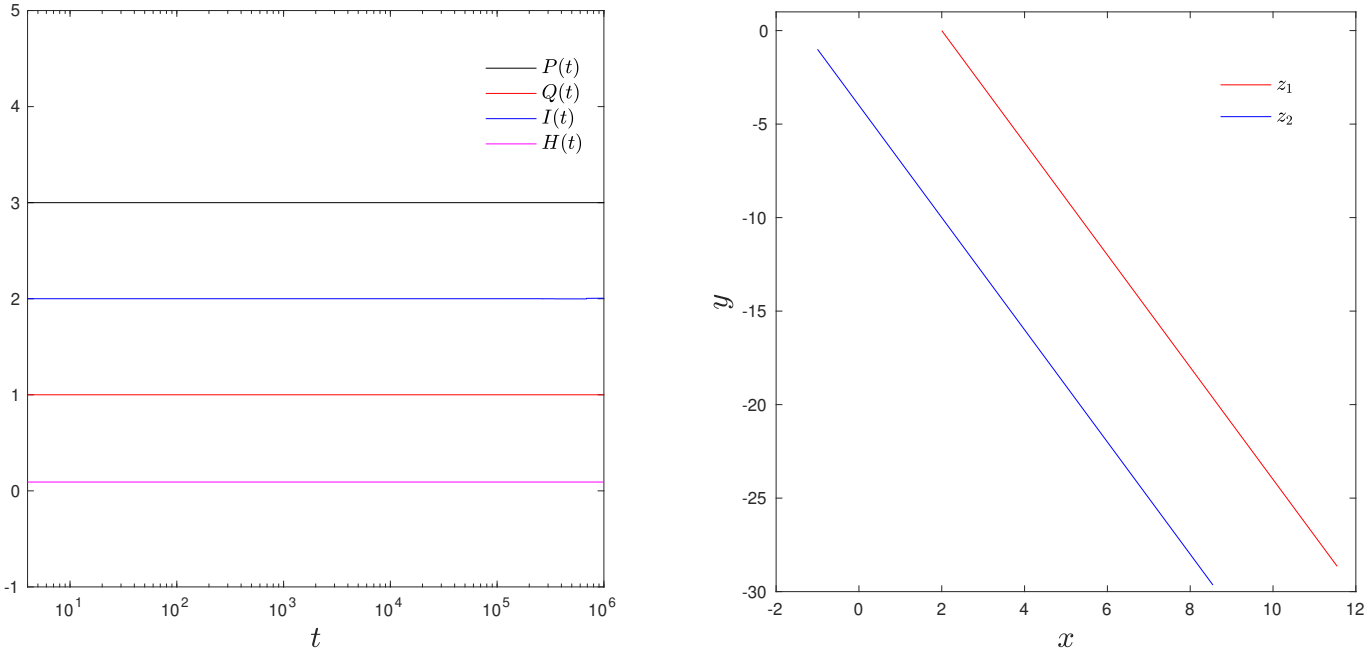

Figure 4.3: Numerical results for the simulation of the system of two inviscid point vortices of circulations $\Gamma_1 = 1$ and $\Gamma_2 = -1$, placed initially at $z_1 = 2$ and $z_2 = -1 - i$. The left panel shows the conserved quantities P, Q, I and H for the whole run of 10^6 units of time. The right panel shows the trajectories of the two vortices: two parallel lines.

The right panel of Figure 4.3 shows the trajectory of the two point vortices in the time interval $[0, 600]$. Depicting the full trajectory for the vortices would only extend the parallel lines, yielding the same behavior as one found analytically in Section 3.1.3.

Any small perturbation on the initial conditions of this problem will result in a similar trajectory for the two vortices. In fact, the distance for the perturbed trajectory to the one presented would be the same at all times and therefore, theoretically, one would have a Lyapunov exponent $\lambda_1 = 0$. Figure 4.4 shows a fast decay of the quantity $\lambda(t)$ that is coherent with what we expect..

4.3.3 Case III: Three inviscid point vortices in an equilateral triangular configuration

For systems with three vortices, while we don't have any explicit solutions available, it is still possible to qualitatively compare the numerical solutions for some configurations. First we show a system with vortices of circulations $\Gamma_1 = 2$, $\Gamma_2 = 1$ and $\Gamma_3 = 2$, initially placed in $z_1 = -1$, $z_2 = 1$ and $z_3 = \sqrt{3}i$, forming an equilateral triangle of side $s = 2$. The integration step was set at $h = 2 \times 10^{-3}$ and the integration ran up until $t = 10^6$. In the left panel of Figure 4.5, we show the conserved quantities of the system, which diverge from their true value due to small numerical oscillations with a relative amplitude of

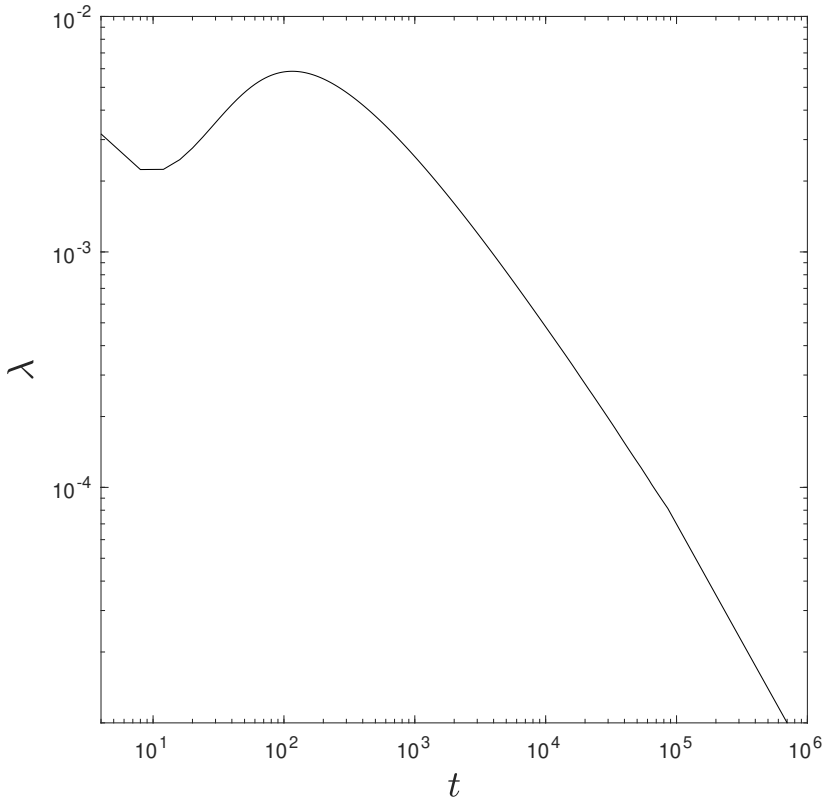

Figure 4.4: Numerical results for $\lambda(t) = \frac{1}{t}\log\frac{|\boldsymbol{\delta}(t)|}{|\boldsymbol{\delta}_0|}$ for the simulation of the system of two inviscid point vortices of circulations $\Gamma_1 = 1$ and $\Gamma_2 = -1$, placed initially at $z_1 = 2$ and $z_2 = -1 - i$. This suggests $\lambda_1 = 0$.

at most $\sim 10^{-12}$. In the right panel of the same Figure, we present the trajectories of the three vortices. Vortices 1 and 3 actually describe the same trajectory (the smallest of the two circumferences), so the plot only depicts two lines instead of three. In Figure 4.6 we plotted the solution at only 8 times in order to see more clearly the equilateral triangle configuration rotating. Numerically, we found that the length of the sides of the triangle stays unchanged up to $\sim 10^{-12}$ throughout the whole run. These errors correspond solely to numerical artifacts.

Figure 4.7 shows a different behavior for $\lambda(t)$ than the two previous cases. This happens because equilateral triangles are, in fact, unstable equilibria of the three vortex system and therefore, any small perturbation will be amplified, giving rise to a completely different solution. Using only values of $\lambda(t)$ for $t > 10^4$ we estimated $\lambda_1 \approx 7.25 \times 10^{-3}$ for this trajectory. We don't include the points of $\lambda(t)$ for $t < 10^4$ in the estimation of λ_1 as the algorithm needs some time to converge and the initial behavior of $\lambda(t)$ is usually not representative of the true value of λ_1.

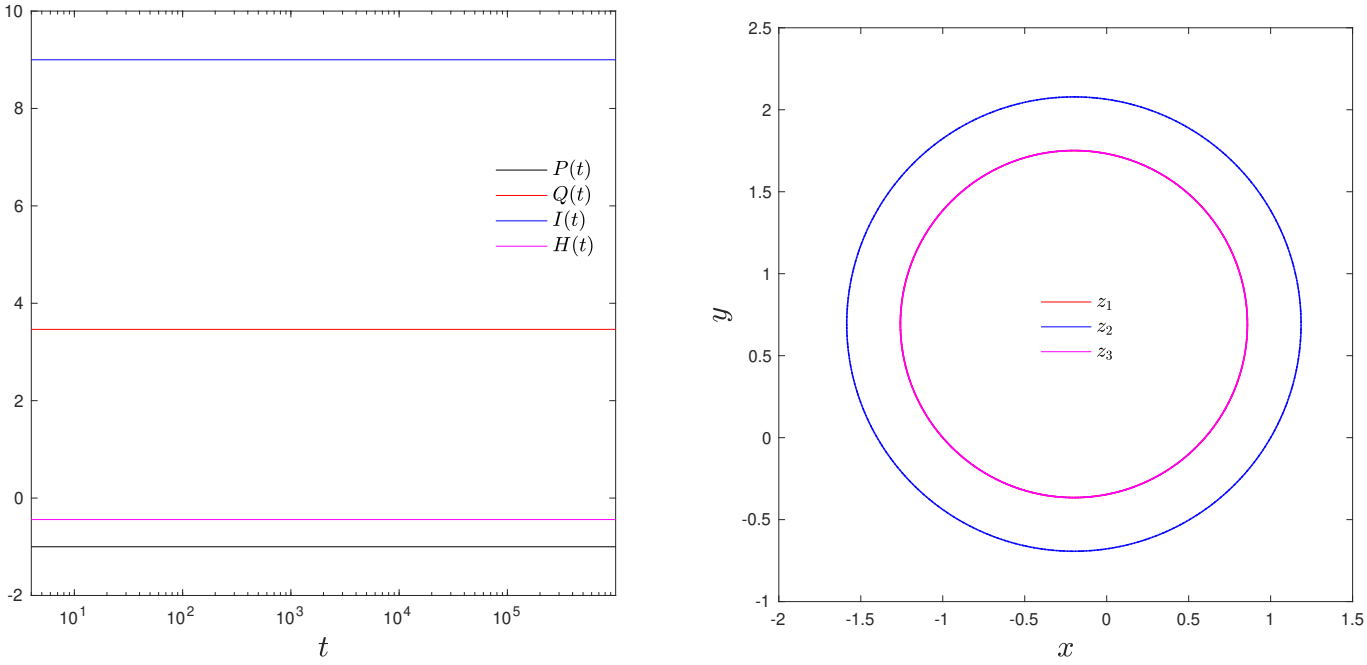

Figure 4.5: Numerical results for the simulation of the system of three inviscid point vortices of circulations $\Gamma_1 = 2$, $\Gamma_2 = 1$ and $\Gamma_3 = 2$, placed initially at $z_1 = -1$, $z_2 = 1$ and $z_3 = \sqrt{3}i$. The left panel shows the conserved quantities P, Q, I and H for the whole run of 10^6 units of time. The right panel shows the trajectories of the three vortices: two closed loops with the same center (the center of vorticity of the system).

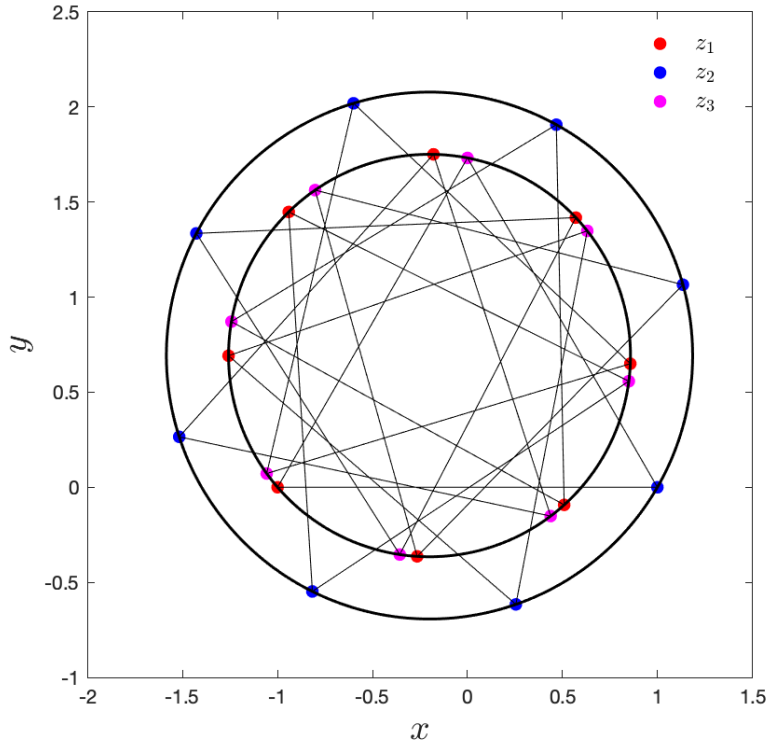

Figure 4.6: Explicit portrait of the equilateral triangular configuration for a system of three inviscid point vortices of circulations $\Gamma_1 = 2$, $\Gamma_2 = 1$ and $\Gamma_3 = 2$, placed initially at $z_1 = -1$, $z_2 = 1$ and $z_3 = \sqrt{3}i$.

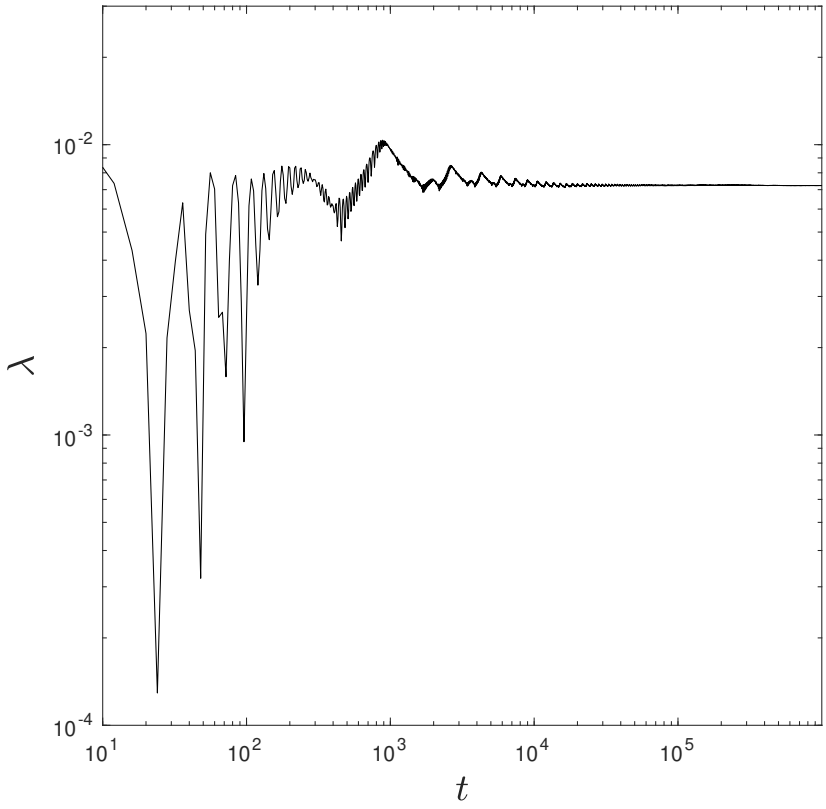

Figure 4.7: Numerical results for $\lambda(t) = \frac{1}{t}\log\frac{|\boldsymbol{\delta}(t)|}{|\boldsymbol{\delta_0}|}$ for the simulation of the system of three inviscid point vortices of circulations $\Gamma_1 = 2$, $\Gamma_2 = 1$ and $\Gamma_3 = 2$, placed initially at $z_1 = -1$, $z_2 = 1$ and $z_3 = \sqrt{3}i$. This suggests $\lambda_1 \approx 7.25 \times 10^{-3}$.

4.3.4 Case IV: Self-similar collapse of three inviscid point vortices

Setting three point vortices with circulations $\Gamma_1 = -3 \times 10^{-3}$, $\Gamma_2 = 2 \times 10^{-3}$ and $\Gamma_3 = -6 \times 10^{-3}$ in the positions $z_1 = -4$, $z_2 = -\frac{9}{2} + i\frac{3\sqrt{3}}{2}$ and $z_3 = \frac{1}{2} + i\frac{\sqrt{3}}{2}$ yields a configuration that satisfies all the conditions of Theorem 3.1.4 and thus will result in a self-similar collapse of the three vortices, as can be seen by their trajectories in the right panel of Figure 4.8. This collapse happens approximately at time $t \approx 2.54 \times 10^4$ at the center of vorticity of the system. The invariants of the system remain unchanged during the whole process, as can be seen in the left panel of the same Figure. There are small numerical oscillations of magnitude at most $\sim 10^{-11}$ in this quantities and thus they are only numerical artifacts.

Figure 4.9 depicts the configuration of the system at some time instants of the evolution leading to collapse. It can be seen that the triangular configuration of vortices rotates around the origin while shrinking, originating spiral trajectories for the vortices. The shrinking is self-similar, as the ratios between the lengths of the sides of the triangle do not change in time.

Any slight deviation from the conditions of collapse will result in a configuration that does not collapse, as such, we expect to have $\lambda_1 > 0$ for this trajectory. Indeed we find results that suggest a positive

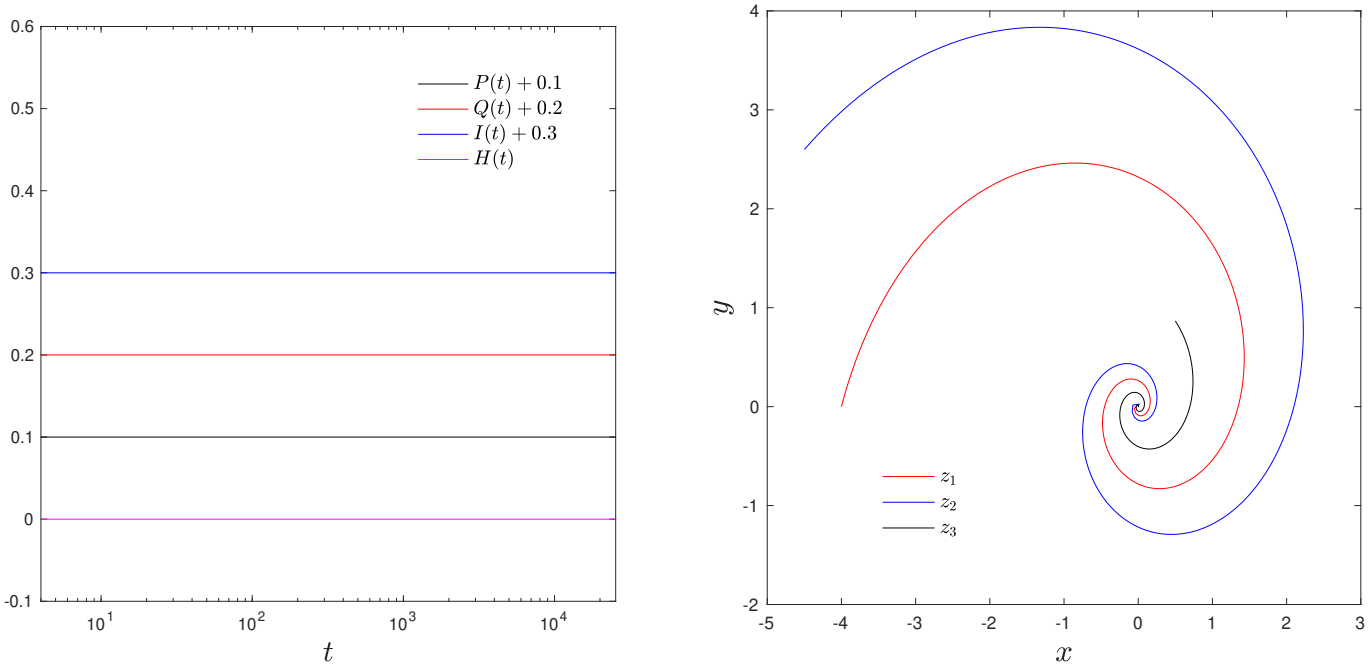

Figure 4.8: Numerical results for the simulation of the system of three inviscid point vortices of circulations $\Gamma_1 = -3 \times 10^{-3}$, $\Gamma_2 = 2 \times 10^{-3}$ and $\Gamma_3 = -6 \times 10^{-3}$, placed initially at $z_1 = -4$, $z_2 = -\frac{9}{2} + i\frac{3\sqrt{3}}{2}$ and $z_3 = \frac{1}{2} + i\frac{\sqrt{3}}{2}$. The left panel shows the conserved quantities P, Q, I and H for the whole run of 10^6 units of time. The right panel shows the trajectories of the three vortices: spirals converging to the same point, the center of vorticity of the system.

Lyapunov exponent, but the method of Benettin does not provide a reasonable estimate for it (see Figure 4.10). This could be explained due to the fact that, as the solution get closer to collapse - a singular point for the equations of motion - it becomes difficult for the numerical integration to proceed with a sufficient precision due to its' resolution being limited by the integration step-size. Also, near the point of collapse, vortices are much closer to one another than the magnitude of the perturbation we impose and thus the assumption of exponential divergence of trajectories might not hold.

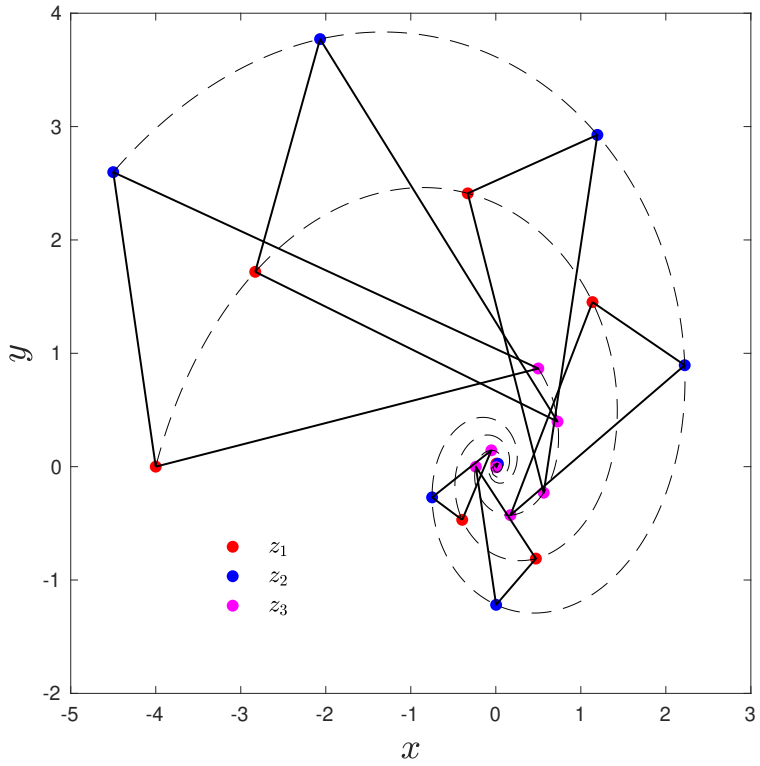

Figure 4.9: Explicit portrait of the evolution of the triangular configuration for a system of three inviscid point vortices undergoing self-similar collapse. Vortex circulations are $\Gamma_1 = -3\times10^{-3}$, $\Gamma_2 = 2\times10^{-3}$ and $\Gamma_3 = -6\times10^{-3}$, with the vortices placed initially at $z_1 = -4$, $z_2 = -\frac{9}{2} + i\frac{3\sqrt{3}}{2}$ and $z_3 = \frac{1}{2} + i\frac{\sqrt{3}}{2}$. Collapse occurs at $t \approx 2.53\times10^4$.

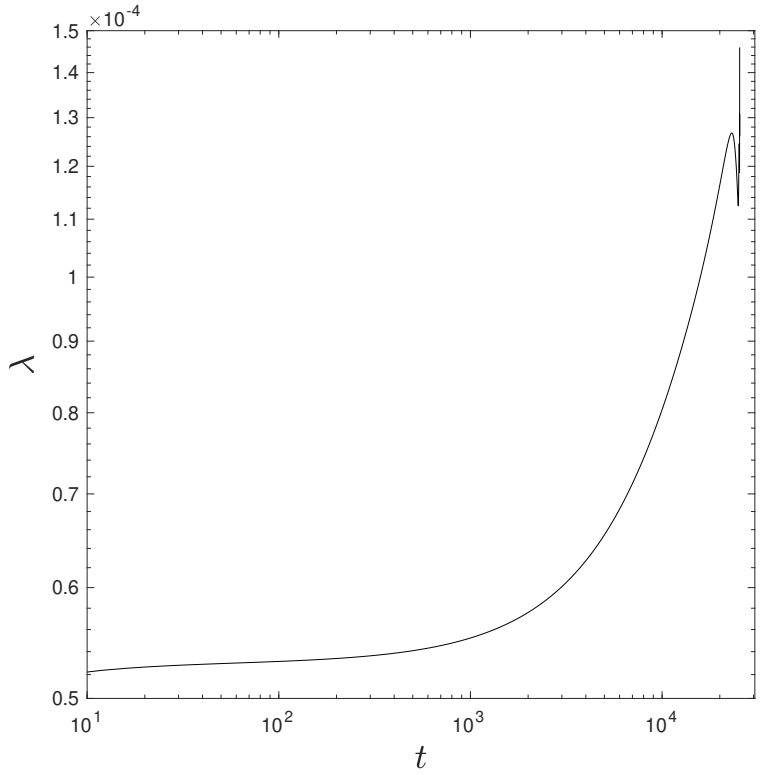

Figure 4.10: Numerical results for $\lambda(t) = \frac{1}{t}\log\frac{|\boldsymbol{\delta}(t)|}{|\boldsymbol{\delta_0}|}$ for the simulation of the system of two inviscid point vortices of circulations $\Gamma_1 = -3\times10^{-3}$, $\Gamma_2 = 2\times10^{-3}$ and $\Gamma_3 = -6\times10^{-3}$, placed initially at $z_1 = -4$, $z_2 = -\frac{9}{2} + i\frac{3\sqrt{3}}{2}$ and $z_3 = \frac{1}{2} + i\frac{\sqrt{3}}{2}$. This suggests $\lambda_1 = 0$.

4.4 VISCOUS VORTICES

In a viscous environment it is not possible to write analytical expressions for the solutions of the n-vortex problem, however, one knows the behaviour of some simple systems and can compare the results qualitatively. Other than that, some of the conserved quantities in the inviscid case are also invariant of the viscous equations and therefore may be used to check the behavior of the developed code.

4.4.1 Cases I and II: Two viscous point vortices

The simulation was made with the exact same circulations and initial positions for the vortices as the inviscid one, documented in Section 4.3.1, but now introducing a viscosity of $\nu = 10^{-4}$ ($Re = 10^4$). Results are similar to the inviscid case: the conserved quantities only present oscillations due to numerical artifacts and are of the same order of magnitude as before; the trajectories describe the exact same loops, but now the velocity of the vortices decays with time due to the dissipation of energy caused by the presence of viscosity. This can be seen in the left panel of Figure 4.11, depicting the intervortex separation D and the velocities of the two vortices. $D/D\,(0)$ is shifted up by 0.1 for a clearer presentation.

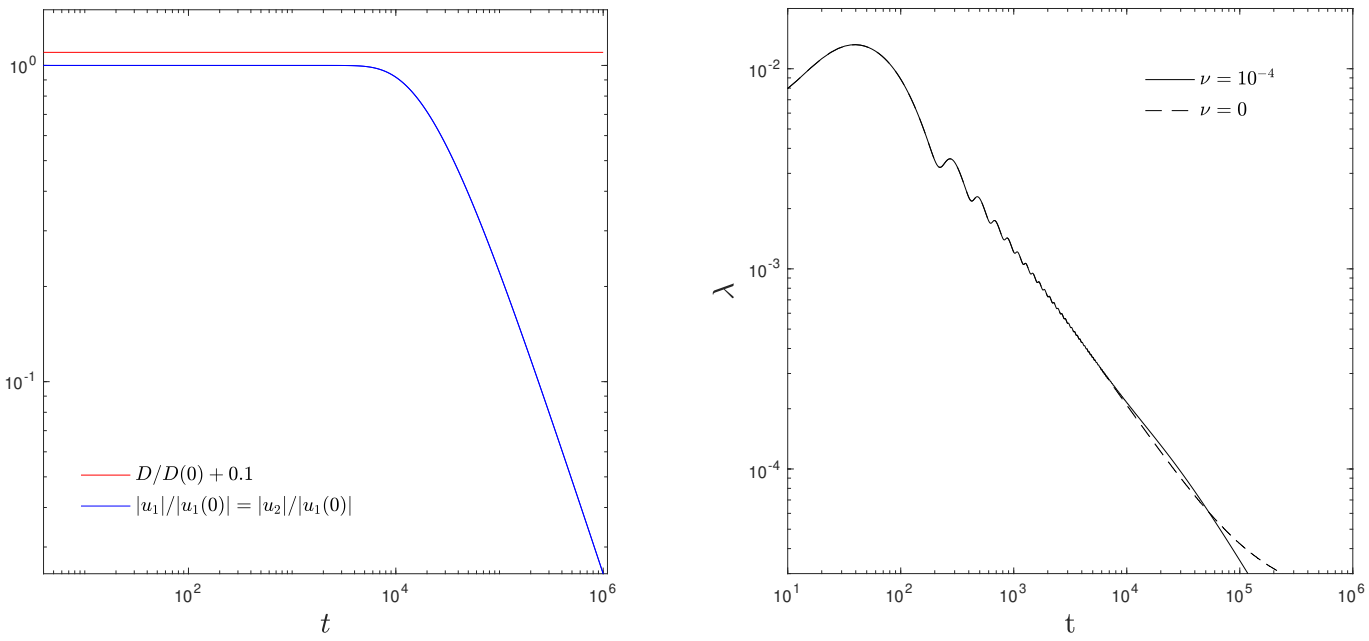

Figure 4.11: Numerical results for the simulation of the system of two viscous point vortices of circulations $\Gamma_1 = 2$ and $\Gamma_2 = -1$, placed initially at $z_1 = 2$ and $z_2 = -1 - i$. The left panel shows that the intervortex separation does not change with time, but velocity does decay due to the presence of viscous forces. The right panel shows the behavior of the quantity $\lambda\,(t)$ for this system, which decays slightly faster than in the inviscid case (dashed line, for comparison), suggesting $\lambda_1 = 0$ once again.

Changing only the circulation Γ_1 to $\Gamma_1 = 1$, one gets the system described in Section 4.3.2. Here,

for a viscous environment, the results are also pretty similar to the inviscid case: all conserved quantities maintain their values throughout the simulation, barring small numerical oscillations, the vortices describe trajectories parallel to one another while maintaining their distance between one another with a velocity decaying in time, as can be seen in the left panel of Figure 4.12. On the right panel of the same Figure, it is possible to notice that viscosity doesn't seem to affect much the computation of $\lambda(t)$. This probably due to the regularity of the straight trajectories themselves.

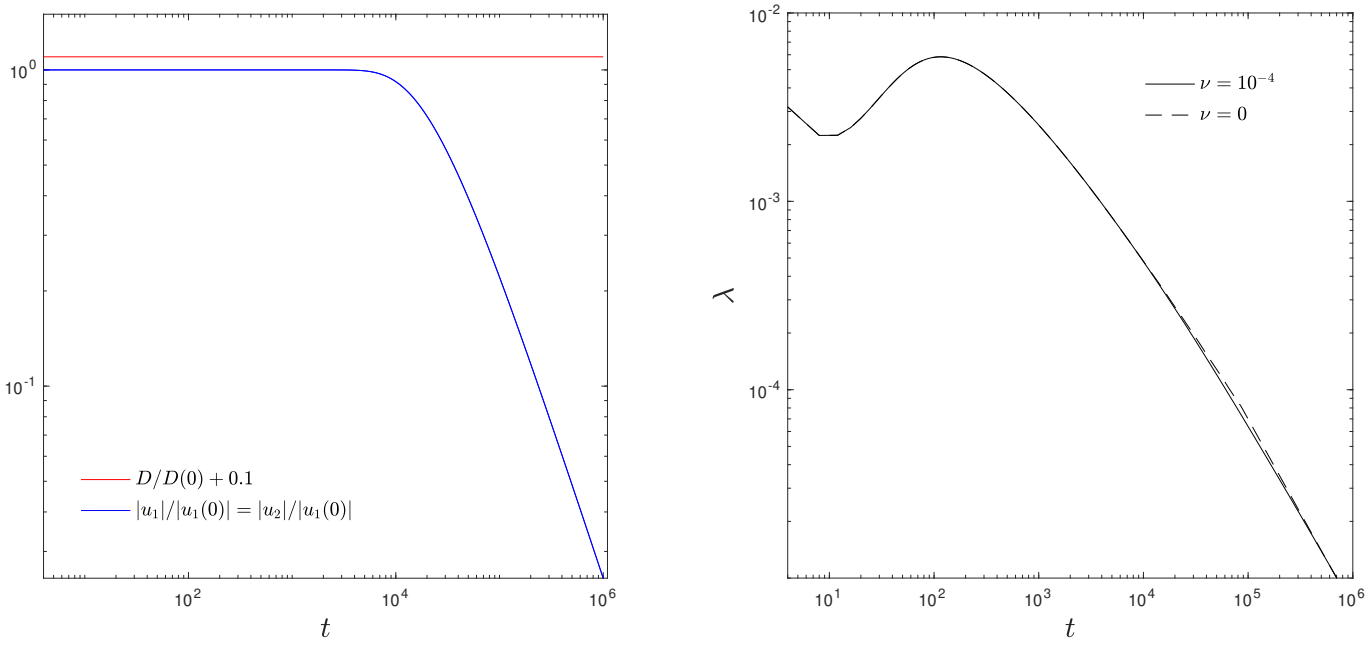

Figure 4.12: Numerical results for the simulation of the system of two viscous point vortices of circulations $\Gamma_1 = 1$ and $\Gamma_2 = -1$, placed initially at $z_1 = 2$ and $z_2 = -1 - i$. The left panel shows that the intervortex separation does not change with time, but velocity does decay due to the presence of viscous forces. The right panel shows the behavior of the quantity $\lambda(t)$ for this system, which decays in a similar fashion as in the inviscid case (dashed line, for comparison), suggesting $\lambda_1 = 0$ once again.

4.4.2 Case III: Two viscous point vortices in an equilateral triangular configuration

As before, we simulate the exact same starting conditions as in the inviscid case described in Section 4.3.3. The results are coincident with the expectations and all the numerical discrepancies seem to be purely artifacts from the computer's limitations. The trajectories of the vortices are still closed loops and the configuration of the vortices forms an equilateral triangle at all times through the whole run of 10^6 units of time. The shape of trajectories are exactly the same as the inviscid case, but with a decaying velocity for all vortices. However, $\lambda(t)$ suggests a different behavior for the maximum Lyapunov Exponent, as can be seen in Figure 4.13. If viscosity has enough time to act and become the ruling force on the system, this suggests that perturbed trajectories won't be able to separate from the original trajectory.

This behavior is expected, as viscosity will make the velocity field approach zero.

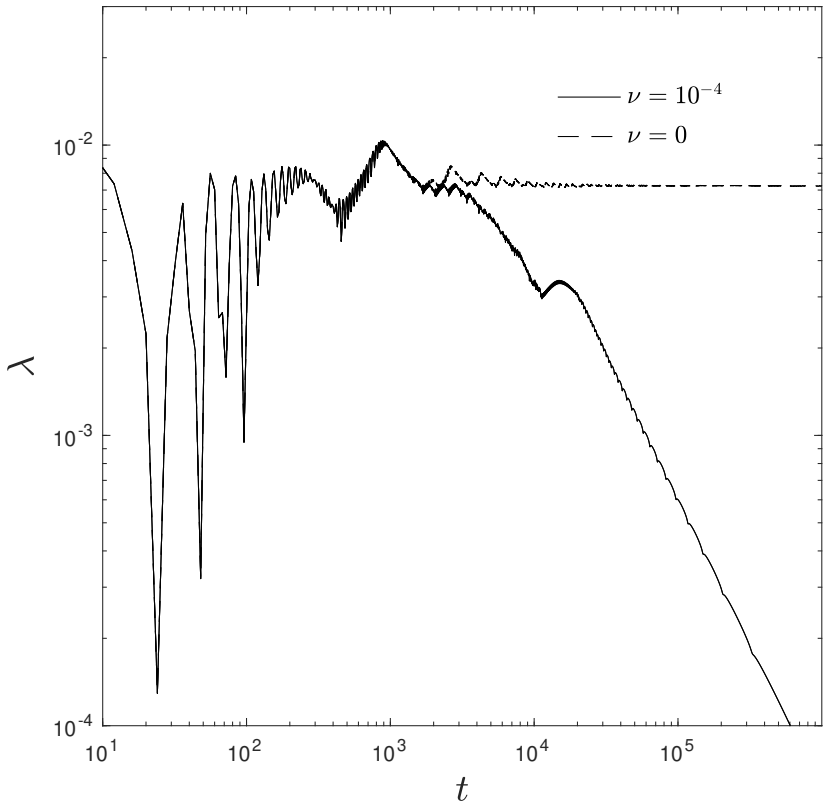

Figure 4.13: Numerical results for $\lambda(t) = \frac{1}{t}\log\frac{|\boldsymbol{\delta}(t)|}{|\boldsymbol{\delta}_0|}$ for the simulation of the system of three inviscid point vortices of circulations $\Gamma_1 = 2$, $\Gamma_2 = 1$ and $\Gamma_3 = 2$, placed initially at $z_1 = -1$, $z_2 = 1$ and $z_3 = \sqrt{3}i$. This suggests $\lambda_1 \to 0$ if viscosity has enough time to act on the system.

4.4.3 Case IV: Comparison with the inviscid collapse

The initial configuration for the inviscid self-similar collapse, however, must evolve in a completely different way, since there is no finite time self-similar collapse for a system of three vortices in a viscous environment. We first noticed that the conserved quantities showed, once more, no signs of variability other than the typical numerical artifacts. The decaying velocity for the vortices prevents the collapse, as they aren't able to progress with their usual motion (i.e., the motion one would expect from the inviscid case) after viscosity starts dominating the system. In fact, while in the inviscid case the trajectories would spiral to the center of viscosity of the system, in the viscous case each of the trajectories of the vortices seems to start accumulating on some loop centered on the center of viscosity of the system. This can be seen in the right panel of Figure 4.14, where we show the viscous trajectories and the inviscid behavior (in dashed lines). On the left panel of the same Figure, one can see that $\lambda(t)$ also presents a distinct behavior: in the viscous case, this seems to suggest $\lambda_1 \to 0$, which agrees with the possibility that the

trajectories of the vortices accumulate on some stable loop.

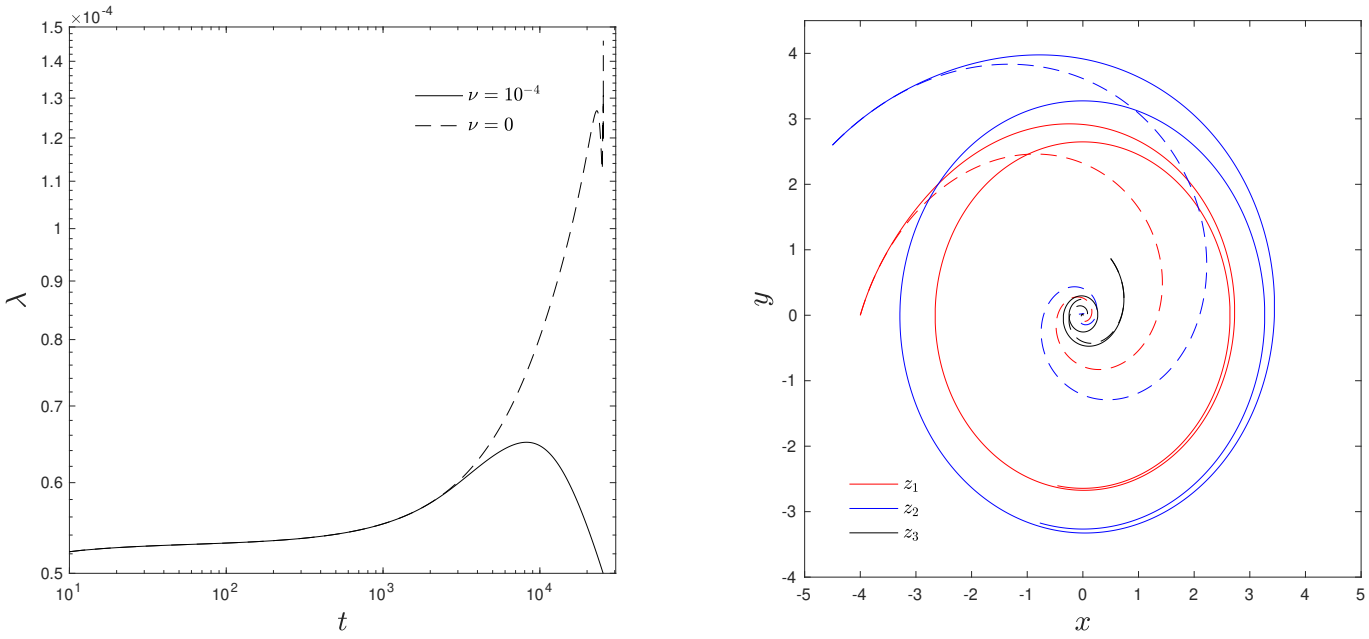

Figure 4.14: Numerical results for the simulation of the inviscid self-similar collapse in a viscous environment. The circulations are $\Gamma_1 = -3 \times 10^{-3}$, $\Gamma_2 = 2 \times 10^{-3}$ and $\Gamma_3 = -6 \times 10^{-3}$, and the vortices are placed initially at $z_1 = -4$, $z_2 = -\frac{9}{2} + i\frac{3\sqrt{3}}{2}$ and $z_3 = \frac{1}{2} + i\frac{\sqrt{3}}{2}$. On the left panel we compare the different behavior of $\lambda(t)$ in the viscous and inviscid cases. On the right panel we see the difference in the viscous trajectories when compared to the inviscid ones (dashed lines).

Chapter 5.

Results

After being confident that the developed code was properly solving the equations of motion for the vortices in a efficient way and the parameters for the computation of the Lyapunov Exponent seemed to return results that matched the expectations, we were able to proceed to more complex studies.

As seen before, a system of n point vortices in a fluid gives rise to a velocity field in that same fluid. This is an alternate modeling of fluid dynamics where the velocity field is commanded by the system of point vortices, avoiding direct integration of the Navier-Stokes equations. Therefore, one would naturally want to know what would happen to some particle of the fluid whose velocity field is governed by those n point vortices. These are usually called test particles or passive particles (because they not interfere with the velocity field).

In systems of $n \geq 4$ inviscid vortices, it is known that the movement of test particles within the flow is chaotic. However, point vortices create regions of stability around them; i.e., while they move chaotically within the fluid, the movement of particles within those regions of stability is predictable with respect to the vortex center [1]. These are usually called stability islands. Furthermore, particles within these islands cannot be ejected from them and particles outside them cannot enter the stability regions.

5.1 PASSIVE PARTICLES IN A SYSTEM OF 4 INVISCID VORTICES

We first considered the inviscid case and a system composed by 4 point vortices of circulations $\Gamma_\alpha = 1$, $\alpha \in \{1, 2, 3, 4\}$ initially located at $z_1 = 2$, $z_2 = -1 - i$, $z_3 = \frac{1}{2} + \frac{1}{2}i$ and $z_4 = -2 + 3i$. This system

was integrated together with a cloud of 10^4 passive particles through the Runge-Kutta-Fehlberg method with a step size of $h = 2 \times 10^{-3}$ during 10^4 units of time. We did two runs with two square clouds of particles: one centered in the vortex initially located at $z_4 = -2 + 3i$ with a side of length 1 and one in the background between the vortices with a side of length 0.1.

For the cloud of particles surrounding the vortex located at $z_4 = -2 + 3i$, we observed that indeed there exists a region of regularity surrouding the vortex, from which particles cannot escape. We also observed that even though the particles aren't able to exit the region, their radial movement (with respect to the vortex) seems to be restricted to some intervals that depend on their initial distance from the vortex. This can be seen from Figure 5.1, where we plot the initial distance from the vortex versus the final distance from the vortex (i.e., at the end of the simulation). In fact, the regularity region appears to be approximately a circular region of radius ~ 0.459 centered on the vortex. A smaller initial distance from the vortex appears to give less freedom of radial movement to a particle. This fact, together with visual observations of the dynamics of the system, point towards the possibility that the shape of these regularity islands changes in time due to the vortex-vortex interactions. This had also already been pointed out by Babiano et al. [1], but without any explicit reasoning. Notice that the discrepancy of this behavior for the particles closer to the vortex is due to the limited resolution of the simulations.

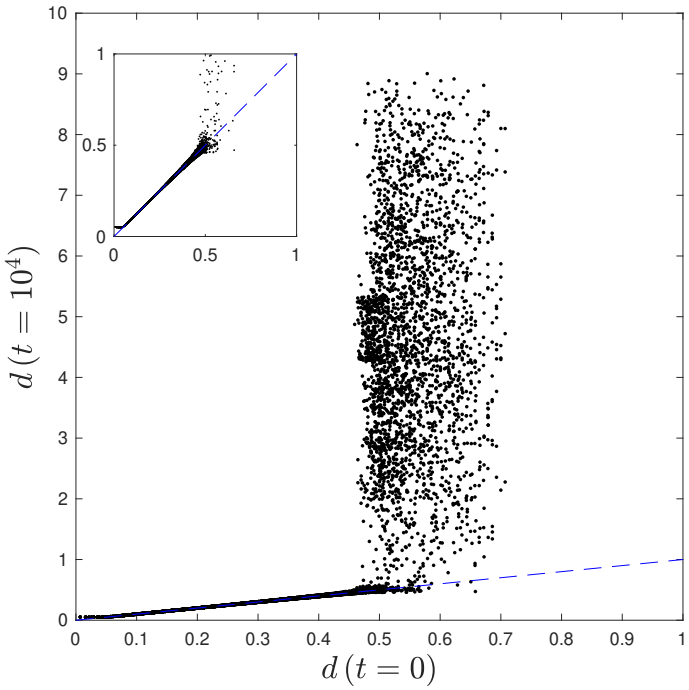

Figure 5.1: Distances between each passive particle and the vortex initially located at $z_4 = -2 + 3i$ at simulation start and end in the inviscid case.

In Figure 5.2 we illustrate the time-evolution of the cloud of passive particles. Red dots correspond to

vortex centers and pink lines represent an estimate of the regularity region (a loop centered in vortex z_4 with a radius of ~ 0.459). Blue dots correspond to particles starting within the estimated radius of the regularity island, while black dots represent the particles starting from a distance greater than ~ 0.459 from the vortex z_4 (other similar figures in the next sections will have the same color scheme). Particles outside of the regularity region appear to move chaotically in the fluid. Given enough time, they seem to permeate space with a homogeneous distribution.

If we place the cloud of particles far from the vortices, we see that all particles remain outside the regularity islands of the vortices at all times. This is illustrated in Figure 5.3. The mixing of particles in the background between the vortices appears to be happen quickly and it looks like particles that were nearby at $t = 0$ will be as further apart as the system permits for some point in time. This suggests chaotic mixing of the particles, whichever their initial position might have been (outside of regularity islands).

In the left panel of Figure 5.4 we plot a part of the trajectories of the vortex z_4 (red) and of two passive particles: one located inside the regularity island (blue) and one located outside of it (black). This illustrates the typical behavior of particles in these two situations. In the right panel, we show $\lambda(t)$ for the system of 4 vortices and for the two passive particles considered. While for the particle inside the regularity island this suggests $\lambda_1 = 0$, for the system of vortices we estimated $\lambda_1 \simeq 1.58 \times 10^{-2}$ and for the particle outside the island of regularity we found $\lambda_1 \simeq 7.62 \times 10^{-3}$.

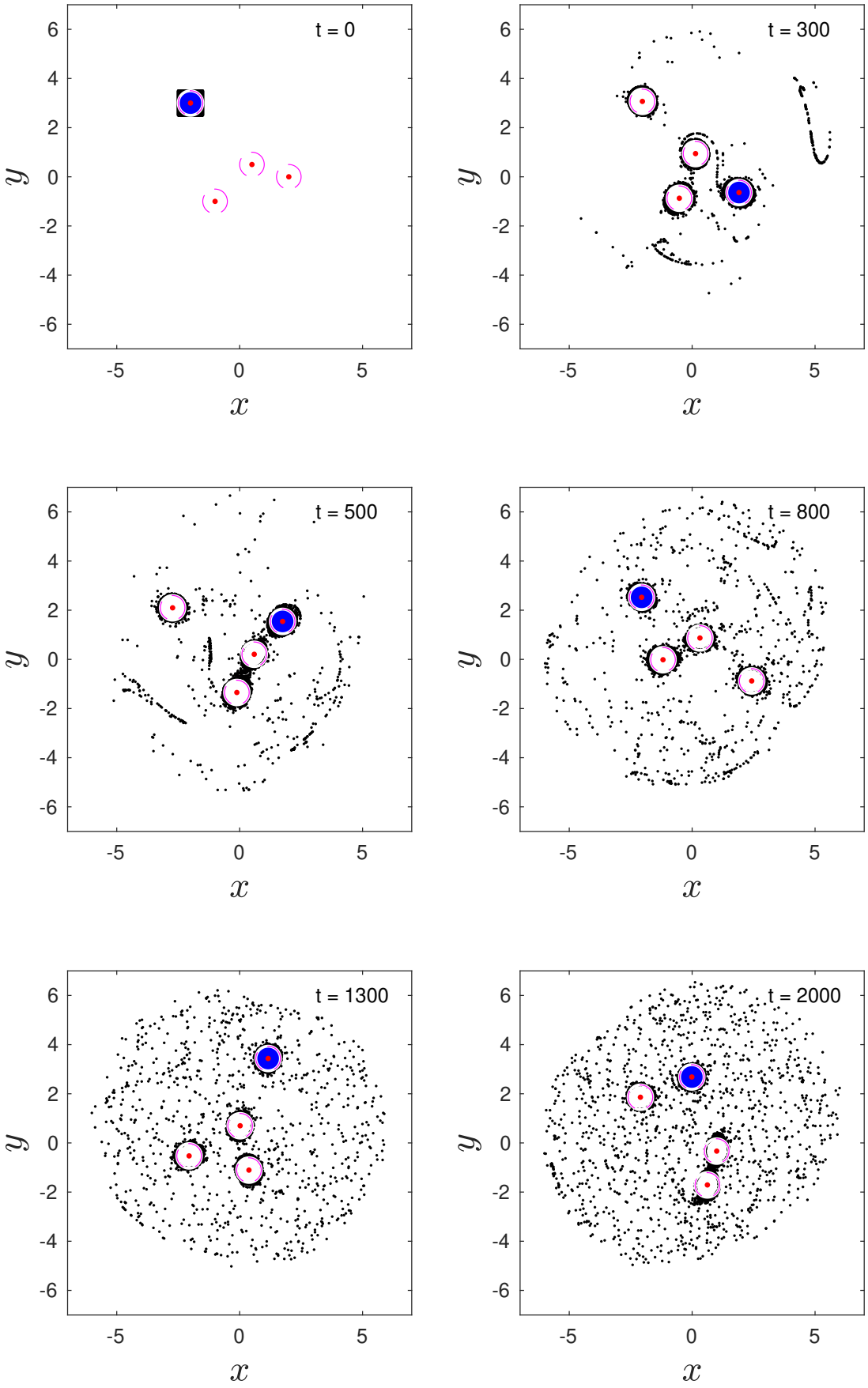

Figure 5.2: Time evolution of a system comprised of 4 inviscid vortices and 10^4 test particles initially located near the vortex at $z_4 = -2 + 3i$.

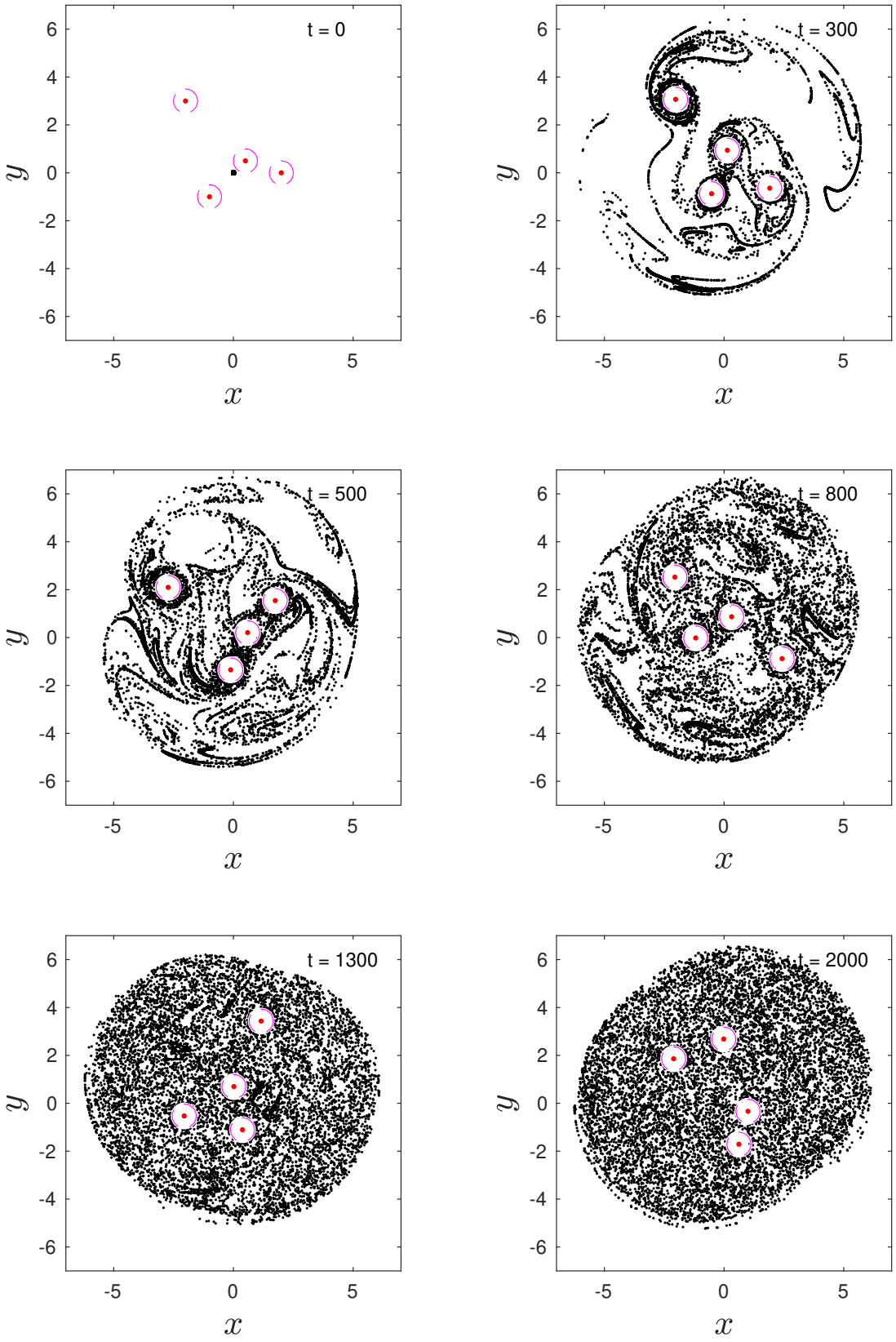

Figure 5.3: Time evolution of a system composed by 4 inviscid vortices and 10^4 passive particles initially located on the background between the vortices.

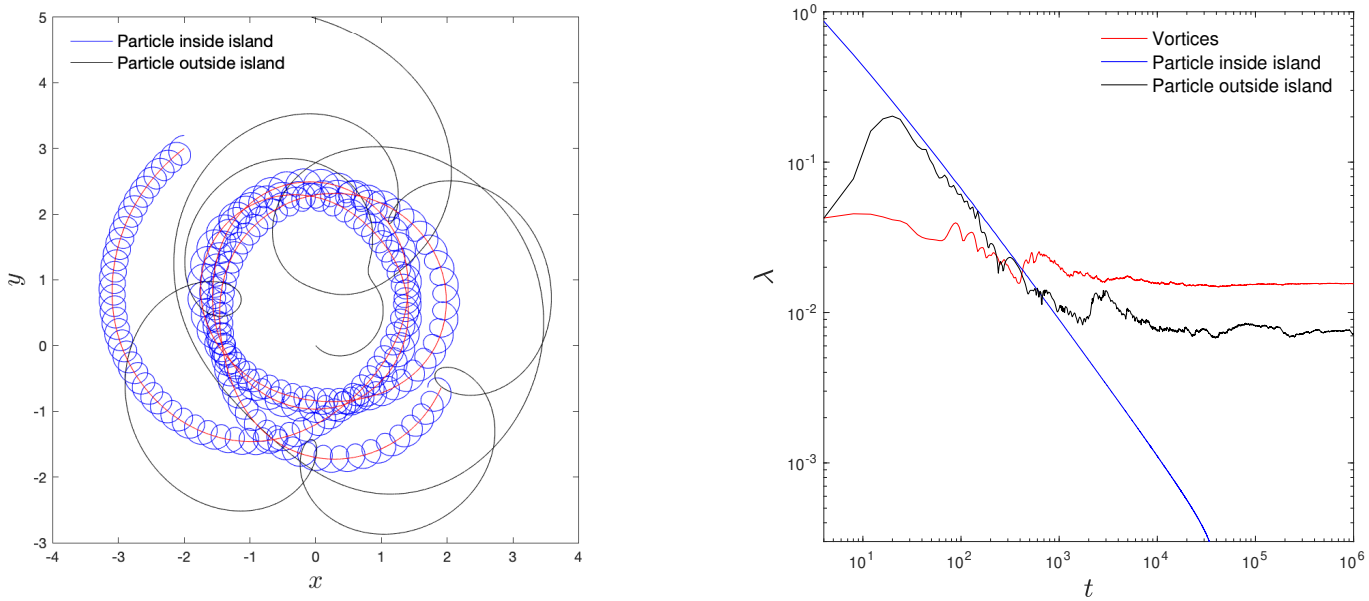

Figure 5.4: Trajectories (left panel) and $\lambda(t)$ (right panel) for the system of 4 inviscid vortices and for one of each kind of passive particles. This suggests $\lambda_1 = 0$ for the particle inside the regularity island, while for the system of vortices and the particle outside of the island we found $\lambda_1 \simeq 1.58 \times 10^{-2}$ and $\lambda_1 \simeq 7.62 \times 10^{-3}$, respectively.

5.2 PASSIVE PARTICLES IN A SYSTEM OF 4 VISCOUS VORTICES

We then moved to a viscous environment with a viscosity of $\nu = 10^{-4}$ ($Re = 10^4$). The physical system is composed by the same 4 point vortices of the inviscid case, i.e., vortices with circulations $\Gamma_\alpha = 1, \alpha \in \{1, 2, 3, 4\}$ initially located at $z_1 = 2$, $z_2 = -1 - i$, $z_3 = \frac{1}{2} + \frac{1}{2}i$ and $z_4 = -2 + 3i$. We also left all the other parameters and conditions unchanged from the inviscid simulations: a step size of $h = 2 \times 10^{-3}$ during 10^4 units of time and two runs with the same two square clouds of particles.

For the cloud of particles surrounding the vortex located at $z_4 = -2 + 3i$, we observed a similar behavior to the inviscid case for small times. However, due to viscosity, the size of the regularity islands starts shrinking and particles that were once inside the stable region find themselves out of the region of influence of the vortex and start moving chaotically within the fluid. Given enough time, all particles will eventually be ejected from the vortex's island of influence as its' strength goes to zero. This can be seen from Figure 5.5, where we plot the initial distance from the vortex versus the final distance from the vortex (i.e., at the end of the simulation): the distribution of points presents no apparent pattern and doesn't seem to hint on any relation between $d\,(t = 10^4)$ and $d\,(t = 0)$. This is typical in chaotic mixing.

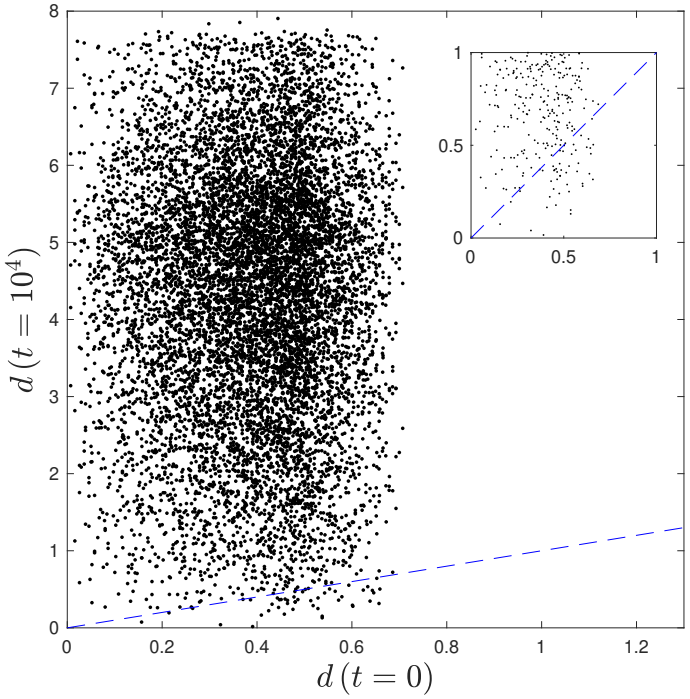

Figure 5.5: Distances between each passive particle and the vortex initially located at $z_4 = -2 + 3i$ at simulation start and end in the viscous case.

Figure 5.6 illustrates this mixing quite well, as in the last panel the distribution of blue and black dots

in the background between the vortices appears to be more or less the same. In fact, at later times this distinction between the two groups of particles will be even less obvious.

Placing the cloud of passive particles far from the vortex centers yields a evolution as the one illustrated in Figure 5.7. The difference from the inviscid case is that, as the vortices lose their strength, the regularity islands shrink and particles will eventually be able to get closer to the vortices. As $t \to \infty$, the vortices would disappear and the velocity field would go to zero everywhere.

Figure 5.8's left panel shows a part of the trajectories of the vortex z_4 (red) and of two passive particles: one located inside the regularity island (blue) and one located outside of it (black). This illustrates the typical behavior of particles in these two situations. We notice that the particle inside the regularity island follows the vortex during the depicted time, albeit its' trajectory isn't as periodic and repetitive as in the inviscid case. Eventually, this particle will be ejected from the regularity island and describe a chaotic trajectory. This claim is verified by the behavior of $\lambda(t)$ that can be seen in the right panel of the figure. Here, we show $\lambda(t)$ for the system of 4 vortices and for the two passive particles considered. This time, all $\lambda(t)$ go to 0, as it is expected from the effects of viscosity. However, one can notice that around $t \sim 10^3$, the particle that was initially inside the regularity island started describing a chaotic trajectory, before almost stopping completely due to the effect of viscosity.

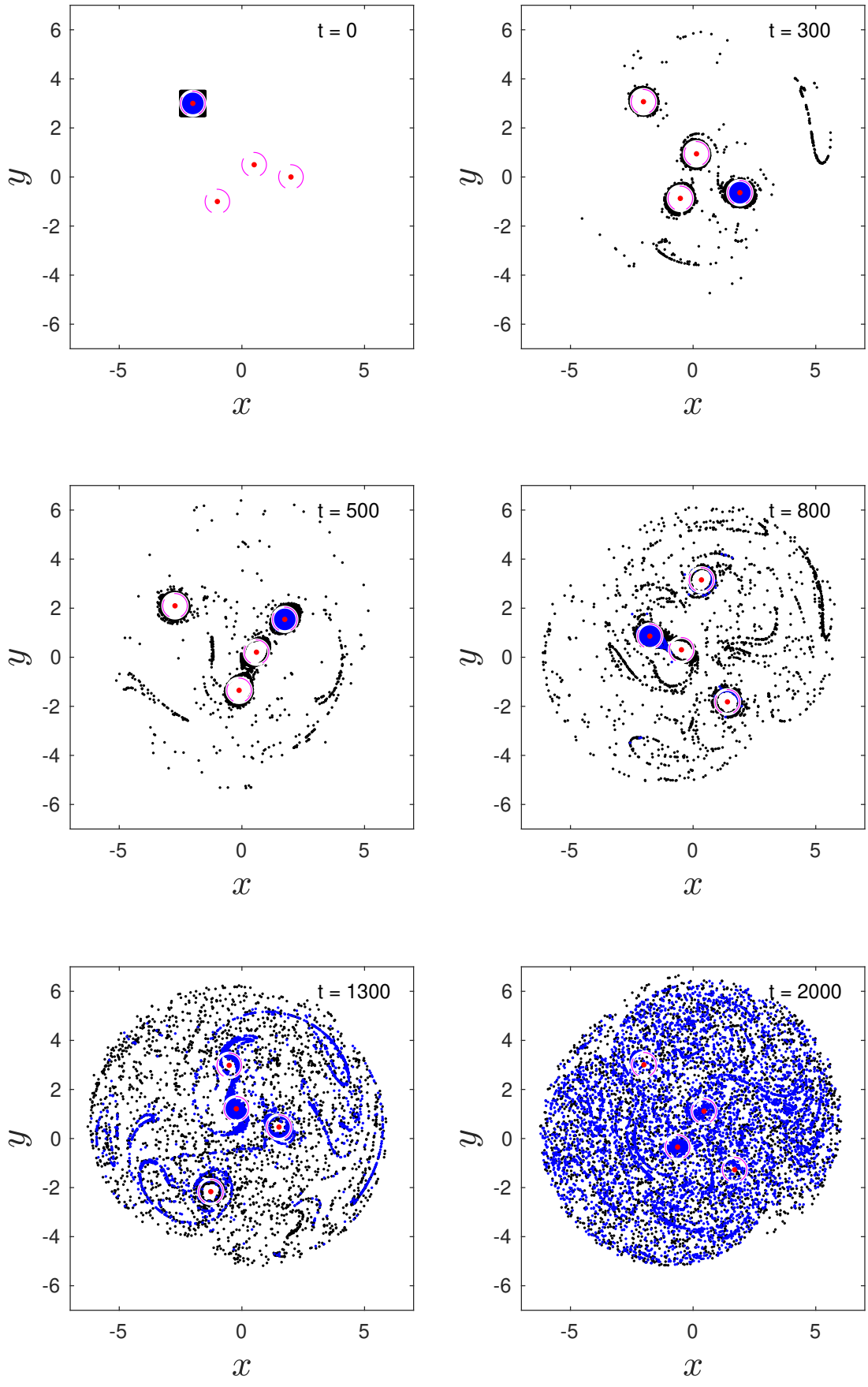

Figure 5.6: Time evolution of a system comprised of 4 viscous vortices and 10^4 test particles initially located near the vortex at $z_4 = -2 + 3i$.

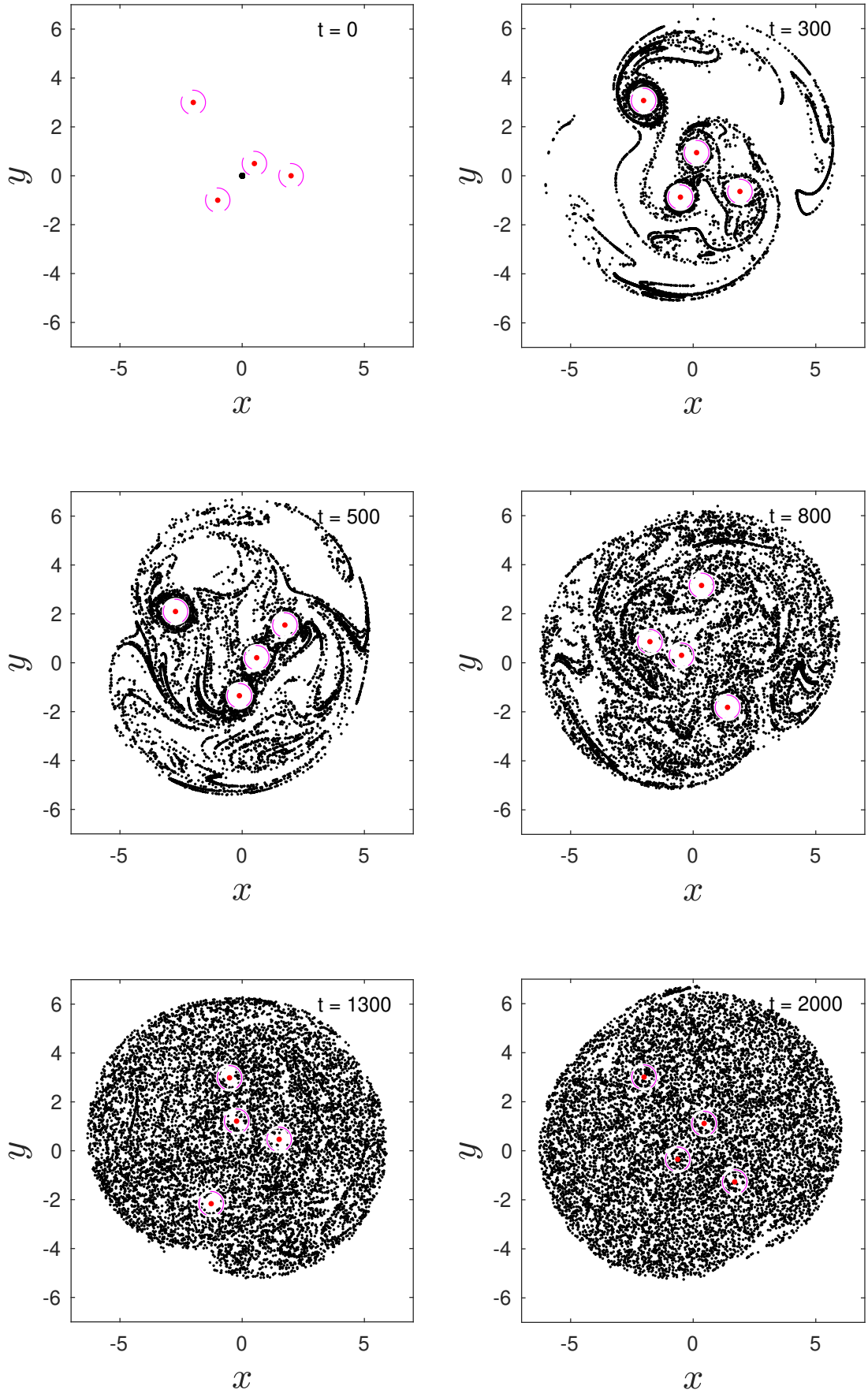

Figure 5.7: Time evolution of a system composed by 4 viscous vortices and 10^4 passive particles initially located on the background between the vortices.

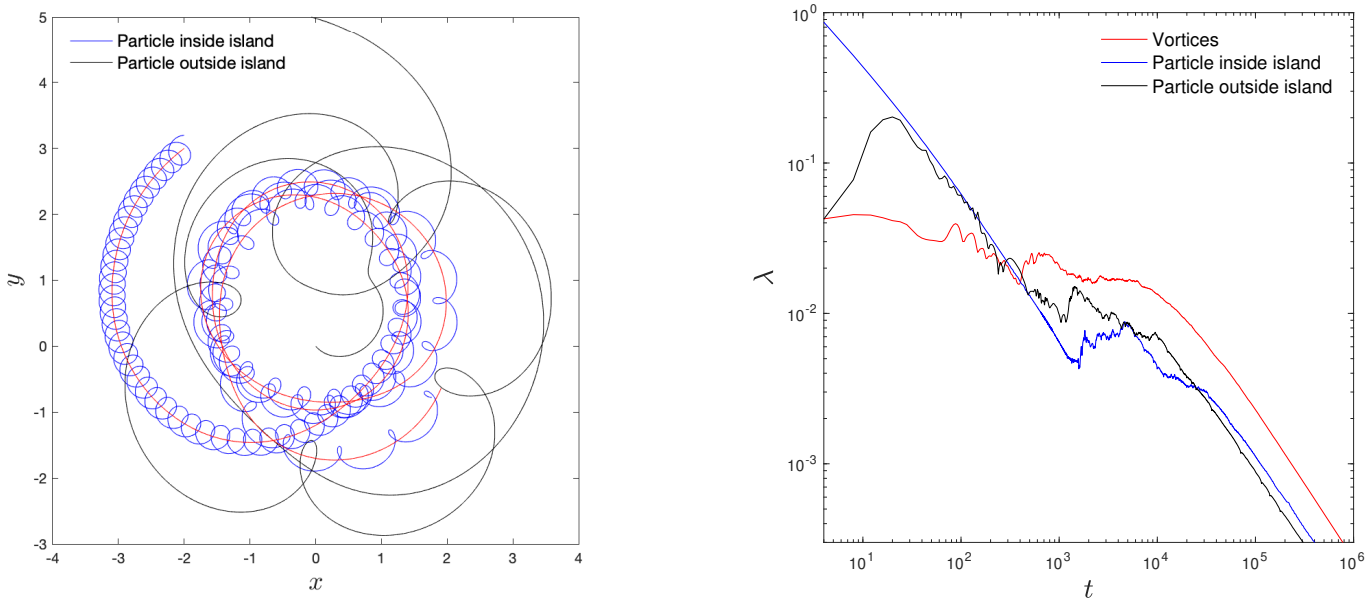

Figure 5.8: Trajectories (left panel) and $\lambda(t)$ (right panel) for the system of 4 viscous vortices and for one of each kind of passive particles.

5.3 CONNECTION BETWEEN VISCOSITY AND DURATION OF CHAOTIC MOTION

A natural question that arises from the behavior we just saw is whether there is any connection between the viscosity coefficient ν and the time period during which a particle (initially located inside a regularity island) can travel chaotically before succumbing to the effects of viscosity.

For that, we considered the exact same system of vortices and a particle located at $z = -2 + 3.2i$, inside the regularity island of vortex z_4, and simulated the system for viscosities $\log_{10}\nu = -1, -2, -3, -4, -5, -6, -7$ during 10^6 units of time. Figure 5.9 shows the results for $\lambda(t)$ for the different viscosities we considered. While it is clear that there exists some period during which chaotic movement occurs for $\nu \leq 10^{-3}$, for $\nu = 10^{-1}, 10^{-2}$ it is difficult to see any indication of chaotic movement. This may be due to the effects of viscosity itself or due to the fact that the computation algorithm for λ needs some time to converge and yield significant results. Figure 5.10 gives clearer visual evidence for the chaotic movement: horizontal lines should correspond to true regularity in the particle's trajectory, while the regions of these curves that highly non-horizontal correspond to time intervals of chaotic movement. As such, from the data of these simulations, one can estimate these time intervals, Δt, for each of the considered viscosities. This yields Figure 5.11, where we left out $\nu = 10^{-1}, 10^{-2}$ because we could not see clear hints of chaotic movement and $\nu = 10^{-7}$ because our simulations were not long enough to sample the times where viscosity starts dominating the system. The point corresponding to $\nu = 10^{-6}$ could also have a higher

position on this plot: while the corresponding curve in 5.10 seems to arrive at a plateau near the end of the simulation, we can't be sure that it's a true plateau without running longer simulations. There seems to be some kind of linear relationship between $\log_{10}\nu$ and $\log_{10}\Delta t$, where environments with smaller viscosities giving rise to longer time periods of chaotic movement for particles initially inside regularity regions. In fact, we estimated $\log_{10}\Delta t = 1.036 - 0.845\log_{10}\nu$, which corresponds to the dashed line in Figure 5.11. Of course, viscosity shouldn't be the only variable affecting these times and further studies can be made to check how the initial distance from the vortex or the circulation of the vortex affect the periods of chaotic motion.

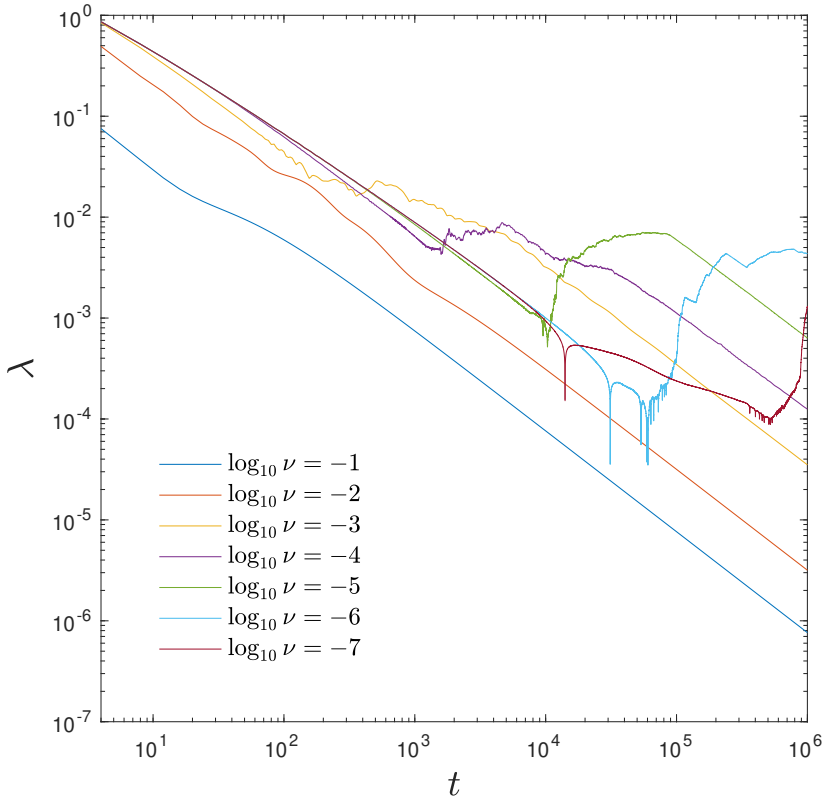

Figure 5.9: $\lambda(t)$ for a particle initially inside a regularity island of the system of 4 viscous vortices for $\log_{10}\nu = -1, -2, -3, -4, -5, -6, -7$

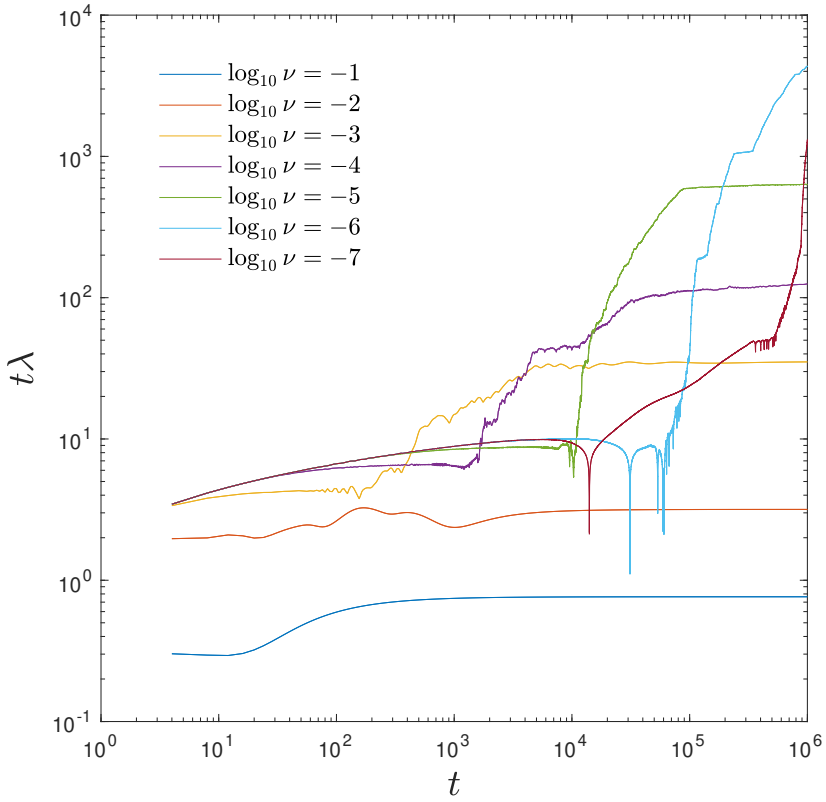

Figure 5.10: $t\lambda\,(t)$ for a particle initially inside a regularity island of the system of 4 viscous vortices for $\log_{10}\nu = -1, -2, -3, -4, -5, -6, -7$

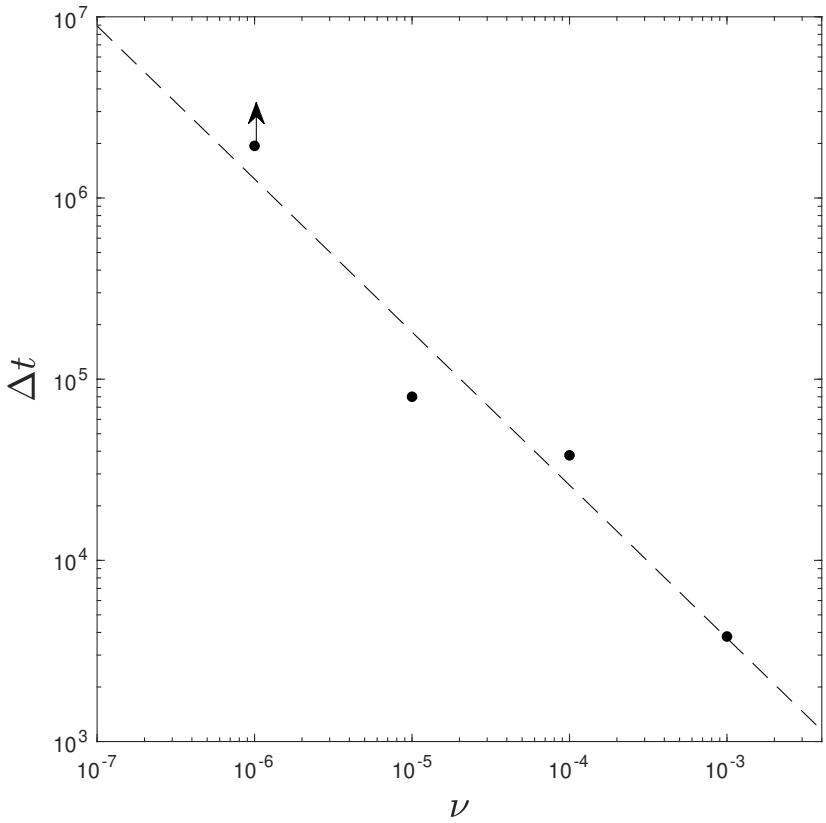

Figure 5.11: Evidence of a linear relationship between the logarithms of the viscosity $\log_{10}\nu$ and the duration of chaotic motion $\log_{10}\Delta t$. The dashed line corresponds to $\log_{10}\Delta t = 1.036 - 0.845\log_{10}\nu$. The point corresponding to $\log_{10}\nu = -6$ could be higher up on the plot due to uncertainties at what is happening near the end of the simulation.

Chapter 6.

Conclusion and Future Work

In this work we presented a short review on the main theoretical results on general fluid dynamics and on the inviscid n-vortex problem. Furthermore, we studied the multi-gaussian model for a viscous description of point vortices based on the Lamb-Oseen solution and tried to make a parallel with the well-known results of the inviscid vortices. We also developed a code in FORTRAN90 to perform the numerical integration of these systems of vortices and validated the code by comparing the numerical and the theoretical results.

The dynamics of passively advected particles by point vortices in the inviscid case has been thoroughly studied over the years. It is known that these systems are characterised by the existence of regularity islands around the vortices, where the particles exhibit regular, non-chaotic, trajectories; in contrast, if the system is composed by more than three vortices, any particle outside of the regularity islands exhibits a chaotic behaviour. The assumption of zero viscosity is, however, questionable in a lot of physical systems and therefore it is important to gain further insight on the dynamics of viscous systems.

We study the dynamics of particles both inside and outside these regularity islands in both inviscid and viscous environments, finding evidence that points towards the fact that these islands change in shape overtime due to the dynamics of the system, even in the inviscid case. There is, however, a barrier that prohibits the exchange of fluid from the inside and outside of these islands. In a viscous environment, the strength of the vortices is diminished by the dissipation of energy through viscosity and these islands shrink in size over time.

We found that, in inviscid environments, Lyapunov exponents seem to predict quite well whether the

movement of vortices and test particles is chaotic or not. In the viscous case, however, some problems arise due to the presence of viscous forces: when trying to identify chaotic motion, if viscosity is too strong, the time interval during which chaotic movement occurs may happen before the algorithm for the computation of Lyapunov exponents converges and yield significant results.

Viscosity makes the dynamics tend towards stability, yet it can also disrupt stable dynamics in the process. In fact, trajectories that initially seem to be stable may start behaving chaotically for some time interval. We found that, in a viscous environment, the time interval of chaotic motion for a passive particle starting inside a regularity island and the coefficient of kinematic viscosity seem to be connected through a linear relationship between their logarithms. In fact, we estimated $\log_{10} \Delta t = 1.036 - 0.845 \log_{10} \nu$. However, further studies are necessary in order to fine-tune this dependency, as this was estimated though a small data set.

Other than fine-tuning the relationship between viscosity and the time length of the chaotic motion, future work on this field could include research on the link between the duration of the chaotic movement and other quantities such as the initial distance of the test particle to the vortex center ou the circulation of the vortex. Another question that could be addressed in future works would be the the dynamics of the regularity islands: in inviscid environments, how does the shape change? Does the area of the islands remain constant? In viscous environments, how does the size or area of the region change with time and viscosity?

Bibliography

[1] Babiano, A., Boffetta, G., Provenzale, A. & Vulpiani, A., *Chaotic advection in point vortex models and two-dimensional turbulence*, 1994, Physics of Fluids 6, Issue 7

[2] Landau, L.D. & Lifshitz, E. M., *Theory of Elasticity*, 3^{rd} edition, 1986, Elsevier

[3] Helmholtz, H.. *Über Integrale der hydrodynamischen Gleichungen, welche den Wirbelbewegungen entsprechen*, 1858, Journal für die reine und angewandte Mathematik, 55, 25-55

[4] Bhatia, H., Norgard, G., Pascucci, V. & Bremer, P-T., *The Helmholtz-Hodge Decomposition - A Survey*, 2013, IEEE Transactions on Visualization and Computer Graphics, 19, 1386-1404

[5] Goldsteion, H., *Classical Mechanics*, 3^{rd} edition, 2001, Addison-Wesley

[6] Arnol'd, V.I., *Mathematical Methods of Classical Mechanics*, 2^{nd} edition, 1997, Springer-Verlag

[7] Struckmeier, J., *Ultimate generalization of Noether's theorem in the realm of Hamiltonian point dynamics*, 2012, Journal of Physics: Conference Series, 380

[8] Benettin, G., Galgani, L., Giorgilli, A. et al., *Lyapunov Characteristic Exponents for smooth dynamical systems and for hamiltonian systems; a method for computing all of them. Part 1: Theory*, 1980, Meccanica, 15, 9-20

[9] Benettin, G., Galgani, L., Giorgilli, A. et al., *Lyapunov Characteristic Exponents for smooth dynamical systems and for hamiltonian systems; A method for computing all of them. Part 2: Numerical application*, 1980, Meccanica, 15, 21-30

[10] Wolf, A., Swift, J.B., Swinney, H.L., & Vastano, J.A., *Determining Lyapunov exponents from a time series*, 1985, Physica D: Nonlinear Phenomena, Volume 16, Issue 3, 285-317

[11] Rosenstein, M.T., Collins, J.J. & De Luca, C.J., *A practical method for calculating largest Lyapunov exponents from small data sets*, 1993, Physica D: Nonlinear Phenomena, Volume 65, Issues 1–2, 117-134

[12] Kantz, H., *A robust method to estimate the maximal Lyapunov exponent of a time series*, 1994, Physics Letters A,

Volume 185, Issue 1, 77-87

[13] Awrejcewicz, J., Krysko, A.V., Erofeev, N.P., Dobriyan, V., Barulina, M.A. & Krysko, V.A., *Quantifying Chaos by Various Computational Methods. Part 1: Simple Systems*, 2018, Entropy, 20, 175

[14] Aref, H., *Stirring by chaotic advection*, 1984, Journal of Fluid Mechanics 143, 1–21

[15] Chapman, D. M. F., *Ideal vortex motion in two dimensions: Symmetries and conservations*, 1978, Journal of Mathematical Physics, 19, 9, 1988-1992

[16] Novikov, E.A. & Sedov, Y.B., *Stochastic properties of a four vortex system*, 1978, Journal of Experimental and Theoretical Physics, 48, 440-444

[17] Aref. H., *Motion of three vortices*, 1979, Physics of Fluids 22, 3, 393- 400.

[18] Adams, M. & Ratiu, T., *The three-point vortex problem: commutative and noncommutative integrability*, 1988, Hamiltonian Dynamical Systems, 81, 245-257

[19] Ziglin, S.L., *Non-integrability of a problem on the motion of four point vortices*, 1980, Doklady Akademii Nauk, 21, 1, 296-299

[20] Koiller, J. & Carvalho, S., *Chaos and non-integrability of point vortex motions*, 1985, Report 010/85, LNCC/CNPq, Rio de Janeiro

[21] Koiller, J. & Carvalho, S., *Non-integrability of the 4-vortex system: analytical proof*, 1989, Communications in Mathematical Physics, 120, 4, 643-652

[22] Castilla, M.S.A.C., Moauro, V., Negrini, P. & Oliva, W.M., *The four positive vortices problem - Regions of chaotic behavior and non-integrability*, 1993, Annales de l'Institut Henri Poincaré - Physique Théorique, 59, 1, 99-115

[23] Lichtenberg, A.J. & Lieberman, M.A., *Regular and Stochastic Motion*, 1982, Springer-Verlag, New York.

[24] Gallay, T. & Wayne, C.E., *Global Stability of Vortex Solutions of the Two-dimensional Navier-Stokes Equation*, 2005, Communications in Mathematical Physics, 255, 1, 97-129

[25] Gallay T., *Interaction of vortices in weakly viscous planar flows*, 2011, Archive for Rational Mechanics and Analysis, 200, 2, 445–490

[26] Jing, F, Kanso, E. & Newton, P.K., *Viscous evolution of point vortex equilibria: The collinear state*, 2010, Physics of Fluids, 22, 12

[27] Fehlberg, E., *Low order Runge-Kutta formulas with step control for heat transfer problems*, 1969, NASA Technical Report 315

Appendix A.

Code for the Simulations

A.1 MAIN PROGRAM

```
program vortex_v0
implicit none



!! Declaração de Parâmetros !!
integer NVORT, NPART
integer LYAPUNOV, TRAJ
integer out_sim, out_z, out_lyap

real*8 PI2
real*8 VISC

!! Inicialização de Parâmetros !!
parameter (NVORT = 2)
parameter (NPART = 0)
parameter (VISC = 0)
```

```
parameter (LYAPUNOV = 1)
parameter (TRAJ = 1)

parameter (out_sim = 20)
parameter (out_z = 40)
parameter (out_lyap = 60)
parameter (PI2 = 8.D0*DATAN(1.D0)) ! 2*pi

!! Declaração de Variáveis !!
complex*16 z(NVORT+NPART), z_perturbed_vort(NVORT+NPART), z_perturbed_part(NVORT+NPART)

real*8 T_final, T, T_out
real*8 h, time
real*8 perturbacao

real*8 gamma(NVORT+NPART)
real*8 dist, somadist
real*8 dist_part(NPART), somadist_part(NPART)
real*8 lyap_vort, lyap_part(NPART)
real*8 P, Q, R, Ham
real*8 hamilt
real*8 start, finish

integer k, s, k_final, k_out, k_int
integer options

!! Inicialização de Variáveis !!
h = 2.D-3 ! Passo de integração
perturbacao = 1.D-5 ! Perturbação inicial
```

```
T_final = 1.D6 ! Tempo final de integração do sistema
T = 1.D0 ! Período de integração para cálculo do expoente de Lyaponov
T_out = 4.D0*T ! Tempo de output

k_out = int(T_out/T) ! iteração de output
k_final = int(T_final/T) ! numero de iterações
k_int = int(T/h) ! iterações por período de integração para cálculo do expoente de
                 ! Lyaponov

options = LYAPUNOV + 2*TRAJ

print*, k_out, k_final, k_int

!! Abertura dos ficheiros de output !!
open (unit=out_sim,file="out_sim_n_vort.txt",action="write",status="replace")
write(out_sim,*) 'SIMULATION START'
write(out_sim,*) ''
write(out_sim,*) 'This simulation was run with ', NVORT, ' vortices and ', NPART,&
         ' particles.'
write(out_sim,*) 'Viscosity: ', VISC
write(out_sim,*) 'Integration Step: ', h
write(out_sim,*) 'Total time of integration: ', T_final
write(out_sim,*) 'Period for Lyapunov Exponent computation: ', T
write(out_sim,*) 'Period for outputs: ', T_out
write(out_sim,*) 'Initial perturbation: ', perturbacao

call cpu_time(start)
```

```
select case( options )

        case( 1 )
                open (unit=out_lyap,file="out_lyap.txt",action="write",status="replace")

                !! Inicialização dos 2 sistemas de vórtices !!
                call InitialConditions (z, gamma, CENTRO, LADO, NVORT, NPART)
                call Perturb_vort(z, z_perturbed_vort, perturbacao, NVORT, NPART, 1)
                call Perturb_part(z, z_perturbed_part, perturbacao, NVORT, NPART, 1)

                !! Inicialização das variáveis do cíclo !!
                k = 0
                somadist = 0.D0
                somadist_part = 0.D0
                time = 0.D0
                lyap_vort = 0.D0
                lyap_part = 0.D0

                !! Invariantes iniciais !!
                P = sum(gamma*dreal(z))
                Q = sum(gamma*dimag(z))
                R = sum(gamma*cdabs(z)**2)
                Ham = hamilt(z, gamma, NVORT, NPART, PI2)

                write(out_lyap,*) k, time, P, Q, R, Ham, lyap_vort, lyap_part

                !! Cíclo de integração e output !!
                do k = 1, k_final
```

```
do s = 1, k_int

        ! Integração dos três sistemas
        call RKF45(h, time, z, gamma, NVORT, NPART, VISC, PI2)
        call RKF45(h, time, z_perturbed_vort, gamma, NVORT, &
                NPART, VISC, PI2)
        call RKF45(h, time, z_perturbed_part, gamma, NVORT, &
                NPART, VISC, PI2)
        time = time + h

end do

!! Cálculo do Expoente de Lyapunov instantâneo !!
dist = dsqrt( sum( cdabs(z(1:NVORT) - &
        z_perturbed_vort(1:NVORT))**2 ) )
somadist = somadist + dlog(dist)

dist_part = cdabs(z(NVORT+1:NVORT+NPART) - &
        z_perturbed_part(NVORT+1:NVORT+NPART))
somadist_part = somadist_part + dlog(dist_part)


!! Escrita de outputs !!
if (k  - (k/k_out)*k_out.EQ.0) then

        lyap_vort = (somadist/float(k) - dlog(perturbacao))
        lyap_part = (somadist_part/float(k) - dlog(perturbacao))

        !! Invariantes !!
```

```
                        P = sum(gamma*dreal(z))
                        Q = sum(gamma*dimag(z))
                        R = sum(gamma*cdabs(z)**2)
                        Ham = hamilt(z, gamma, NVORT, NPART, PI2)

                        write(out_lyap,*) k, time, P, Q, R, Ham, lyap_vort, &
                                lyap_part

                end if

                ! Re-perturbar os sistemas
                call Perturb_vort(z, z_perturbed_vort, perturbacao, NVORT, &
                        NPART, 2)
                call Perturb_part(z, z_perturbed_part, perturbacao, NVORT, &
                        NPART, 2)

        end do

        close(out_lyap)

case( 2 )
        open (unit=out_z,file="out_z.txt",action="write",status="replace")

        !! Inicialização do sistema de vórtices !!
        call InitialConditions (z, gamma, CENTRO, LADO, NVORT, NPART)

        !! Inicialização das variáveis do cíclo !!
        k = 0
```

```
                write(out_z,*) k, time, z

                !! Cíclo de integração e output !!
                do k = 1, k_final

                        do s = 1, k_int

                                ! Integração dos dois sistema de vórtices
                                call RKF45(h, time, z, gamma, NVORT, NPART, VISC, PI2)
                                time = time + h

                        end do

                        !! Escrita de outputs !!
                        if (k  - (k/k_out)*k_out.EQ.0) then

                                write(out_z,*) k, time, z
!                                print*, k, '/', k_final

                        end if

                end do

                close(out_z)

        case ( 3 )
                open (unit=out_lyap,file="out_lyap.txt",action="write",status="replace")
                open (unit=out_z,file="out_z.txt",action="write",status="replace")
```

```
!! Inicialização dos 3 sistemas !!
call InitialConditions (z, gamma, CENTRO, LADO, NVORT, NPART)
call Perturb_vort(z, z_perturbed_vort, perturbacao, NVORT, NPART, 1)
call Perturb_part(z, z_perturbed_part, perturbacao, NVORT, NPART, 1)

!! Inicialização das variáveis do cíclo !!
k = 0
somadist = 0.D0
somadist_part = 0.D0
time = 0.D0
lyap_vort = 0.D0
lyap_part = 0.D0

!! Invariantes e escrita das condições iniciais !!
P = sum(gamma*dreal(z))
Q = sum(gamma*dimag(z))
R = sum(gamma*cdabs(z)**2)
Ham = hamilt(z, gamma, NVORT, NPART, PI2)

write(out_lyap,*) k, time, P, Q, R, Ham, lyap_vort, lyap_part
write(out_z,*) k, time, z

!! Cíclo de integração e output !!
do k = 1, k_final

        do s = 1, k_int

                ! Integração dos dois sistema de vórtices
                call RKF45(h, time, z, gamma, NVORT, NPART, VISC, PI2)
```

```
        call RKF45(h, time, z_perturbed_vort, gamma, NVORT, &
                NPART, VISC, PI2)
        call RKF45(h, time, z_perturbed_part, gamma, NVORT, &
                NPART, VISC, PI2)
        time = time + h

end do

!! Cálculo do Expoente de Lyapunov instantâneo !!
dist = dsqrt( sum( cdabs(z(1:NVORT)- &
        z_perturbed_vort(1:NVORT))**2 ) )
somadist = somadist + dlog(dist)

dist_part = cdabs(z(NVORT+1:NVORT+NPART)- &
        z_perturbed_part(NVORT+1:NVORT+NPART))
somadist_part = somadist_part + dlog(dist_part)

!! Escrita de outputs !!
if (k  - (k/k_out)*k_out.EQ.0) then

        !! Invariantes !!
        P = sum(gamma*dreal(z))
        Q = sum(gamma*dimag(z))
        R = sum(gamma*cdabs(z)**2)
        Ham = hamilt(z, gamma, NVORT, NPART, PI2)

        lyap_vort = (somadist/float(k) - dlog(perturbacao))
        lyap_part = (somadist_part/float(k) - dlog(perturbacao))
```

```
                                write(out_lyap,*) k, time, P, Q, R, Ham, lyap_vort, &
                                        lyap_part
                                write(out_z,*) k, time, z
!                                print*, k, '/', k_final

                        end if

                        ! Re-perturbar os sistemas
                        call Perturb_vort(z, z_perturbed_vort, perturbacao, NVORT, &
                                NPART, 2)
                        call Perturb_part(z, z_perturbed_part, perturbacao, NVORT, &
                                NPART, 2)

                end do

                close (out_z)
                close (out_lyap)

        case default
                write(out_sim,*) 'Não foi pedido nenhum output.'

end select

call cpu_time(finish)


write(out_sim,*) ''
write(out_sim,*) 'Time of simulation: ', finish - start, 'seconds'
write(out_sim,*) ''
```

```
write(out_sim,*) 'SIMULATION END'
close (out_sim)

end program vortex_v0
```

A.2 SUBROUTINE TO PERTURBATE THE VORTICES

```
subroutine Perturb_vort(z, z_perturbed, perturbacao, NVORT, NPART, opt)
implicit none

integer, parameter :: out_unit=20

integer NVORT, NPART, opt
complex*16 z(NVORT + NPART), z_perturbed(NVORT + NPART)
real*8 x, y, perturbacao

integer seed(121)
complex*16 aux(NVORT)

select case (opt)

        ! Perturbação inicial
        case (1)
                !! Seed para RNG !!
                seed = 121
                call RANDOM_SEED(PUT = seed)

                call RANDOM_NUMBER(x)
                call RANDOM_NUMBER(y)
```

```
                z_perturbed = z
                z_perturbed(1) = z(1) + perturbacao*complex(0.0697565D0,0.997564D0)

        ! Re-perturbações na direcção de maior crescimento
        case(2)
                aux = z_perturbed(1:NVORT) - z(1:NVORT)
                z_perturbed(1:NVORT) = z(1:NVORT) + &
                        perturbacao/dsqrt(dfloat(NVORT)) * aux/cdabs(aux)
end select

return
end
```

A.3 SUBROUTINE TO PERTURBATE THE PARTICLES

```
subroutine Perturb_part(z, z_perturbed, perturbacao, NVORT, NPART, opt)
implicit none

integer, parameter :: out_unit=20

integer NVORT, NPART, opt
complex*16 z(NVORT + NPART), z_perturbed(NVORT + NPART)
real*8 x, y, perturbacao

integer seed(121)
complex*16 aux(NPART)

select case (opt)
```

```
        ! Perturbação inicial
        case (1)
                !! Seed para RNG !!
                seed = 121
                call RANDOM_SEED(PUT = seed)

                call RANDOM_NUMBER(x)
                call RANDOM_NUMBER(y)

                z_perturbed = z
                z_perturbed(NVORT+1:NVORT+NPART) = z(NVORT+1:NVORT+NPART) + &
                         perturbacao*complex(0.0697565D0,0.997564D0)

        ! Re-perturbações na direcção de maior crescimento
        case(2)
                aux = z_perturbed(NVORT+1:NVORT+NPART) - z(NVORT+1:NVORT+NPART)
                z_perturbed(NVORT+1:NVORT+NPART) = z(NVORT+1:NVORT+NPART) + &
                        perturbacao * aux/cdabs(aux)
end select

return
end
```

A.4 SUBROUTINE FOR RUNGE-KUTTA-FEHLBERG INTEGRATION

```
subroutine RKF45(h, time, z, gamma, NVORT, NPART, VISC, PI2)
implicit none
```

```
   interface                                    !! Declare function
    function modelo(t, z, gamma, NVORT, NPART, VISC, PI2) result(dz)
     integer :: NVORT, NPART
         real*8 :: VISC
         real*8 :: Pi2
     real*8 :: t
     real*8, dimension(NVORT+NPART) :: gamma
     complex*16, dimension(NVORT+NPART) :: z
     complex*16, dimension(NVORT+NPART) :: dz
    end function
   end interface

real*8 PI2
real*8 VISC
real*8 time
integer NVORT, NPART
complex*16 z(NVORT+NPART)
real*8 gamma(NVORT+NPART)
real*8 h, h2, h4, h38, h1213
complex*16 K1(NVORT+NPART), K2(NVORT+NPART), K3(NVORT+NPART), K4(NVORT+NPART), &
        K5(NVORT+NPART), K6(NVORT+NPART)

h2 = h/2.D0
h4 = h/4.D0
h38 = 3.D0*h/8.D0
h1213 = 12.D0*h/13.D0

K1 = h * modelo(time, z, gamma, NVORT, NPART, VISC, PI2)
```

```
K2 = h * modelo(time + h4, z + K1/4.D0, gamma, NVORT, NPART, VISC, PI2)
K3 = h * modelo(time + h38, z + 3.D0*K1/32.D0 + 9.D0*K2/32.D0, &
        gamma, NVORT, NPART, VISC, PI2)
K4 = h * modelo(time + h1213, z + 1932.D0*K1/2197.D0 - 7200.D0*K2/2197.D0 + &
         7296.D0*K3/2197.D0 , gamma, NVORT, NPART, VISC, PI2)
K5 = h * modelo(time + h, z + 439.D0*K1/216.D0 - 8.D0*K2 + 3680.D0*K3/513.D0 - &
        845.D0*K4/4104.D0 , gamma, NVORT, NPART, VISC, PI2)
K6 = h * modelo(time + h2, z - 8.D0*K1/27.D0 + 2.D0*K2 - 3544.D0*K3/2565.D0 + &
        1859.D0*K4/4104.D0 - 11.D0*K5/40.D0 , gamma, NVORT, NPART, VISC, PI2)

z = z + 16.D0*K1/135.D0 + 6656.D0*K3/12825.D0 + 28561.D0*K4/56430.D0 - &
        9.D0*K5/50.D0 + 2.D0*K6/55.D0

return
end
```

A.5 FUNCTION TO COMPUTE THE DYNAMICAL EQUATIONS

```
FUNCTION modelo(t, z, gamma, Nvort, Npart, VISC, PI2) result(dz)
implicit none

integer Nvort, Npart
real*8 PI2
real*8 VISC
complex*16 z(Nvort+Npart)
real*8 gamma(Nvort+Npart), t

complex*16 aux
complex*16 aux2
```

```
complex*16, dimension(Nvort+Npart) :: dz

integer k, j

dz(1:Nvort+Npart) = (0.D0,0.D0)
aux = (0.D0,0.D0)

if (VISC.EQ.0) then

        ! Vórtices
        do k = 1, Nvort, 1
                do j = k+1, Nvort, 1

                        aux = (1.D0,0.D0)/(z(k)-z(j))
                        aux = dconjg(aux)

                        dz(k) = dz(k) + gamma(j)*aux
                        dz(j) = dz(j) - gamma(k)*aux

                end do
        end do

        ! Partículas
        do k = Nvort+1, Nvort+Npart, 1
                do j = 1, Nvort, 1

                        aux = (1.D0,0.D0)/(z(k)-z(j))
                        aux = dconjg(aux)
```

```
                        dz(k) = dz(k) + gamma(j)*aux


                end do
        end do



else
        ! Vórtices
        do k = 1, Nvort, 1
                do j = k+1, Nvort, 1

                        aux = z(k)-z(j)
                        aux2 = 1 - dexp( - cdabs(aux)**2/(4.D0*VISC*t))

                        aux = (1.D0,0.D0)/(z(k)-z(j))
                        aux = dconjg(aux) * aux2

                        dz(k) = dz(k) + gamma(j) * aux
                        dz(j) = dz(j) - gamma(k) * aux

                end do
        end do

        ! Partículas
        do k = Nvort+1, Nvort+Npart, 1
                do j = 1, Nvort, 1

                        aux = z(k)-z(j)
                        aux2 = 1 - dexp( - cdabs(aux)**2/(4.D0*VISC*t))
```

```
                        aux = (1.D0,0.D0)/(z(k)-z(j))
                        aux = dconjg(aux) * aux2

                        dz(k) = dz(k) + gamma(j) * aux

                end do
        end do

end if

dz = -dz/complex(0.D0, PI2)

return
end
```

A.6 SUBROUTINE TO DEFINE INITIAL CONDITIONS (EXAMPLE)

```
subroutine InitialConditions(z, gamma, NVORT, NPART)
implicit none

integer NVORT, NPART
complex*16 z(NVORT + NPART)
real*8 gamma(NVORT + NPART)

integer k
real*8 x, y

!! Seed para RNG !!
```

```
integer seed(101)

seed = 101

call RANDOM_SEED(PUT = seed)


do k = 1, NVORT, 1
        call RANDOM_NUMBER(x)
        call RANDOM_NUMBER(y)
        z(k) =  complex(x, y)
        gamma(k) = 1.D0
end do


do k = NVORT+1, NVORT+NPART, 1
        call RANDOM_NUMBER(x)
        call RANDOM_NUMBER(y)
        z(k) =  complex(x, y)
        gamma(k) = 0.D0
end do


! z(1) = complex(2.D0, 0.D0)
! z(2) = complex(-1.D0, -1.D0)
! gamma(1) = 1.D0
! gamma(2) = -1.D0


return
end
```